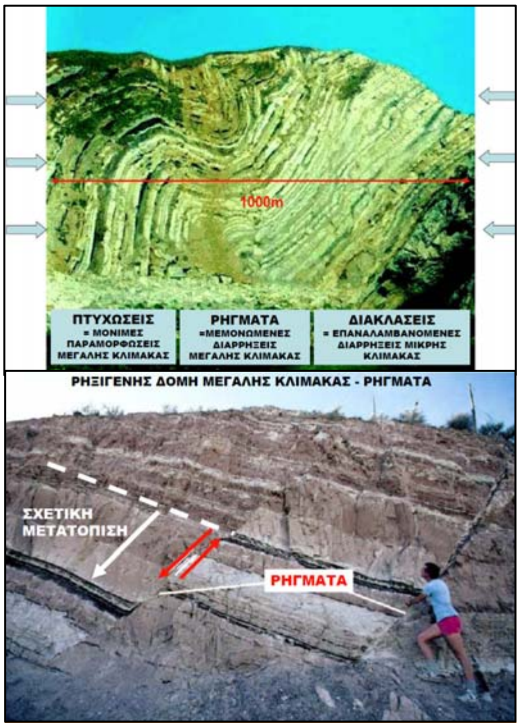

Από τις σημειώσεις του Σταύρου Μπαντή «ΒΡΑΧΟΜΗΧΑΝΙΚΗ»

ΕΛΛΗΝΙΚΗ ΕΠΙΣΤΗΜΟΝΙΚΗ ΕΤΑΙΡΕΙΑ ΕΔΑΦΟΜΗΧΑΝΙΚΗΣ & ΓΕΩΤΕΧΝΙΚΗΣ ΜΗΧΑΝΙΚΗΣ

Τα Νέα της Ε Ε Ε Ε Γ Μ

88

Αρ. 88 – ΜΑΡΤΙΟΣ 2016

Safe geotechnics by observation

In geotechnics more than in other engineering disciplines much can be learnt from the behaviour of finished structures regardless of where they are located in the world. This is certainly true for major collapses such as the Nicoll Highway or the centuries of mitigation attempted on the still-leaning tower of Pisa.

But we do not need to rely on catastrophes or mistakes to enhance our understanding of soil behaviour and of how man-made structures interact with it. By monitoring the behaviour of structures during and after construction we have the opportunity to compare the predictions made at design stage with their real behaviour.

(συνέχεια στην σελίδα 2)

Σταύρος Μπαντής 1951 – 2016

Καθηγητής Τεχνικής Γεωλογίας και Βραχομηχανικής του Τμήματος Πολιτικών Μηχανικών της Πολυτεχνικής Σχολής του Αριστοτελείου Πανεπιστημίου Θεσσαλονίκης. Απεβίωσε στο γραφείο του στις 11 Ιανουαρίου 2016.

(αφιέρωμα στην σελίδα 3)

SIMSG ISSMGE

ISRM

Π Ε Ρ Ι Ε Χ Ο Μ Ε Ν Α

(συνέχεια από την 1η σελίδα)

Beyond a validation of the design, I believe we should habitually ‘back-analyse’ the behaviour to assess whether the input parameters could have been more accurate. In this way we can generate deeper insights into the geotechnics of a given project or location, arriving at valuable conclusions that we can share with our peers.

The monitoring industry is ever evolving thanks to advancements in instrumentation, such as the use of fibre-optics and post-processing tools which now also include those used for big data. This then creates data that can be shared in the cloud and made available in real-time and shared with users via web portals such as the Global Analyser.

But industry codes and regulations do not typically prescribe back-analyses, which means that if they take place at all, they’re left to the initiative of the designers for whom they’re not a priority and who may not have access to the monitoring data. I firmly believe that whenever there is this sort of disconnection between a project’s design and construction activities the construction industry misses a golden opportunity to improve.

As a geotechnical engineer I always look for precedents when a new project starts. Published case histories in the project area or with comparable features are particularly valuable to designers as they can contain a wealth of information on what went well but also on what might have been problematic in previous construction projects. The International Society for Soil Mechanics and Geotechnical Engineering publishes a journal on this topic for example and encourages academics and practitioners to contribute to it.

Looking forward, we have the opportunity to bring together all this data into a single, shared computer model for the behaviour of say Copenhagen till, Milan gravels, London clay, San Francisco Bay mud and so on.

I believe the time is right for legislators to consider adding back-analyses as a requirement to the virtuous circle of design > construction > observed behaviour > improved design. Ultimately this will lead to safer and more sustainable assets.

Francesco Petrella / ARUP Geotechnics, 31 March 2016

http://thoughts.arup.com/post/details/534/safe-geotechnics-by-observation

ΣΤΑΥΡΟΣ ΜΠΑΝΤΗΣ (1951 – 2016)

ΣΤΗ ΜΝΗΜΗ ΤΟΥ ΑΠΟ ΧΡΗΣΤΟ ΑΝΑΓΝΩΣΤΟΠΟΥΛΟ

Δυστυχώς έτυχε σε μένα ο κλήρος να αποχαιρετίσω το στενό μου φίλο Σταύρο Μπαντή, που μας άφησε ξαφνικά στις 11.01.2016, μέσα στο γραφείο του στο Εργαστήριο Τεχνικής Γεωλογίας και Βραχομηχανικής στο Τμήμα Πολιτικών Μηχανικών του ΑΠΘ εν ώρα εργασίας.

Η ακαδημαϊκή του εξέλιξη ήταν γρήγορη.

Το 1973 αποφοίτησε από τη Φυσικομαθηματική Σχολή του Αριστοτελείου Πανεπιστημίου Θεσσαλονίκης και το 1976 έλαβε το μεταπτυχιακό του δίπλωμα (MSc in Engineering Geology & Geotechnics) από το University of Leeds, UK.

Από το ίδιο Πανεπιστήμιο το 1980 έλαβε το διδακτορικό του δίπλωμα στη Βραχομηχανική (PhD in Engineering Rock Mechanics).

Στη συνέχεια (1981-1985) έκανε τη μεταδιδακτορική του έρευνα (Postdoctoral Research Fellowship) με υποτροφία του Εθνικού Ιδρύματος Ερευνών της Νορβηγίας (NTNF) στο Νορβηγικό Γεωτεχνικό Ινστιτούτο (Norwegian Geotechnical Institute, NGI).

Ο Σταύρος Μπαντής εκλέχθηκε το 1986 ως Λέκτορας στο Εργαστήριο Τεχνικής Γεωλογίας του Τμήματος Πολιτικών Μηχανικών του ΑΠΘ ενώ το 1996 εξελέγη Διευθυντής του Εργαστηρίου Τεχνικής Γεωλογίας. Το 1998 εξελέγη καθηγητής του Τμήματος Πολιτικών Μηχανικών του ΑΠΘ.

Η μεγάλη και ουσιαστική συνεισφορά του Σταύρου Μπαντή στο ΑΠΘ συνοψίζεται σε δύο τομείς:

α. Την αναδιοργάνωση του Εργαστηρίου Τεχνικής Γεωλογίας, το συστηματικό εξοπλισμό του και τη συνεχή ανάπτυξη της λειτουργίας του.

β. Την εισαγωγή και καθιέρωση των αντικειμένων της Βραχομηχανικής και της Περιβαλλοντικής Τεχνικής Γεωλογίας

Η επιστημονική και ερευνητική του εξέλιξη ήταν λαμπρή.

Σε συνεργασία με τον Dr. Nicholas Barton εργάστηκε συστηματικά στον τομέα των καταστατικών νόμων συμπεριφοράς των ασυνεχειών σε βραχώδη εδάφη. Ο νόμος συμπεριφοράς ασυνεχειών «Barton-Bandis Model of Engineering Properties of Joints» έγινε παγκόσμια αποδεκτός και χρησιμοποιείται ευρέως στα σχετικά λογισμικά (UDEC-BB and FLAC by Itasca, Inc., Phase2, Swedge, etc. by RocScience of Canada).

Ο Σταύρος Μπαντής ήταν επιστήμονας διεθνούς κύρους και ακτινοβολίας και έχαιρε παγκόσμιας αναγνώρισης. Ήταν μέλος πολλών διεθνών επιτροπών, κριτής στα εγκυρότερα επιστημονικά περιοδικά του χώρου, προσκεκλημένος ομιλητής σε διάφορα συνέδρια ανά τον κόσμο, επιστημονικός υπεύθυνος εκπόνησης πολλών ερευνητικών προγραμμάτων και συγγραφέας πάνω από 100 επιστημονικών εργασιών που δημοσιεύτηκαν σε έγκριτα διεθνή περιοδικά και συνέδρια.

Το τελευταίο του πόνημα, το βιβλίο με τίτλο "Engineering in Jointed and Faulted Rock" που συνέγραφε με τον Dr. N. R. Barton, έμεινε δυστυχώς ημιτελές. Ο Dr. Barton δήλωσε θα καταβάλει κάθε προσπάθεια να εκδοθεί σύντομα.

Ο Σταύρος Μπαντής, με όπλο τη βαθιά επιστημονική του γνώση, απέκτησε μεγάλη επαγγελματική εμπειρία στο σχεδιασμό και την παρακολούθηση δύσκολων γεωτεχνικών έργων και ειδικότερα στα στις σήραγγες και τα υπόγεια έργα, τη σταθεροποίηση κατολισθήσεων και βραχωδών πρανών, τα φράγματα και τις θεμελιώσεις γεφυρών σε βράχο.

Ήταν Τεχνικός Σύμβουλος διαφόρων Οργανισμών, Μελετητικών Γραφείων και Κατασκευαστικών Εταιρειών. Ενδεικτικά αναφέρονται το Νορβηγικό Γεωτεχνικό Ινστιτούτο, World Bank (Expert Panelist), Geo-Engineering, Jersey, U.K., Haswell Consulting Engineers,U.K., Golder Associates Ltd, Canada, Atkins China Ltd., TVX GOLD,Inc., Sir Alexander Gibb and Partners, U.K., McDowels Consulting Engineers, U.K., Maunsell PTY LTD, Sydney, Rail Link Engineering Ltd, U.K., Μηχανική Α.Ε., Τμήμα Αναπτύξεως Υδάτων Κύπρου, Ελληνική Μελετών Α.Τ.Ε., Α.Ε.Γ.Ε.Κ., ΜΕΤΩΝ Α.Ε., Αναστηλωτική Α.Τ.Ε., ΒΑΣΙΣ ΣΥΣΜ Α.Ε.., Υπουργείο Πολιτισμού, ΔΑΒΜΜ, ΕΓΝΑΤΙΑ ΟΔΟΣ Α.Ε., Εδαφοστατική, Scott Wilson (U.K.), Flint and Neil Partnership (UK), Charles Haswell & Partners (UK), CityTunnel Konsortiet, Malmo (Sweden), Halcrow (UK).

Η μεγάλη επαγγελματική και πρακτική του εμπειρία σε θέματα σηράγγων, φραγμάτων και κατολισθήσεων του επέτρεψαν να μεταδώσει σε πολλές γενιές Πολιτικών Μηχανικών ουσιαστικές και άμεσα αξιοποιήσιμες γνώσεις σε ένα καινούριο τομέα.

Ο Σταύρος Μπαντής συνδύασε με ιδιαίτερα αρμονικό τρόπο την ιδιότητα του ακαδημαϊκού δασκάλου, του ερευνητή και του γεωτεχνικού μηχανικού της πράξης.

Η οικογένειά του, οι φίλοι του, το Τμήμα Πολιτικών Μηχανικών, το ΑΠΘ και η Ελληνική κοινωνία, ήταν τυχεροί που είχαν κοντά τους το Σταύρο.

Φίλε μου καλό σου ταξίδι.

Χρήστος Αναγνωστόπουλος, Μάρτιος 2016

ΣΤΗ ΜΝΗΜΗ ΤΟΥ ΑΠΟ NICK BARTON

With a heavy heart mixed with unfading warm memories we must report the sudden death of Prof. Stavros Bandis, who was at work in the University of Thessaloniki on 11th January 2016. He died of sudden heart failure. He was head of the department and Chair of Rock Mechanics and Civil Engineering. His many past and future students, and his staff, have suffered a very great loss. Two who have also had long association with him, Dr. Nick Barton and Dr. John Sharp, have provided these images of his important contributions to rock mechanics and rock engineering, on behalf of ISRM.

Nick Barton was first contacted by Stavros when he was a Ph.D. student with Prof. Dearman, in Leeds University: Out of the blue in 1978 or 1979, Stavros wrote a detailed, beautifully illustrated, and several page letter in his inimitable italic hand, with his latest research on scale effects in rock joint replicas. By good fortune for those in rock mechanics who value an alternative to Mohr-Coulomb for describing rock joints, he was already making thorough use of JRC and JCS, as recently detailed with shear tests, tilt tests and profiling, in Barton and Choubey, 1977. His thesis of 1980 'Experimental studies of scale effects on shear strength, and deformation of rock joints', was soon awarded a highly deserved (5th) Rocha Medal by the ISRM. Bandis's superb research helped to set the scene for the development of the Barton-Bandis joint behaviour criterion. The recommended scale-effects for JRC and JCS, which are block-size dependent, were derived from his and the writer's physical model and jointed rock experiments. Bandis alone was responsible for the hyperbolic normal closure and stiffness behaviour. By 1982 the Barton-Bandis model, with physical and conducting apertures included, was up and running in TerraTek, Salt Lake City (thanks to Dr. Khosrow Bakhtar's programable HP calculator expertise).

In 1985, Mark Christianson of Itasca installed BB in Peter Cundall's UDEC, of course with some assistance from Bandis since he was with us at NGI at the time. We immediately applied UDEC-BB to the Ekofisk reservoir compaction (and joint shearing) study. Bandis was actually the first to test Ekofisk joints for their shear strength, after Philips had been surprised at the writer's NGI request for jointed core samples.

We had the pleasure and great benefit of several visits for summer and sabbatical work by Stavros at NGI, perhaps most notably during a physical model study of 3D borehole/wellbore stability and failure, conducted for various oil companies in the late 1980's. The most detailed study of log-spiral failure patterns, for holes drilled in various directions in relation to applied 3D stresses, was strongly contributed to by Bandis, including a personal (anisotropic) gift to the project manager, shown here, and carefully preserved in my Oslo office. (See Addis et 1991, SPE for project details).

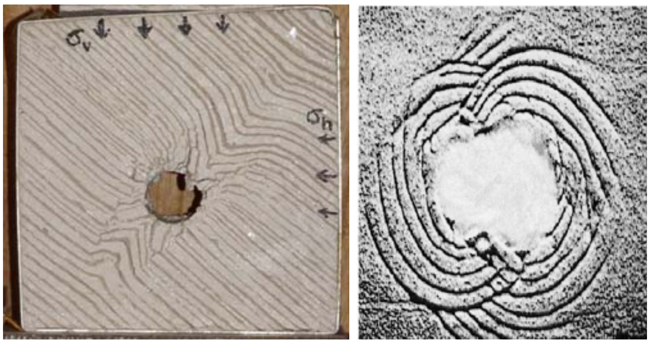

An example of Bandis's quest for reality, in this case anisotropic behaviour, to contrast with isotropic log-spirally failing model wellbores. Here he proved that shearing was occurring using coloured sand in miniature pre-drilled boreholes.

In 1990 we held the Rock Joints conference in Loen, and naturally Bandis was one of the keynote lecturers. A gathering of rock mechanics friends prior to this event, also illustrated here, includes ISRM president John Franklin, 1987-1991. The ISRM has also lost Prof. Kawamoto in the intervening years.

Stavros Bandis, as you will read from John Sharp, had an uncanny wish to achieve reality when characterizing and then modelling rock mass and rock excavation behaviour with UDEC-BB or 3DEC. His modelling work was outstanding and has probably not been matched due to his constant attention to detail. As his friend and colleague John Sharp has written: 'His loss as a world leader in his field with such an enormous insight and depth of knowledge is unaccountable. He spoke to everyone as an equal, with interest and humour, always making a substantial and yet understated impression.' A selection of his many contributions will be included in our joint book-project, which has been progressing for the last four years, during chapter by chapter sessions, mostly undertaken in a deserted village high in the Greek mountains, cut off from the internet.

From right (ISRM only): Pinto da Cunha, Bandis, Makurat, Franklin, Johanson, Martin, Aydan, Barton, Kawamoto, pictured in 1990 prior to the Loen conference of Rock Joints. Sadly, three are now departed.

Sadly, Stavros is no longer in the University of Thessaloniki, but he left behind a team of expertly trained and gifted colleagues who will attempt via his inspiration to continue his unique legacy and reputation for geologic inquisition, realistic simulation and applied engineering solutions. Stavros leaves his wife Christina, and two adult sons Konstantinos and Nickolas.

Nick Barton, March 2016

ΓΙΑΤΙ ΣΤΗ ΓΕΩΤΕΧΝΙΚΗ

Does anybody have an idea why do we use 25 blows in the standard compaction test? As well as why do we compact with 3 layers?

Η ερώτηση υπεβλήθη στον ιστοχώρο Research Gate από τον Omar Hamdi Jasim, φοιτητή του Department of Civil Engineering, Yildiz Technical University, Κωνσταντινούπολη. Η παρακάτω απάντηση ήρθε από την Madhavi Latha Gali, Καθηγήτρια στο Department of Civil Engineering, Indian Institute of Science, Bengaluru.

"Proctor was doing road development projects where he needed to estimate the practically possible density of soil, which is different from theoretical density. He tried to solve this through laboratory tests by using various moulds and compactors and different combinations of blows and lift thicknesses. In this process he settled with 25 blows and 3 lifts.

The original Proctor Compaction Test of 1933 used cylindrical mold 4 inches in diameter and 4.6 inches high, with a removable mold collar 2.5 inches high. The mold volume is 1/30th cubic foot.

A 5.5 pound hammer, 2 inches in diameter, was pulled upward and allowed to free-fall 12 inches, onto the soil (5.5 ft-lbs per blow).

The soil was compacted in three lifts, with an average thickness of 1.33 inches/lift. 25 blows were exerted per lift, which equals 25 x 5.5 = 137.5 ft-lbs. **The total input energy for the three lifts was 3 x 137.5 = 412.50 ft-lbs on a soil sample with a volume of 1/30th cubic foot. This equals 12,400 ft-lbs of compactive energy per cubic foot of soil**.

This energy simulates the field compactive effort closely and hence he settled for this. Read the enclosed document for more details on the development of this test."

ΑΡΘΡΑ

Γεφύρωση της κατολίσθησης της Τσακώνας Γεωτεχνικές προκλήσεις και διαχείριση του γεωτεχνικού κινδύνου στη διάρκεια της κατασκευής

Κων. Σεφέρογλου, Πολ. Μηχ., M.Sc.*, Φρ. Χρυσοχοϊδης Τεχν. Γεωλόγος, M.Sc.**
ΟΔΟΤΕΧΝΙΚΗ Ε.Π.Ε.

Bridging over Tsakona Landslide Geotechnical challenges and management of geotechnical risk during construction

K. Seferoglou, Dipl. Civil Engineer, M.Sc. and F. Chrysohoidis, Eng. Geologist, M.Sc.
ODOTECHNIKI LTD, Athens-Greece

Abstract

The article presents the geotechnical challenges during the construction of a 390m long bridge over an active landslide in southern Greece. The project consisted of an access bridge of about 130m long, followed by a 260m long steel arch with a suspended deck. The arch was designed to bridge over a major landslide, which was active and moved downstream at an average rate of about 1.5-2.0mm/month. The rates of movements of the landslide increased dramatically during the winter, exceeding for short periods of time, 30mm/month, following excessive rainfalls. During the construction period, it was required to use the landslide body as a foundation ground to support 16 steel piers up to 60mm high. The towers aimed at heavy lifting and final assembly at height of the steel arch parts, preassembled on the ground. At the same time, the highway traffic was deviated to pass on top of the slide's body. The fact that the slide was active and the margins of safety against failures ware very small, led to the implementation of a monitoring and instrumentation network, consisting of conventional inclinometers, piezometers and optical targets as well as fully automated inclinometric arrays, located at key depths within the sliding surface, combined with electrical piezometers and rain gauges. The automated instruments provided real time records of the movements and the piezometric levels. They continuously updated a software application (developed on Excel), which provided real time evaluation of the readings and the trends of the phenomena. The system was accessible at any time by the key engineers of the monitoring and construction team and was used to assess at any point the potential risk of the landslide. Further to the continuous evaluation of the readings, alert and alarm limits were introduced in the data logger and provided SMS messages to the engineers in charge, in an effort to take actions preventing any accidents due to potential excessive movements or slides. The preparation of the project started early 2012 and was completed on January 2016. During that period, several incidents of excessive movements were observed and special instructions were issued to the construction team. The early collected data about the mode of the landslide behavior were also used to optimize the design of the deep foundations (within the sliding mass), structured to support the assembly towers and the retaining of the temporary traffic.

1. Εισαγωγή

Η μεγάλη κατολίσθηση της Τσακώνας στον Αυτοκινητόδρομο Τρίπολης-Καλαμάτας αντιμετωπίσθηκε με την κατασκευή γέφυρας συνολικού μήκους 390m. Η συγκεκριμένη γέφυρα περιλαμβάνει στο άκρο της προς Τρίπολη, ένα τμήμα προσβασης, μήκους 130m, το οποίο οδηγεί προς το κύριο άνοιγμα (τόξο), μήκους 260m, μέσω του οποίου επιτυγχάνεται η υπέρβαση της ενεργούς μάζας της κατολίσθησης. Στην Εικόνα 1 παρουσιάζονται φωτογραφίες από την αστοχία αλλά και η τελική κατάσταση με τη γέφυρα ολοκληρωμένη. Ανάμεσα στις δυο ακραίες φάσεις οι οποίες αποτυπώνονται στις φωτογραφίες αυτές, την αρχική της καταστροφής και την τελική της υπέρβασης, μεσολάβησε η φάση της κατασκευής (2012-2016), στη διάρκεια της οποίας δύο θέματα κυριάρχησαν. Το πρώτο ήταν η διαχείριση των εξαιρετικά δυσμενών γεωτεχνικών συνθηκών και το δεύτερο η μεθοδολογία ανέγερσης της γέφυρας και κυρίως του μεταλλικού τόξου.

Εικόνα 1. Άποψη της κατολίσθησης με διαφορά 13 ετών (2003-2016)

2. Γενική περιγραφή του έργου - Γεωτεχνικές προκλήσεις

Η κατολίσθηση ήταν και συνεχίζει να είναι αποδεδειγμένα ενεργή, όπως αυτό αποτυπώνεται στις μετρήσεις των οργάνων που είχαν εγκατασταθεί στην περιοχή. Η κατασκευή του μεταλλικού τόξου σύμφωνα με τον σχεδιασμό της γέφυρας προέβλεπε τη χρήση 16 προσωρινών χαλύβδινων πύργων, ύψους μέχρι και 60m, οι οποίοι θα εδράζονταν μέσα στη μάζα της κατολίσθησης. Ταυτόχρονα και στη διάρκεια της κατασκευής, η κυκλοφορία του αυτοκινητοδρόμου θα διερχόταν μέσω προσωρινής παρακαμπτήριας οδού μέσα από το σώμα της κατολίσθησης (Εικόνα 2). Η ασφαλής και απρόσκοπτη κατασκευή της γέφυρας καθώς και η ασφαλής διέλευση της κυκλοφορίας, μέσα από μία κινηματικά ενεργή μάζα και σε συνθήκες πιθανών γεωτεχνικών αστοχιών, προκάλεσαν την απαίτηση γεωτεχνικών διερευνήσεων μελετών και συνεχούς ενόργανης γεωτεχνικής παρακολούθησης.

(*) sef@oodotechniki.gr
(**) franxgr@hotmail.com

3. Έργα υποδομής για την ανέγερση

Η εκτέλεση των εργασιών ανέγερσης περιλάμβανε την κατασκευή σημαντικών δομικών συστημάτων (έργα υποδομής), για τη συναρμολόγηση των χαλύβδινων σπονδύλων των τόξων και του καταστρώματος, την ανύψωση των επιμέρους τμημάτων και την τελική σταδιακή συναρμολόγηση (συγκόλληση) στον «αέρα» (Εικόνα 3). Συγκεκριμένα περιλαμβάνονταν, (α) 14 δίδυμοι χαλύβδινοι πύργοι βαριάς ανύψωσης (Π1Α-Π7Α και Π1Δ-Π7Δ), (β) δύο ειδικοί χαλύβδινοι πύργοι (ΜΤΑ και ΜΤΔ) με δυνατότητα να φέρουν 12000KN ο καθένας καθώς και ειδικές διατάξεις έδρασης και ρύθμισης στην κεφαλή τους (**Εικόνα 4**), (γ) 16 ανεξάρτητες θεμελιώσεις (πάσσαλοι συνδεδεμένοι με κεφαλοδέσμους) για κάθε πύργο, (δ) διαδρόμους από οπλισμένο σκυρόδεμα επί του εδάφους για την προσυναρμολόγηση των υποτμημάτων των μεταλλικών τόξων, (ε) διαδρόμους/γέφυρες σε θέσεις που το ανάγλυφο δεν επέτρεπε την ανάπτυξη χωματουργικών διαμορφώσεων, και (στ) ένα πασσαλότοιχο αντιστήριξης για τη βελτίωση της ευστάθειας του πρανούς της προσωρινής οδού διέλευσης του αυτοκινητοδρόμου. Τα παραπάνω δομικά έργα συνδυάσθηκαν με χωματουργικές διαμορφώσεις, η έκταση των οποίων σε κάθε περίπτωση όφειλε να είναι περιορισμένη ώστε να αποφεύγεται η περαιτέρω προσθήκη φορτίων στο σώμα της αστοχίας και η επιδείνωση των συνθηκών ευστάθειας. Μία γενική άποψη των απαιτούμενων έργων υποδομής δίνεται στην Εικόνα 5.

Εικόνα 2. Η προσομοίωση της ανέγερσης στη φάση μελέτης και η πραγματική κατάσταση στη φάση ανέγερσης σε σχέση με την ολισθαίνουσα μάζα

Εικόνα 3. Έργα υποδομής και εργασίες για την ανέγερση του τόξου

Εικόνα 4. Κατασκευή αντηρίδων μεσοβάθρου με τους πύργους ΜΤ (ΜΤΑ και ΜΤΔ)

Εικόνα 5. Συνολική άποψη των έργων υποδομής (λήψη προς Καλαμάτα)

4. Ιστορικό κατολίσθησης – Γεωλογικές / γεωτεχνικές συνθήκες

Η καταστροφική φάση της κατολίσθησης συνέβη τον Φεβρουάριο του 2003 μετά από περίοδο εξαιρετικών βροχοπτώσεων. Ως αποτέλεσμα, αποκόπηκε η Εθνική Οδός σε μηκος 200 m περίπου και μετατοπίστηκε οριζοντιογραφικά κατά 100m και υψομετρικά κατά 40m (κατά μέγιστο). Τα καταστροφικά αποτελέσματα του φαινομένου εκτάθηκαν 400m ανάντι και 700m κατάντι της Ε.Ο.

Η περιοχή δομείται κυρίως από φλύσχη ψαμμιτικής και ιλυολιθικής σύστασης, ενώ αμέσως ανάντι της κατολίσθησης δεσπόζει εμφάνιση ασβεστόλιθων. Τα παράγωγα των σχηματισμών αυτών, κολλούβια, κορήματα και μανδύες αποσάθρωσης, επικαλύπτουν σε σημαντικό πάχος (>30m κατά θέσεις) το βραχώδες υπόβαθρο. Η περιοχή της κατολίσθησης χαρακτηρίζεται από ένα μορφολογικό βύθισμα που αποτέλεσε τη λεκάνη αποθέσεως των εδαφικών υλικών, ενώ η επιφάνεια ολίσθησης εντοπίζεται κοντά στο όριο αυτών με τους υποκείμενους βραχώδεις σχηματισμούς.

Στο Σχήμα 1, όπου δίνεται μία ενδεικτική γεωτεχνική διατομή, παρουσιάζεται η χαρακτηριστική εικόνα του γεωλογικού – γεωτεχνικού περιβάλλοντος. Σημειώνεται το όριο του βραχώδους υποβάθρου (φλύσχης) καθώς και τα υπερκείμενα ολισθαίνοντα εδαφικά υλικά (κορήματα ποικίλης προέλευσης και σύστασης), τα οποία έρπουν πάνω στο σταθερό υπόβαθρο του φλύσχη. Επισημαίνονται ιδιαίτερα 2 στοιχεία της γεωλογίας της κατολίσθησης: (α) το κυμαινόμενο πάχος της (15-40m) και (β) οι αλλαγές της κλίσης του υποβάθρου (12^0 -30^0), η οποία τοπικά στην περιοχή κατασκευής των έργων του αριστερού κλάδου και του πασσαλότοιχου υποστήριξης Ε.Ο.) γίνεται πολύ απότομη (>40^0). Αυτή η υπόγεια μορφολογία της επαφής «εδαφικών-υποβάθρου» δημιουργούσε αφενός μεγάλη αβεβαιότητα ως προς τη μορφή της γεωτεχνικής διατομής (πάχος χαλαρών υλικών, κλπ.) κατά μήκος του έργου και αφετέρου ευνοούσε και ευνοεί την ανάπτυξη απότομων ολισθήσεων. Αυτές ακριβώς οι σημαντικές αβεβαιότητες ως προς τη συμπεριφορά της ολισθαίνουσας μάζας, σε συνδυασμό με το γεγονός ότι η κινηματική δραστηριότητα των εδαφικών μαζών στο διάστημα 2000 έως 2010 παρουσίαζε φάσεις έντασης και ύφεσης, προκάλεσαν την αναγκαιότητα καταγραφής και αξιολόγησης της εξέλιξης των μετακινήσεων. Η αποτύπωση των πραγματικών τάσεων στο διάστημα της κατασκευής της γέφυρας θεωρήθηκε ως βασικό προαπαιτούμενο για τον αποτελεσματικό γεωτεχνικό σχεδιασμό των έργων υποδομής αλλά και των έργων ανωδομής (πύργοι συναρμολόγησης).

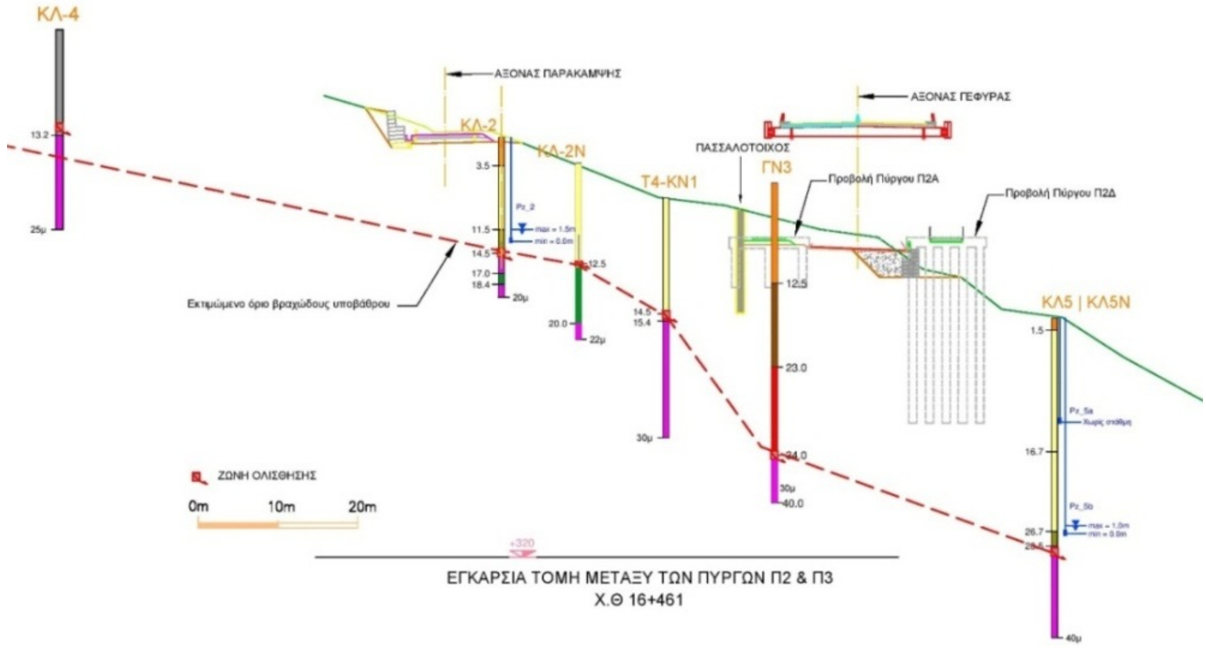

Σχήμα 1. Χαρακτηριστική γεωτεχνική τομή με τις θέσεις ερευνών και γεωτεχνικής παρακολούθησης

5. Στοχευμένες γεωτεχνικές έρευνες για τα προσωρινά έργα ανέγερσης

Προκειμένου να διερευνηθούν οι γεωτεχνικές συνθήκες με τη μέγιστη δυνατή ακρίβεια στη θέση του έργου, υλοποιήθηκε από τον ανάδοχο (αρχικά Κ/Ξ Alpine Bau-ΤΕΡΝΑ Α.Ε. και στη συνέχεια ΤΕΡΝΑ Α.Ε), υπό της οδηγίες της εταιρείας «ΟΔΟΤΕΧΝΙΚΗ Ε.Π.Ε.» (μελετητή και συμβούλου του αναδόχου κατά την κατασκευή), ένα πρόγραμμα γεωτρήσεων, διασκοπήσεων και εγκατάστασης πρόσθετων γεωτεχνικών οργάνων παρακολούθησης. Εκτελέσθηκαν δειγματοληπτικές γεωτρήσεις στη θέση καθενός από τους επτά προσωρινούς πύργους, από τις οποίες έγινε αναγνώριση των σχηματισμών και εκτίμηση της θέσης της επιφάνειας ολίσθησης σε κάθε θέση. Οι γεωτρήσεις συμπληρώθηκαν με κατακόρυφες και πλάγιες διασκοπήσεις με διατρητικό φορείο (wagon drill), όπως ενδεικτικά απεικονίζεται στο Σχήμα 2 για την περιοχή του πύργου Π6. Η εφαρμογή των διασκοπήσεων χρησίμευσε ώστε να εντοπισθεί το ανάγλυφο του υποβάθρου με σχεδόν απόλυτη ακρίβεια σε διατομή και σε κάθε πύργο. Η πληροφορία αυτή ήταν αναγκαία για το σχεδιασμό της βαθιάς θεμελίωσης των έργων υποδομής για την ανέγερση (θεμελίωση πύργων, θεμελίωση προσωρινών διαδρόμων/γεφυρών, κλπ.), καθώς και των έργων προσωρινής προστασίας της οδού παράκαμψης. Ταυτόχρονα, η αναγνώριση της μορφολογίας του υποβάθρου έδωσε και τη δυνατότητα βελτιστοποίησης των θέσεων και του βάθους των οργάνων παρακολούθησης.

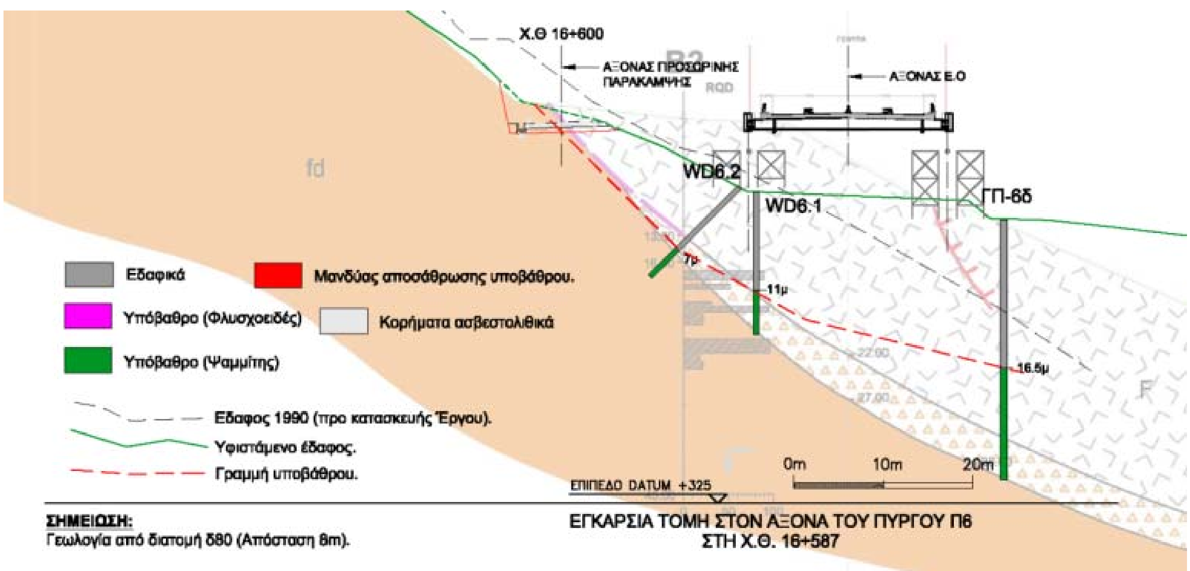

Σχήμα 2. Ερευνητικές διατρήσεις για τον εντοπισμό του υποβάθρου στην περιοχή του πύργου Π6

6. Γεωτεχνική παρακολούθηση κατά την κατασκευή

6.1. Γενικά

Η γεωτεχνική παρακολούθηση κατά τη διάρκεια της κατασκευής (συνολική διάρκεια περίπου τέσσερα χρόνια) επέβαλε την ανάπτυξη ενός συστήματος παρακολούθησης μέσω οργανομετρήσεων με αντικειμενικό σκοπό (α) τον συνεχή έλεγχο και εκτίμηση της συμπεριφοράς της κατολίσθησης ώστε να γίνονται οι αναγκαίες ρυθμίσεις ανάλογα με τις αναπόφευκτες μετακινήσεις των έργων θεμελίωσης, (β) την εκτίμηση του γεωτεχνικού κινδύνου ο οποίος αφορούσε τόσο στη ζώνη των εργασιών όσο και στην ανάντι ζώνη διέλευσης συνεχούς και σημαντικής κυκλοφορίας του αυτοκινητοδρόμου, (γ) την βελτιστοποίηση του σχεδιασμού και της κατασκευής των δομικών έργων υποδομής. Η εμπειρία από τις γεωλογικές συνθήκες στην περιοχή και ειδικότερα από την μακρόχρονη παρακολούθηση της συμπεριφοράς των ασταθών περιοχών του συγκεκριμένου έργου αλλά και στη ευρύτερη ζώνη της οδού έδειχναν την άμεση σχέση της δράσης των υδάτων στην ενεργοποίηση των αστοχιών. Η αμεσότητα αντίδρασης της ολίσθησης σε σχέση με τις βροχοπτώσεις (αποτέλεσμα μάλλον των μικρών υδρογεωλογικών λεκανών ανάντι του έργου) είναι εντυπωσιακή και καταγεγραμμένη.

Η ξαφνική αύξηση του ρυθμού μετακίνησης και κατά συνέπεια αύξησης του κινδύνου αστοχιών, ειδικά στην περίοδο των βροχοπτώσεων (Περίοδος Νοεμβρίου-Απριλίου), σε συνδυασμό με την κρισιμότητα των έργων (οδός σε κυκλοφορία, παρουσία μεγάλου αριθμού προσωπικού και βαρειών μηχανημάτων) και τις κατασκευές με αυξημένες απαιτήσεις θεμελίωσης και γεωμετρικών περιορισμών, οδήγησαν στο συμπέρασμα ότι η συνεχής εκτίμηση του γεωτεχνικού κινδύνου μέσω ενός εκτεταμένου δικτύου οργανομετρήσεων ήταν επιβεβλημένη. Κρίθηκε απαραίτητη για τον σκοπό αυτό, εκτός των συμβατικών γεωτεχνικών οργάνων, η εγκατάσταση ενός συστήματος συνεχούς αυτόματης παρακολούθησης και καταγραφής των κρίσιμων παραμέτρων της δραστηριότητας της αστοχίας, σε πραγματικό χρόνο. Αντικειμενικός σκοπός αυτής της επιλογής ήταν να υπάρχει δυνατότητα πρώιμης αναγνώρισης ενός πιθανού κατολισθητικού φαινομένου (τοπικού ή γενικευμένου), το οποίο θα έβαζε σε κίνδυνο την κυκλοφορία, τους εργαζόμενους και τα έργα. Δεν πρέπει να διαφεύγει ότι όλο το εγχείρημα (κυκλοφορία και κατασκευή) εδραζόταν προσωρινά σε μια εδαφική μάζα, η οποία, τοπικά τουλάχιστον, βρισκόταν σε συνθήκες οριακής ισορροπίας και συνεχώς «γλιστρούσε» προς τα κατάντι. Χαρακτηριστικό είναι το **Σχήμα 3** και παρουσιάζει την εξέλιξη του ρυθμού μετακίνησης (mm/month), στο διάστημα 12/2008-10/2012 με βάση τα εγκατεστημένα αρχικά, συμβατικά όργανα.

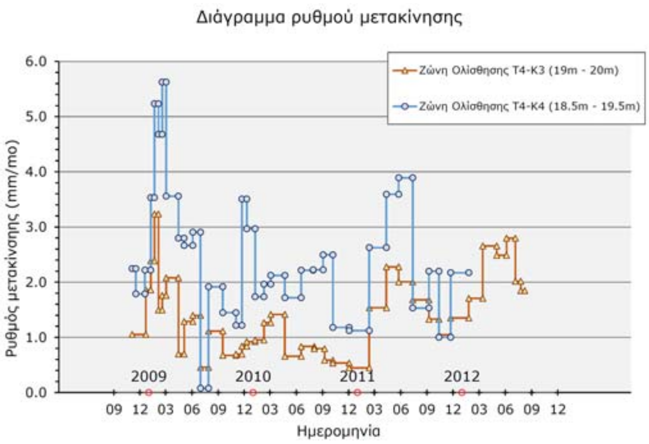

Σχήμα 3. Ρυθμοί μετακίνησης 2008-2012 (συμβατικά όργανα)

Σημειώνεται ότι την περίοδο πριν από τη μεγάλη ενεργοποίηση του 2003, οι καταγραφόμενες μετρήσεις των κλισιομέτρων στο βάθος της ολίσθησης είχαν ρυθμό εξέλιξης ~15-30mm/month, ενώ ο ρυθμός των επιφανειακών μετακινήσεων (μετρούμενες σε τοπογραφικά βάθρα) ήταν 17-63mm/month. Αν και οι ρυθμοί αυτοί ήταν 10πλάσιοι περίπου συγκρινόμενοι με τους αντίστοιχους της περιόδου 2008-2012, δίνοντας την εικόνα ήπιας κινηματικής δραστηριότητας, δεν ισχύει το ίδιο αν το χρονικό παράθυρο ελέγχου είναι μικρότερο και με συνεχείς καταγραφές. Το γεγονός δηλαδή ότι οι χειροκίνητες μετρήσεις είχαν μικρή συχνότητα (π.χ. μία φορά το μήνα) δεν επέτρεπε την καταγραφή «επιταχύνσεων» της κατολίσθησης στα μεσοδιαστήματα. Έτσι όπως φαίνεται στο δεύτερο διάγραμμα (Σχήμα 4) από τις καταγραφές του αυτοματοποιημένου συστήματος, υπάρχουν «χρονικά παράθυρα» (π.χ πρώτες ημέρες Μαρτίου 2013), μέσα στα οποία ο ρυθμός τοπικά ήταν πολλαπλάσιος του μεγέθους της περιόδου της αστοχίας (ευτυχώς μόνο για λίγες μέρες ή ώρες). Από τα παραπάνω επιβεβαιώνεται ότι τουλάχιστον τοπικά υπήρχαν χρονικά διαστήματα στα οποία ο κίνδυνος ενός κατολισθητικού φαινομένου ήταν εξαιρετικά μεγάλος.

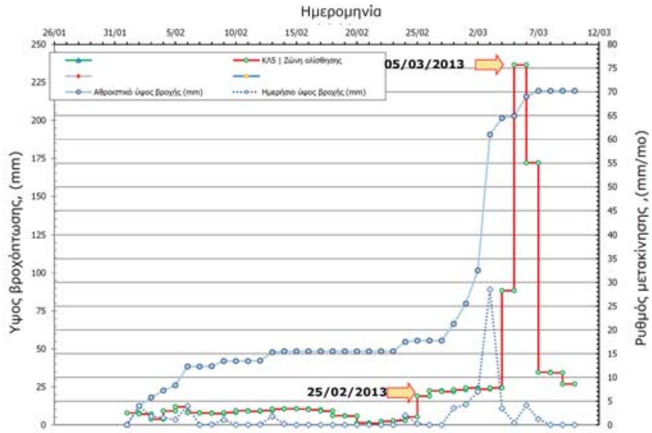

Σχήμα 4. Χαρακτηριστική καταγραφή ενός αυτοματοποιημένου οργάνου που δείχνει επεισόδιο επιτάχυνσης για λίγες μόνο μέρες (καταγραφή εντός της επιφάνειας αστοχίας)

6.2. Δίκτυο αυτόματων και συμβατικών οργάνων

Η ανάγκη για παρακολούθηση της δυναμικής της κατολίσθησης προτάθηκε και αποφασίστηκε να καλυφθεί με τη σύνθεση ενός αξιόπιστου δικτύου οργάνων, καθώς και συμβατικών και αυτοματοποιημένων μετρήσεων, τα οποία θα έδιναν τη δυνατότητα στην ομάδα παρακολούθησης (ΟΔΟΤΕΧΝΙΚΗ Ε.Π.Ε. και ΤΕΡΝΑ Α.Ε.) να εκτιμούν τους κινδύνους και να προγραμματίζουν το επίπεδο των μέτρων επαγρύπνησης ή και των μέτρων αναστολής εργασιών και κυκλοφορίας (αν αυτό ήταν αναγκαίο). Το δίκτυο των αυτοματοποιημένων οργάνων θα ικανοποιούσε ακριβώς την ανάγκη συνεχούς (real time) ενημέρωσης σχετικά με την κινηματική κατάσταση της κατολίσθησης και σχεδιάστηκε να περιλαμβάνει (Σχήμα 5):

- 4 κλισιομετρικές στήλες στις γεωτρήσεις ΚΛ2, ΚΛ3, ΚΛ4 και ΚΛ5 (και μετέπειτα μεταφέρθηκαν στις ΚΛ2Ν, ΚΛ3Ν, ΚΛ5Ν)
- 4 ηλεκτρικά πιεζόμετρα (ΠΖ-2, ΠΖ-3 και ΠΖ-5) μέτρησης της πίεσης των πόρων σε ξεχωριστές γεωτρήσεις δίπλα στις ΚΛ2, ΚΛ3 και ΚΛ5 (2τεμ.)
- ένα βροχομετρικό σταθμό

Κάθε κλισιομετρική στήλη αποτελείται από μια συνεχή «αλυσίδα» μόνιμων κλισιομέτρων (in place inclinometers) τα οποία λαμβάνουν μετρήσεις ανά καθορισμένα από τον χρήστη χρονικά διαστήματα, μαζί και τα υπόλοιπα γεωτεχνικά όργανα του αυτοματοποιημένου δικτύου μετρήσεων. Στο Σχήμα 6 απεικονίζεται (α) σχηματικά η διασύνδεση των οργάνων με την κεντρική καταγραφική μονάδα, (β) η διάταξη μιας στήλης («τρενάκι») μόνιμων κλισιομέτρων (IPI chain) εντός γεώτρησης, εξοπλισμένης με κλισιομετρικούς σωλήνες και (γ) η διάταξη εγκατάστασης 2 ηλεκτρικών πιεζομέτρων εντός γεώτρησης. Τα παραπάνω αυτόματα όργανα συνδυάσθηκαν με 7 ακόμα συμβατικά κλισιόμετρα και με συμβατικά πιεζόμετρα, καθώς και με 4 επιφανειακούς οπτικούς στόχους (3D κάτοπτρο) για την εξακρίβωση των μετακινήσεων στην επιφάνεια. Στη συνέχεια και ακολουθώντας την εξέλιξη της κατασκευής τοποθετήθηκαν 26 οπτικοί στόχοι παρακολούθησης σε χαρακτηριστικά δομικά στοιχεία των έργων υποδομής. Επίσης, χρειάσθηκε η επανατοποθέτηση κλισιομέτρου ύστερα από υπερβολική παραμόρφωση του σωλήνα, η οποία δεν επέτρεπε τη λειτουργία του. Το σύνολο των οργάνων αυτών παρείχε ολοκληρωμένη πληροφόρηση για την κινηματική κατάσταση της κατολίσθησης και τις επιπτώσεις του φαινομένου στα δομικά έργα, πάνω σε 2 κύριες γεωτεχνικές τομές.

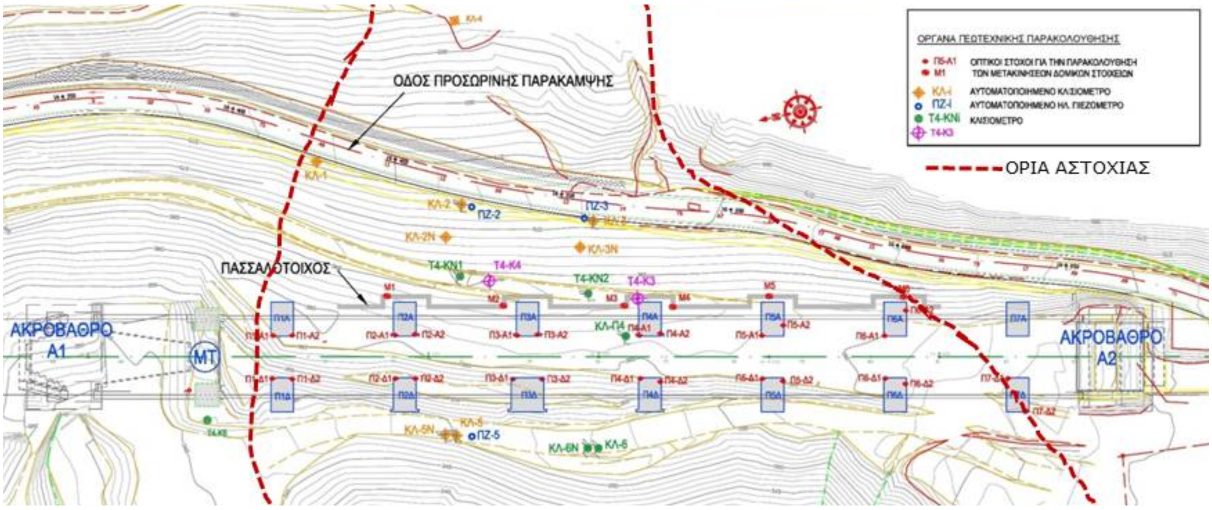

Σχήμα 5. Οριζοντιογραφία της περιοχής του Έργου όπου σημειώνονται τα προσωρινά έργα και οι θέσεις γεωτεχνικών ερευνών

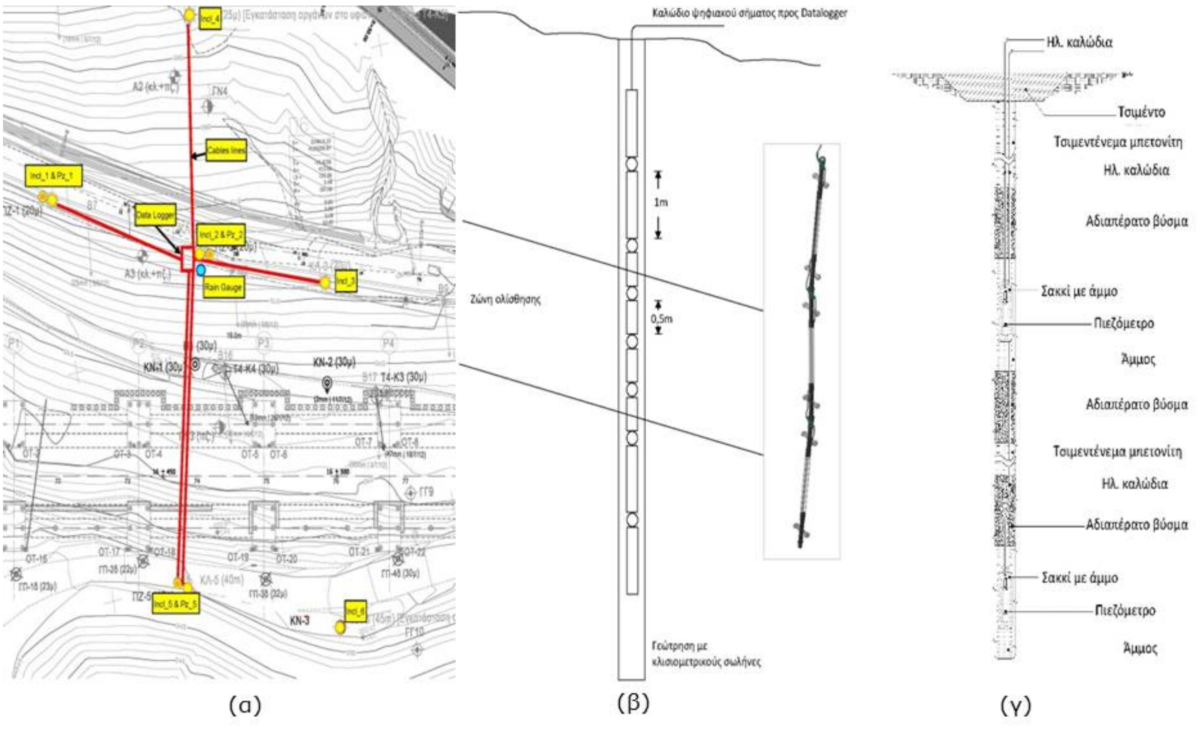

Σχήμα 6. (α) Δίκτυο οργάνων αυτοματοποιημένων μετρήσεων, (β) στήλη αυτόματων κλισιομέτρων, (γ) εγκατάσταση ηλ. πιεζόμετρου

6.3. Διαχείριση και αξιολόγηση μετρήσεων αυτοματοποιημένων οργάνων

Η επικοινωνία με το σύστημα των οργάνων (Σχήμα 7) και ο προγραμματισμός του γινόταν μέσω υπολογιστή εξοπλισμένου με GSM modem και τη χρήση ειδικού λογισμικού (Multilogger). Σε κάθε σύνδεση με την καταγραφική μονάδα γινόταν το «κατέβασμα» των πρωτογενών δεδομένων (raw data), τα οποία στη συνέχεια επεξεργάζονταν μέσω ειδικού λογισμικού (Excel spreadsheet) που αναπτύχθηκε για το σκοπό αυτό. Στόχος ήταν η μετατροπή των ανεπεξέργαστων στοιχείων σε γεωτεχνική πληροφορία (μετακίνηση, πιεζομετρική στάθμη, ύψος βροχής), αλλά και η ολοκληρωμένη παρουσίαση και αξιολόγηση των στοιχείων αυτών με τη βοήθεια πινάκων και διαγραμμάτων τα οποία συνόψιζαν, απεικόνιζαν και συσχέτιζαν όλη την συλλεγόμενη πληροφορία (Σχήμα 8). Η διαδικασία της ενημέρωσης του λογιστικού φύλλου είχε προγραμματιστεί να γίνεται αυτόματα ανά τακτά χρονικά διαστήματα, όσες φορές δηλαδή γίνεται και η λήψη μετρήσεων στα γεωτεχνικά όργανα (6-12 φορές ανά ημέρα). Το ενημερωμένο αυτό λογιστικό φύλλο ήταν προσβάσιμο από συγκεκριμένα άτομα, για κατέβασμα (download) σε σταθερό σύνδεσμο (link). Η καταγραφική μονάδα (εξοπλισμένη με GSM modem) παρείχε επιπλέον τη δυνατότητα αποστολής μηνυμάτων (SMS), κατά την υπέρβαση καθορισμένων ορίων τιμών (alarm limits), σε επιλεγμένα όργανα. Η δυνατότητα αυτή χρησιμοποιήθηκε για τα μόνιμα (αυτόματα) κλισιόμετρα (εντός των ζωνών ολίσθησης), για τα οποία καθορίζονταν ανά τακτά διαστήματα όρια τιμών μετακίνησης που πληρούσαν το 1^{ο} όριο ελέγχου.

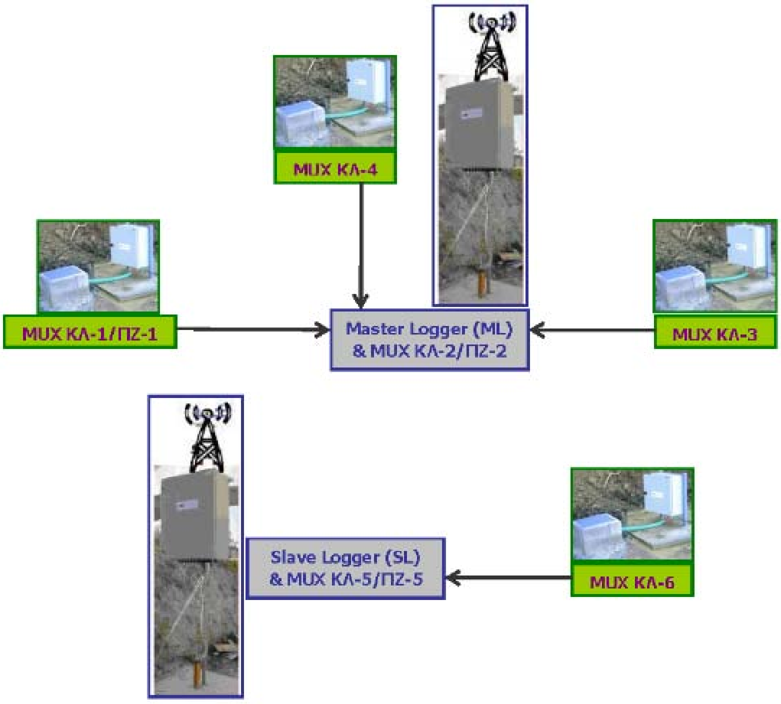

Σχήμα 7. Εικόνα από την πραγματική συνδεσμολογία

Σχήμα 8. Διάγραμμα λειτουργίας του αυτόματου δικτύου

6.4. Κριτήρια παρακολούθησης

Μετά την εγκατάσταση και την πλήρη λειτουργική αποκατάσταση του εξοπλισμού, καθώς και των αναγκαίων ρυθμίσεων, καθορίσθηκαν τα κριτήρια με βάση τα οποία θα γινόταν η αξιολόγηση του γεωτεχνικού κινδύνου. Αποφασίσθηκε ότι τα μόνα κριτήρια τα οποία μπορούσαν να αξιολογούνται άμεσα και σε πραγματικό χρόνο ήταν (α) ο ρυθμός της μετακίνησης σε σχέση με τη θεωρούμενη ως καταστροφική με βάση την εμπειρία του 2003, (β) η έκταση και θέση των παρατηρούμενων ρυθμών μετακίνησης, στην ουσία κρινόταν αν η επιτάχυνση της κινηματικής δραστηριότητας αφορούσε στο σύνολο της ζώνης του έργου ή απλά σε μια μικρή τοπική αστάθεια. Το πρώτο κριτήριο ήταν απολύτως αντικειμενικό και επιλέχθηκε ως η παράμετρος η οποία θα σχετιζόταν με την ανάπτυξη του συστήματος έγκαιρης προειδοποίησης σε πραγματικό χρόνο. Ο Πίνακας 1 παραθέτει τα όρια ελέγχου σύμφωνα με τα οποία αξιολογήθηκε η διαβάθμιση της επικινδυνότητας της κινηματικής δραστηριότητας. Το δεύτερο κριτήριο αποτελούσε αντικείμενο συστηματικής αξιολόγησης όλων των μετρήσεων καθώς και επιτόπου μακροσκοπικών παρατηρήσεων. Σημειώνεται ότι οι μακροσκοπικές παρατηρήσεις αποτελούσαν τμήμα του προγράμματος παρακολούθησης με συχνότητα τουλάχιστον μια φορά την ημέρα κατά την κρίσιμη περίοδο των έντονων ρυθμών μετακίνησης. Η προσπάθεια ήταν να εντοπίζονται βυθίσματα ή ρωγμές στο οδόστρωμα της παρακαμπτήριας οδού, επιφανειακές αναβλύσεις ύδατος στα πρανή, τοπικές αστοχίες στην επιφάνεια των πρανών, ορατές αλλαγές στις θέσεις αρμών τάφρων, κεφαλοδέσμων, δομικών στοιχείων.

Πίνακας 1. Προτεινόμενα Όρια Ελέγχου για τις μετακινήσεις των κλισιομέτρων

	Ρυθμός μετακίνησης	Χρονικό διάστημα	Αθροιστική μετακίνηση	Ενέργεια
Όριο 1	≥ 3.0mm/month	≥ 30 days	3.0mm	Αξιολόγηση δεδομένων και πύκνωση μετρήσεων συμβατικών οργάνων σε 2 ανά εβδομάδα.
Όριο 2	≥ 6.0mm/month	≥ 15 days	3.0mm	Αξιολόγηση δεδομένων και πύκνωση σε 1 ανά ημέρα, αύξηση συχνότητας λήψης δεδομένων από το αυτόματο σύστημα σε 6 την ημέρα, μακροσκοπικές παρατηρήσεις 2 φορές την ημέρα.
Όριο 3	≥ 10.0mm/month ≥ 30.0mm/month	≥ 15 days ≥ 7 days	5.0 mm 7.0 mm	Αξιολόγηση δεδομένων πύκνωση μετρήσεων ως άνω και διακοπή εργασιών στην περιοχή του τόξου, απομάκρυνση βαρειών μηχανημάτων, προετοιμασία για πιθανή διακοπή κυκλοφορίας.
Όριο 4	≥ 30.0mm/month	≥ 15 days	15.0 mm	Όπως ανωτέρω και οδηγία για κλείσιμο κυκλοφορίας.

7. Χαρακτηριστικά αποτελέσματα και γενικά συμπεράσματα από την ενόργανη παρακολούθηση κατά την κατασκευή

Ο όγκος των δεδομένων από την μακροχρόνια ενόργανη παρακολούθηση της κατολίσθησης είναι εξαιρετικά μεγάλος και απαιτεί εκτενή ανάλυση και χώρο για να παρουσιαστεί με πληρότητα, ιδιαίτερα δε για να επιχειρηθεί η αξιολόγηση και ο συσχετισμός των επιμέρους παραμέτρων που επηρεάζουν το κατολισθητικό φαινόμενο. Στη συνέχεια θα παρατεθούν κάποια βασικά στοιχεία και συμπεράσματα που δίνουν αντιπροσωπευτική εικόνα.

Α. Μέσος ρυθμός μετακίνησης – Βάθος ολίσθησης

Ο Πίνακας 2 συνοψίζει τις μετακινήσεις και τους μέσους ρυθμούς που υπολογίστηκαν σε 11 θέσεις ερευνών. Εξ αυτών προκύπτει πως ο ρυθμός μετακίνησης διαφέρει ανάλογα με τη θέση της κατολίσθησης που εξετάζεται. Αυτός κυμαίνεται από ~15-40mm/year, με μία μέση τιμή 25-30mm/year να μπορεί να θεωρηθεί αντιπροσωπευτική. Η διακύμανση αυτή εκτιμάται πως οφείλεται κυρίως στην επίδραση δύο βασικών γεωμετρικών παραμέτρων του φαινομένου: (α) του βάθους της ολίσθησης (πάχος) και (β) της κλίσης του υποβάθρου πάνω στο οποίο ολισθαίνει η εδαφική μάζα. Από την επεξεργασία των μετρήσεων προέκυψε πως αυξανομένου του βάθους και της κλίσης της επιφάνειας ολίσθησης επιδεινώνεται και η αστάθεια της εδαφικής μάζας. Ο τρόπος συσχέτισης των παραμέτρων αυτών υποστηρίζεται και από το σχετικό γράφημα (Σχήμα 9) που αφορά στο κοινό διάστημα παρακολούθησης 6 κλισιομέτρων. Μια τέτοια σχέση ήταν βέβαια αναμενόμενη μια και απλά επιβεβαιώνει ότι όσο πιο έντονη είναι η κλίση αλλά και μεγάλου πάχους η ολισθαίνουσα μάζα, τόσο αυξάνεται ο ρυθμός κίνησης. Η χρησιμότητα όμως της συγκεκριμένης συσχέτισης ήταν μεγάλη για την εκτίμηση της πιθανής μέγιστης μετακίνησης σε κάθε θέση βάθρου και της πιθανής πρόσθετης καταπόνησης πάνω στους πασσάλους θεμελίωσης. Το πρόβλημα αυτό αντιμετωπίσθηκε στο επόμενο στάδιο σχεδιασμού της θεμελίωσης.

Πίνακας 2. Σύνοψη των μετακινήσεων στα εγκατεστημένα κλισιόμετρα (2012-2016)

Κλισιόμετρο	Περίοδος Παρακολούθησης	Ζώνη Ολίσθησης	Συνολική μετακίνηση (mm)	Μέσος ρυθμός (mm/year)
Στήλες κλισιομέτρων (αυτοματοποιημένες μετρήσεις)				
ΚΛ2	01/13 - 06/14	13.5 - 15.0μ	26.4	18
ΚΛ2Ν	07/14 – 02/16	10.5 – 12.0μ	8.4	5.4
ΚΛ3	01/13 – 05/14	16.5 – 17.5μ	23.1	17
ΚΛ3Ν	09/14 – 02/16	15.0 – 17.0μ	19.1	13
ΚΛ4	01/13 – 04/14	-	-	-
ΚΛ5	01/13 – 03/14	29.5 – 31.0μ	35.6	30
ΚΛ5Ν	05/14 – 02/16	27.5 – 29.5μ	35.2	20
Συμβατικά κλισιόμετρα (χειροκίνητες μετρήσεις)				
Τ4-ΚΝ1	07/12 – 03/15	14.0 – 15.0μ	77.1	28
Τ4-ΚΝ2	06/12 – 03/15	19.0 – 19.5μ	77.5	27
ΚΛ6	10/12 – 03/14	39.5 – 40.0μ	53.4	39
ΚΛ6Ν	05/14 – 04/15	37.0 – 37.5μ	21.1	20

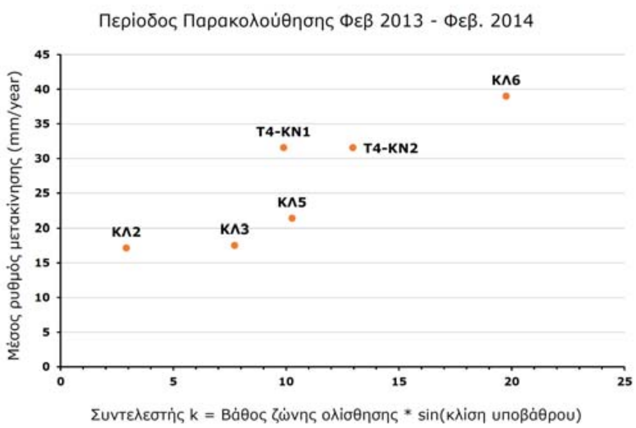

Σχήμα 9. Συσχέτιση ρυθμού μετακίνησης με βάθος ολίσθησης/κλίση υποβάθρου

Β. Μέσος ρυθμός μετακίνησης – Πιεζομετρικές στάθμες – Βροχόπτωση

Η αύξηση της κινηματικής δραστηριότητας της κατολίσθησης στη διάρκεια του χειμώνα, ειδικά στο διάστημα Ιανουάριος – Μάρτιος, ήταν αναμενόμενη και συνήθης σε κάθε περίπτωση. Η ταχύτητα απόκρισης της κατολίσθησης στην αύξηση της πιεζομετρικής στάθμης, αμέσως μετά από έντονες βροχοπτώσεις, είχε πρακτικό ενδιαφέρον κυρίως στα πλαίσια της πρόβλεψης – επαγρύπνησης και έγκαιρης προειδοποίησης. Στο **Σχήμα 10** και στο Σχήμα 11 δίνονται διαγράμματα βροχόπτωσης και στάθμης πιεζόμετρων που καλύπτουν τις περιόδους έξαρσης των βροχοπτώσεων για τα έτη 2013 και 2014, αντίστοιχα. Φαίνεται χαρακτηριστικά η συσχέτιση που έχουν οι βροχοπτώσεις, ιδιαίτερα οι μεγάλου ύψους, με την αύξηση της πιεζομετρικής στάθμης η οποία είναι εντονότερη στα πιεζόμετρα ΠΖ-2 και ΠΖ-3, δηλαδή στο σχετικά ρηχό τμήμα της κατολίσθησης (βλ. γεωτεχνική διατομή, Σχήμα 1). Παράλληλα στα Σχήματα 12-14 δίνονται διαγράμματα ρυθμού μετακίνησης για τις περιόδους 2012-2013, 2013-2014 και 2014-2015, αντίστοιχα, όπου η αύξηση του ρυθμού της κίνησης είναι σαφής και ακολουθεί τις φάσεις μεγάλων βροχοπτώσεων και άρα αύξησης της πιεζομετρικής στάθμης.

Γ. Μετακινήσεις στα δομικά στοιχεία

Ενδιαφέρον παρουσιάζουν τα αποτελέσματα της καταγραφής των επιπτώσεων της κατολίσθησης πάνω στα δομικά στοιχεία των προσωρινών έργων που εδράζονταν μέσα στην ασταθή εδαφική μάζα, με βάση την τοπογραφική παρακολούθηση οπτικών στόχων. Σε σχέση με τις επιπτώσεις στην κατασκευή, αυτά τα μεγέθη είχαν μεγαλύτερη αξία διότι συγκρίνονταν με τις προβλέψεις συνολικών μετακινήσεων στη διάρκεια της κατασκευής αλλά κυρίως με τις επιβεβλημένες διαφορικές μετακινήσεις μεταξύ βάθρων στα πλαίσια της μελέτης. Τα στοιχεία αυτά ήταν βέβαια συστηματικά διαθέσιμα στον ανάδοχο ώστε να προγραμμάτιζε διορθώσεις στους πύργους ανέγερσης αν αυτό κρίνονταν αναγκαίο.

Προκειμένου να είναι συγκρίσιμα τα μεγέθη των μετακινήσεων, τα διαγράμματα των οριζόντιων (Σχήμα 15) και κατακόρυφων (Σχήμα 16) μετατοπίσεων αφορούν στο διάστημα παρακολούθησης 03/2013-03/2014 και όχι σε όλη την διάρκεια του Έργου. Με βάση αυτά διαπιστώνονται διαφορές στις μετατοπίσεις, τόσο μεταξύ δύο διαδοχικών βάθρων του ίδιου κλάδου (π.χ. Π2Δ-Π3Δ), όσο και μεταξύ του δεξιού και αριστερού βάθρου του ίδιου Πύργου (π.χ. Π2Α-Π2Δ). Οι διαφορές αυτές αφορούν τόσο στις οριζόντιες μετακινήσεις όσο και στις κατακόρυφες (διαφορικές καθιζήσεις). Στο οριζόντιο

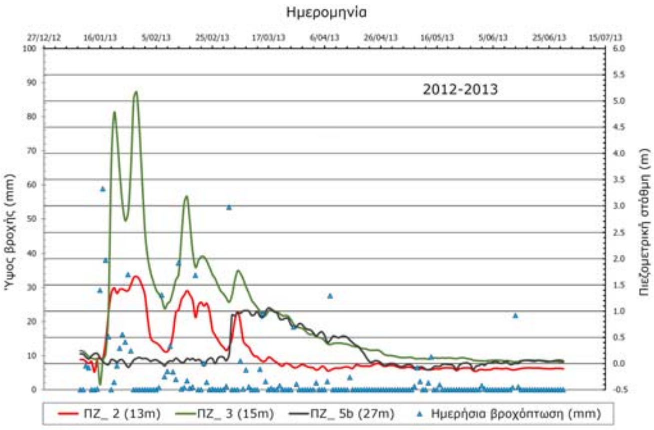

Σχήμα 10. Διαγράμματα βροχόπτωσης – στάθμης πιεζόμετρων 2013

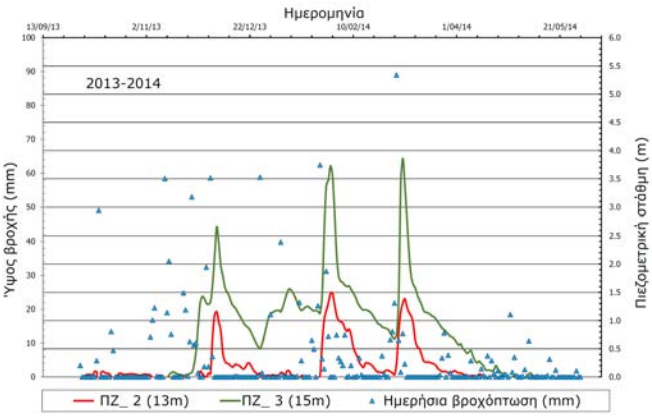

Σχήμα 11. Διαγράμματα βροχόπτωσης – στάθμης πιεζόμετρων 2014

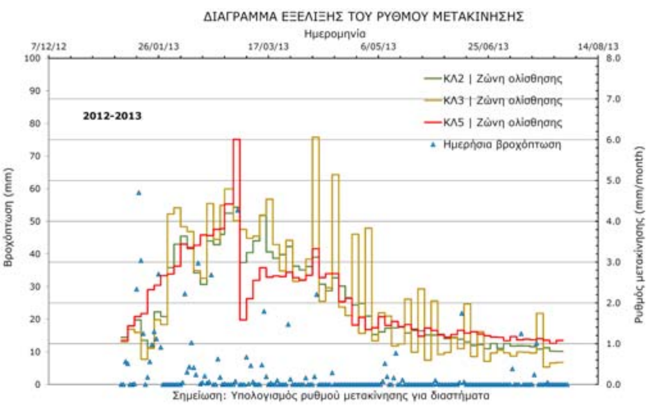

Σχήμα 12. Διακύμανση του ρυθμού μετακίνησης στα αυτόματα κλισιόμετρα (2012-2013)

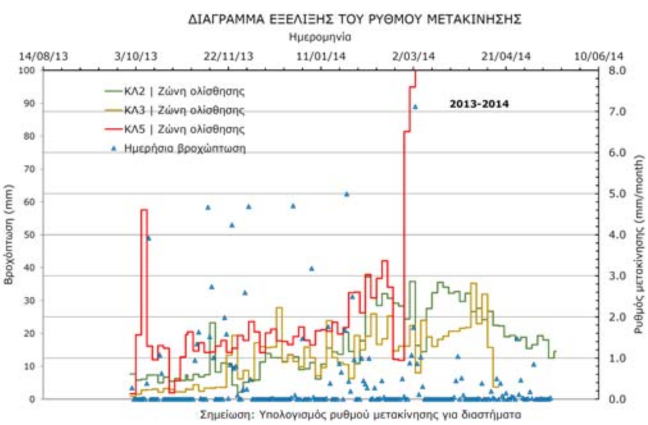

Σχήμα 13. Διακύμανση του ρυθμού μετακίνησης στα αυτόματα κλισιόμετρα (2013-2014)

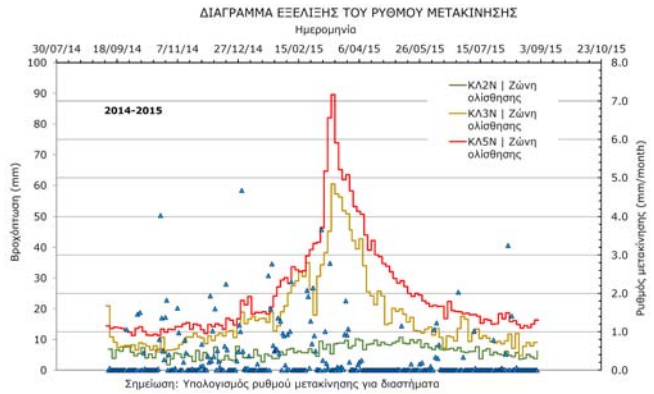

Σχήμα 14. Διακύμανση του ρυθμού μετακίνησης στα αυτόματα κλισιόμετρα (2014-2015)

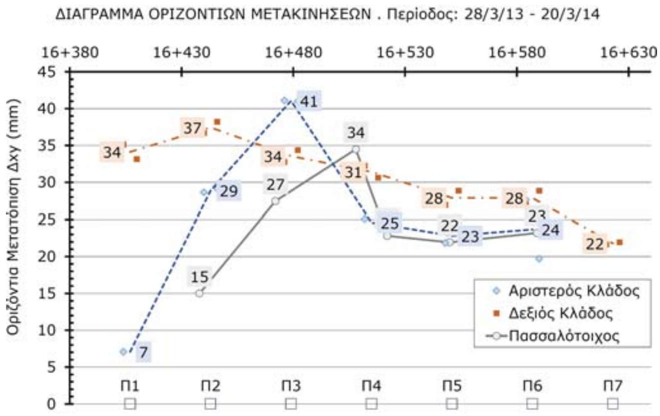

Σχήμα 15. Οριζόντιες μετατοπίσεις στα βάθρα θεμελίωσης των πύργων ανέγερσης της γέφυρας και στον Πασσαλότοιχο

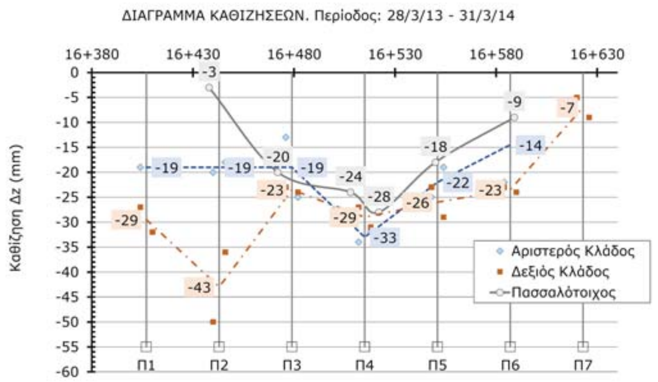

Σχήμα 16. Κατακόρυφες μετατοπίσεις στα βάθρα θεμελίωσης των πύργων ανέγερσης της γέφυρας και στον Πασσαλότοιχο

επίπεδο η μεγαλύτερη απομάκρυνση καταγράφηκε μεταξύ των βάθρων Π1Α και Π2Α (2.2,2cm), ενώ οι μεγαλύτερες διαφορικές καθιζήσεις παρατηρούνται μεταξύ των κεφαλοδέσμων Π2Δ και Π3Δ (20cm) και Π2Α-Π2Δ(2,4cm).

Τέλος, συγκρίνοντας τις επιφανειακές με τις εις βάθος μετακινήσεις οδηγούμαστε στα εξής συμπεράσματα:

(1) οι μετακινήσεις που καταγράφονται πάνω στα δομικά στοιχεία του Έργου (Πασσαλότοιχος & Κεφαλόδεσμοι Πύργων) αυξάνονται με την αύξηση του βάθους εμφάνισης του υποβάθρου, δηλαδή του πάχους της εδαφικής μάζας που ολισθαίνει στο εξεταζόμενο σημείο.

(2) το μέγεθος των επιφανειακών μετακινήσεων είναι συγκρίσιμο με αυτό της επιφάνειας ολίσθησης, όπως προκύπτει συγκρίνοντας (α) τις μετατοπίσεις του Πασσαλότοιχου (25 mm) με αυτές των κλισιομέτρων Τ4-ΚΝ1 και Τ4-ΚΝ2 (27 mm) και (β) των κεφαλοδέσμων του αριστερού κλάδου (34

mm) με αυτές των κλισιομέτρων ΚΛ5, ΚΛ6 (32mm) (**Πίνακας 3**).

(3) Τόσο η μορφή αυτής της μετακίνησης όσο και τα μεγέθη επαλήθευσαν τις εκτιμήσεις της μελέτης, στην οποία, για την προβλεπόμενη διετία ως απαραίτητο χρονικό διάστημα για την ανέγερση του τόξου, προτάθηκε ως κύρια μετακίνηση σχεδιασμού (εγκάρσια στον άξονα της γέφυρας) η τιμή των 30mm/year και για την διαμήκη διεύθυνση θεωρήθηκε συνολική σχετική μετακίνηση μεταξύ προσωρινών βάθρων 15 mm/year

Πίνακας 3. Σύγκριση επιφανειακών και σε βάθος μετακινήσεων (28/03/13÷7/03/14)

Θέση καταγραφής μετακίνησης	Βάθος ολίσθησης	Μέση συνολική μετακίνηση
Ζώνες ολίσθησης Τ4-ΚΝ1 και Τ4-ΚΝ2	15-20μ	27mm
Οπτικοί Στόχοι Πασσαλότοιχου Μ2, Μ3, Μ4	18-22μ	25mm
Οπτικοί στόχοι κεφαλοδέσμων Π2Δ, Π3Δ, Π4Δ	18-20μ	29mm
Οπτικοί στόχοι κεφαλοδέσμων Π2Α, Π3Α, Π4Α	30-34μ	34 mm
Ζώνες ολίσθησης ΚΛ5 και ΚΛ6	35-40μ	32mm

8. Σύνοψη

Στο άρθρο αυτό περιγράφηκε η μοναδική εμπειρία της λεπτομερούς γεωτεχνικής παρακολούθησης και καταγραφής της συμπεριφοράς της ευρύτατης ενεργού κατολίσθησης της Τσακώνας και της συνεχούς αξιολόγησης των γεωτεχνικών μετρήσεων. Η αξιολόγηση αυτή χρησιμοποιήθηκε ως εργαλείο εκτίμησης του γεωτεχνικού κινδύνου και των επιπτώσεων στα προσωρινά έργα ανέγερσης της τοξωτής γέφυρας της Τσακώνας και κυρίως στη διερχόμενη παρακαμπτήρια οδό τους αυτοκινητόδρομου. Εξίσου χρήσιμη ήταν η ορθολογική αντίληψη της συμπεριφοράς της κατολίσθησης στον γεωτεχνικό και δομοστατικό σχεδιασμό των έργων υποδομής.

9. Ευχαριστίες

Η «περιπέτεια» της γεωτεχνικής και δομοστατικής υποστήριξης του αναδόχου στη φάση κατασκευής του έργου και η ανταπόκριση στην πρόκληση της θεμελίωσης σημαντικών έργων αλλά και της προσωρινής έδρασης της Εθνικής Οδού, στο σώμα μιας ευρύτατης ενεργού κατολίσθησης, ήταν έργο ομαδικής εργασίας των στελεχών της εταιρείας «ΟΔΟΤΕΧΝΙΚΗ Ε.Π.Ε.». Συγκεκριμένα εργάσθηκαν, οι Κ. Σεφέρογλου, Πολ. Μηχ., Φ. Χρυσοχοΐδης, Τεχν. Γεωλόγος, Ι. Βασιλοπούλου, Δρ. Πολ. Μηχ., Γ. Προυντζόπουλος, Δρ. Πολ. Μηχ., Π. Φορτσάκης, Δρ. Πολ. Μηχ., Κ. Νίκας, Πολ. Μηχ., Γ. Σκάρπα, Τεχν. Μηχ. και Κ. Σταμούλη, Σχεδιάστρια. Η ομάδα στηρίχθηκε αποτελεσματικά από τα στελέχη του αναδόχου (Κ/Ξ ALPINE BAU-ΤΕΡΝΑ Α.Ε. και στη συνέχεια ΤΕΡΝΑ Α.Ε.), όπως επίσης και από στελέχη του Υπουργείου Υποδομών.

10. Βιβλιογραφία

1 ΓΕΦΥΡΑ Τ4 - ΓΕΩΤΕΧΝΙΚΕΣ ΕΚΘΕΣΕΙΣ ΕΝΟΡΓΑΝΗΣ ΠΑΡΑΚΟΛΟΥΘΗΣΗΣ, ΠΑΡΟΥΣΙΑΣΗ ΚΑΙ ΑΞΙΟΛΟΓΗΣΗ ΜΕΤΡΗΣΕΩΝ ΣΥΣΤΗΜΑΤΟΣ (No1-No18) για το έργο: «ΕΡΓΑΣΙΕΣ ΑΠΟΚΑΤΑΣΤΑΣΗΣ ΠΡΟΒΛΗΜΑΤΙΚΩΝ ΤΜΗΜΑΤΩΝ ΤΗΣ Ε.Ο. ΤΡΙΠΟΛΗΣ - ΚΑΛΑΜΑΤΑΣ ΣΤΟ ΤΜΗΜΑ ΠΑΡΑΔΕΙΣΙΑ – ΤΣΑΚΩΝΑ», ΟΔΟΤΕΧΝΙΚΗ Ε.Π.Ε., 2012-2015.

2 ΓΕΦΥΡΑ Τ4 - ΓΕΩΤΕΧΝΙΚΗ ΚΑΙ ΣΤΑΤΙΚΗ ΜΕΛΕΤΗ ΘΕΜΕΛΙΩΣΗΣ ΠΥΡΓΩΝ για το έργο: «ΕΡΓΑΣΙΕΣ ΑΠΟΚΑΤΑΣΤΑΣΗΣ ΠΡΟΒΛΗΜΑΤΙΚΩΝ ΤΜΗΜΑΤΩΝ ΤΗΣ Ε.Ο. ΤΡΙΠΟΛΗΣ - ΚΑΛΑΜΑΤΑΣ ΣΤΟ ΤΜΗΜΑ ΠΑΡΑΔΕΙΣΙΑ – ΤΣΑΚΩΝΑ», ΟΔΟΤΕΧΝΙΚΗ Ε.Π.Ε., 2012.

3 ΓΕΦΥΡΑ Τ4 - ΓΕΩΤΕΧΝΙΚΗ ΜΕΛΕΤΗ ΠΡΟΣΩΡΙΝΗΣ ΠΑΡΑΚΑΜΨΗΣ Ε.Ο. για το έργο: «ΕΡΓΑΣΙΕΣ ΑΠΟΚΑΤΑΣΤΑΣΗΣ ΠΡΟΒΛΗΜΑΤΙΚΩΝ ΤΜΗΜΑΤΩΝ ΤΗΣ Ε.Ο. ΤΡΙΠΟΛΗΣ - ΚΑΛΑΜΑΤΑΣ ΣΤΟ ΤΜΗΜΑ ΠΑΡΑΔΕΙΣΙΑ – ΤΣΑΚΩΝΑ», ΟΔΟΤΕΧΝΙΚΗ Ε.Π.Ε., 2012.

4 ΓΕΦΥΡΑ Τ4 - ΓΕΩΤΕΧΝΙΚΗ ΜΕΛΕΤΗ - ΑΥΤΟΜΑΤΟΠΟΙΗΜΕΝΟ ΣΥΣΤΗΜΑ ΓΙΑ ΤΗΝ ΠΑΡΑΚΟΛΟΥΘΗΣΗ ΤΗΣ ΚΑΤΟΛΙΣΘΗΣΗΣ ΚΑΙ ΤΗΝ ΕΓΚΑΙΡΗ ΠΡΟΕΙΔΟΠΟΙΗΣΗ για το έργο: «ΕΡΓΑΣΙΕΣ ΑΠΟΚΑΤΑΣΤΑΣΗΣ ΠΡΟΒΛΗΜΑΤΙΚΩΝ ΤΜΗΜΑΤΩΝ ΤΗΣ Ε.Ο. ΤΡΙΠΟΛΗΣ - ΚΑΛΑΜΑΤΑΣ ΣΤΟ ΤΜΗΜΑ ΠΑΡΑΔΕΙΣΙΑ – ΤΣΑΚΩΝΑ», ΟΔΟΤΕΧΝΙΚΗ Ε.Π.Ε., 2012.

5 ΟΡΙΣΤΙΚΗ ΓΕΩΤΕΧΝΙΚΗ ΜΕΛΕΤΗ ΤΕΧΝΙΚΟΥ Τ4, ΘΕΜΕΛΙΩΣΗ ΓΕΦΥΡΑΣ για το έργο: «ΕΡΓΑΣΙΕΣ ΑΠΟΚΑΤΑΣΤΑΣΗΣ ΠΡΟΒΛΗΜΑΤΙΚΩΝ ΤΜΗΜΑΤΩΝ ΤΗΣ Ε.Ο. ΤΡΙΠΟΛΗΣ - ΚΑΛΑΜΑΤΑΣ ΣΤΟ ΤΜΗΜΑ ΠΑΡΑΔΕΙΣΙΑ – ΤΣΑΚΩΝΑ», ΕΔΑΦΟΣ Α.Ε., 2008.

6. ΟΡΙΣΤΙΚΗ ΜΕΛΕΤΗ ΓΕΦΥΡΑΣ Τ4 για το έργο: «ΕΡΓΑΣΙΕΣ ΑΠΟΚΑΤΑΣΤΑΣΗΣ ΠΡΟΒΛΗΜΑΤΙΚΩΝ ΤΜΗΜΑΤΩΝ ΤΗΣ Ε.Ο. ΤΡΙΠΟΛΗΣ - ΚΑΛΑΜΑΤΑΣ ΣΤΟ ΤΜΗΜΑ ΠΑΡΑΔΕΙΣΙΑ – ΤΣΑΚΩΝΑ», ΔΟΜΗ Α.Ε., 2008.

XVI European Conference on Soil Mechanics and Geotechnical Engineering, Edinburgh, 13-17 September 2015

Παρουσίαση άρθρων, στην συγγραφή των οποίων μετείχαν Έλληνες (κατ' αλφαβητική σειρά, στα ελληνικά, του ονόματος του πρώτου συγγραφέα).

Seismic demand of coupled soil-foundation-pier systems

Demande sismique des systèmes sol-fondation-piliers

A. Karatzetzou and D. Pitilakis

ABSTRACT The scope of the present study is to investigate and demonstrate the effects of soil-foundation-structure interaction on seismic demand of bridge piers ideally founded on ground surface. For the studied soil-foundation-pier systems (SFPS) we choose various geometric and dynamic characteristics in order to cover a wide range of systems. Ten judiciously-chosen earthquake records are used to excite the SFPS and dynamic response at foundation level is calculated directly. The results clearly show modification of the response at foundation level with respect to the free-field. Soil conditions and structure's stiffness are found to play the most significant role in modifying the acceleration at the foundation level. We demonstrate that effective foundation motion (foundation level motion) is an appropriate index describing soil-foundation-structure interaction effects on seismic demand of structures. Effective foundation motion includes both kinematic and inertial components of the interaction. This effective foundation motion is directly comparable to actual recordings. We compare our results from parametric analyses with strong motion recordings from the vast database of European project SHARE, and we conclude that they are in accordance with findings published in the very few recent studies that attest both amplification and de-amplification in recorded strong motion at foundation level from the free-field, because of soil-foundation-structure interaction.

1 INTRODUCTION

In current engineering practice, ground motion recorded at free-field conditions is commonly assumed when evaluating seismic demand of a structure. The term "free-field motion" (FFM) implies that ground response to seismic excitation is not affected by the presence and oscillation of nearby structures. Naturally, response at foundation level to an earthquake event deviates from the free-field motion because of soil-foundation-structure interaction (SFSI) (Gazetas, 1983)

FEMA440 (Federal Emergency Management Agency, 2005), one of the few design guidelines accounting for SFSI, adopts a two-step procedure in estimating foundation motion. First, kinematic interaction effects are incorporated assuming that the structure and foundation are massless, producing the so-called foundation input motion (FIM). Next, inertial interaction effects are added to FIM, introducing damping at foundation level because of base shear and moment originating from the oscillating structure. The foundation motion including both kinematic and inertial effects will be called herein effective foundation motion (EFM). Therefore, the response at foundation level recorded during an earthquake event is EFM (and obviously neither FFM nor FIM).

Due to lack of well correlated strong motion recordings between free-field and foundation, relatively few studies provide insight in the deviation of EFM from FFM. Boore et al. (1980) showed that ground motions at the base of the buildings decrease with increasing building height. More recently, Fraino et al. (2012) studied the SFSI effects on instrumented bridges, and demonstrated clearly that foundation motion is not always de-amplified from FFM, while Pitilakis et al. (2013) argued that EFM deviates from FFM not only due to soil-foundation-structure interaction, but because of nonlinear soil behavior as well.

The principal objective of this paper is to elucidate the deviation of EFM from FFM because of SFSI, for the simplest case of linear structures on shallow foundations. Foundation motion deviates from the free-field because of the combined effect of both inertial and kinematic interaction. We compare our results with actual records from a large database compiled in the framework of European project Seismic Hazard Harmonization in Europe" (SHARE) (Yenier et al. 2010). Strong motion recordings validate our finding that actual foundation motion might as well increase from free-field due to soil-foundation-structure interaction.

2 MODEL CONFIGURATION

A single-degree-of-freedom structure (SDOF) is used for simplicity, the degree of freedom being the horizontal displacement of the structural mass, m_s. The SDOF structure is characterized by its stiffness k_s, its damping c_s and its height h. The structure is founded on a rigid surface foundation of width equal to *2B* resting on the soil surface. Details on the system properties are given in Table 1.

Table 1. Characteristics of the two distinct soil-foundation-structure systems at hand.

h(m)	2B (m)	m_s (Mg)	V_s (m/s)
5	10	100	100
		200	200
10	10	400	300
		800	400

Soil and structural properties are judiciously chosen, such as to represent a large variety of actual soil-foundation-structure systems. Material and geometrical properties of the systems vary based on the governing parameters of soil-foundation-structure interaction problems, notably the relative structure-to-soil stiffness ratio $1/\sigma$ ($=f_0*h/V_s$, where f_0= resonant frequency of fixed-base structure, h=distance from the base to the centroid of inertia force and V_s=shear wave velocity of soil), and the slenderness h/B (B=half-width of foundation) of the structure (Veletsos and Meek, 1974).

Material properties of the structure are kept constant (modulus of elasticity E=32GPa, corresponding to concrete type C30/37), while the fictitious circular cross-section diameter d of the pier ranges from 0.6m to 3.0m. The structure's height is 5m and 10m, so as to cover typical bridge piers that could potentially be founded on shallow footings. The footing is 10m wide. The mass of superstructure *ms* is 100Mg, 200Mg, 400Mg and 800Mg, standing for the concentrated mass of the two adjacent half spans of the bridge deck and half of the pier. Therefore, relative stiffness $1/\sigma$ varies between 0.01 and 0.98 and slenderness h/B between, 1 and 2. Slenderness ratio values h/B were selected after conducting some preliminary dynamic analyses of soil-foundation-structure systems, and after evaluating the bearing capacity of the soil below the selected footings. From these analyses we concluded that low-slenderness structures are mainly affected by interaction effects, whereas evaluation of the soil bearing capacity revealed that it was impossible to choose a realistic surface foundation for slenderness values larger than 2.

From all configurations, we did not retain the ones that gave very low, non-realistic values for fixed base period T_{fix} (lower than 0.1s), as well as the combinations where safety factor for bearing capacity under earthquake loading, according to Eurocode 8 (CE de Normalisation, 1998), was lower than unity.

All selected earthquakes for the analyses were recorded on rock or very stiff sites with $V_{s,30}$ larger than 600m/s. No scaling was applied, whereas a Butterworth band-pass filter with corner frequencies 0.25Hz and 25Hz was used. The selected records have peak acceleration amplitude varying form 1.03m/s^2 to 4.14m/s^2. Details on the earthquake records are given in Table 2, while corresponding time histories and corresponding elastic response spectra are plotted in Figure 1.

Table 2. Earthquake records used in the parametric analyses.

No	Location	Station	R (km)	M_w
1	Friuli/Italy	ITACA_16	21.70	6.4
2	Loma Prieta/USA	NGA_765	28.64	6.93
3	Northridge/USA	NGA_1011	18.99	6.69
4	Northridge/USA	NGA_994	25.42	6.69
5	Northridge/USA	NGA_1078	14.66	6.69
6	Kozani/Greece	ISESD_1210	16.00	5.3
7	Izmit/Turkey	T-NSMP_1105	42.77	7.6
8	Izmit/Turkey	T-NSMP_1109	3.40	7.6
9	Kyushu/Japan	C&F_442	36.00	6.6
10	L Aquila/Italy	ITACA_974	15.10	5.6

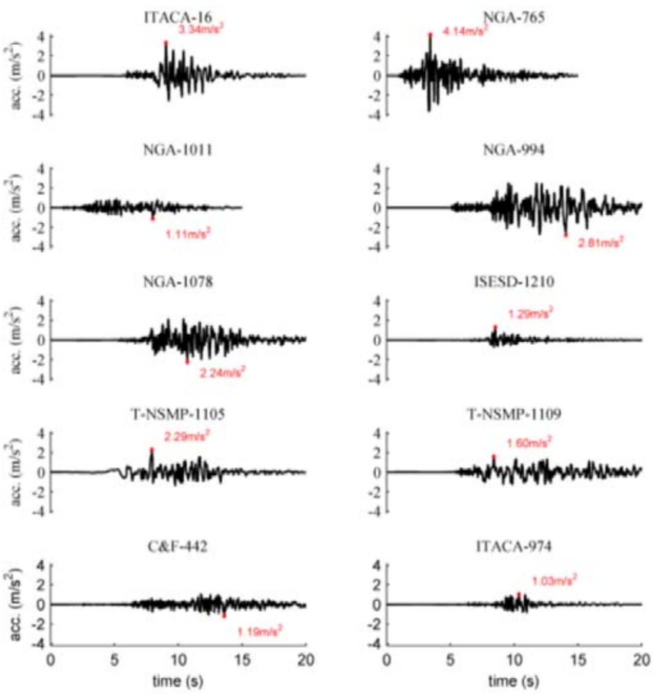

Figure 1. Acceleration-time histories of the utilized earthquakes.

3 NUMERICAL ANALYSES RESULTS

Two-dimensional plane strain analyses are performed in time domain with Opensees software (PEER, 2008) to determine response at foundation level and at free-field conditions. In our finite element model, the soil is simulated by 4 node linear elastic elements. Elastic bedrock is simulated using Lysmer-Kuhlemeyer (1969) dashpots at the base of the soil profile. The rigid foundation is simulated by 4 node linear elastic elements. The structure is simulated by linear elastic beam elements.

In Figure 2, peak ground acceleration at free-field $a_{FFM,max}$ is compared with the peak acceleration calculated at the foundation, notably $a_{EFM,max}$. Each point in the plot refers to a single analysis of the specific structure, for different mass, soil properties and earthquake input at bedrock. Deviation from the 1:1 line suggests modification of the EFM from FFM due to soil-foundation-structure interaction, including both inertial and kinematic effects.

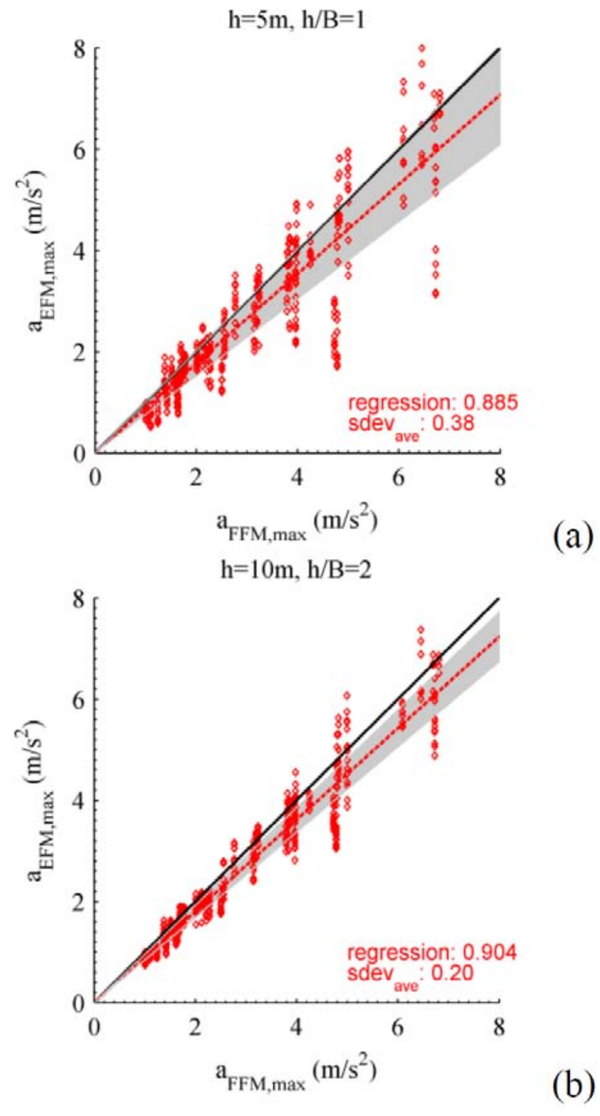

Figure 2. Variation of ratio of maximum acceleration of EFM to FFM ($a_{EFM,max}$ / $a_{FFM,max}$) with respect to the ratio of the predominant earthquake record period T_p to the resonant period of the soil-foundation-structure system, for structures (a) with slenderness h/B=1 and for height h=5m and (b) with slenderness h/B=2 and for height h=10.

For relatively squatty structures (h/B=1), the linear regression line of maximum EFM values for all acceleration levels deviates from $a_{FFM,max}$ at free-field conditions (1:1 radial line). The slope of the regression line of EFM values is 0.885 for the model of height h=5m, as seen in Table 3. This corresponds to 11% decrease on average from $a_{FFM,max}$. The average SD, sd_{ave}, is 0 0.38, for h= 5. Table 3 presents the linear regression line of the moving SD.

For more slender structures with h/B ratio equal to 2 (Figure 2b), EFM peak acceleration is as low as 90% of the free-field motion on average (Table 3), for structures with height h=10m, due to soil-foundation compliance. Moreover, in slender structures scatter is significantly lower than for squatty structures, while for the majority of structures EFM de-amplifies from FFM. This implies that, besides kinematic effects that mostly reduce acceleration demand of the structure, as witnessed in actual strong motion recordings by Kim and Stewart (2003), inertial effects - more important for taller and more slender structures - add up to that modification from freefield.

Table 3. Average values and standard deviation of $a_{EFM,max}$ with respect to $a_{FFM,max}$.

$a_{EFM,max}$ / $a_{FFM,max}$	h=5m, h/B=1	h=10m, h/B=2
average	0.885	0.904
average+stdev (reg)	1.008	0.965
average-stdev (reg)	0.762	0.843
stdevave	0.38	0.20

Figures 3 demonstrates the variation of $a_{EFM,max}$ /$a_{FFM,max}$ with T_p /T_{SFSI}, for squatty and more slender structures, highlighting the important effect of the predominant period of the strong motion on the response. Evidently, for T_p /T_{SFSI} less than 1, acceleration motion at foundation is less than at free-field for most systems and especially for slender structures (*h/B*=2). More specifically, for *h/B*=1, EFM is lower than FFM in 70% of cases (for *h*=5m), while for *h/B*=2 in 87% of cases (for heights *h*=10m). We could note that these rates (especially for *h/B*=2) are in accordance with design codes that consider the beneficial effect of soil-foundation-structure interaction. Maximum reduction of EFM with respect to FFM can be up to 65% for squatty structures and up to 40% for more slender structures.

On the other hand, for T_p /T_{SFSI} less than 1, there exists an important 35% of case studies for squatty and 10% for more slender structures, which reveals that EFM increases, and interaction can be detrimental for the structure, as described in Pandey et al., (2012). This increase of acceleration demand in some cases might reach 50% of free-field motion. Moreover, it is apparent that if T_p is in the region where inertial interaction effects are concentrated, around T_{SFSI}, EFM amplifies with respect to FFM for all structures (Figures 3). In this period range (T_p /T_{SFSI} ≈1), SFSI is potentially damaging to the structure.

Finally, for predominant record period T_p larger than the system period T_{SFSI} (T_p /$_{TSFSI}$ >1), in more than 95% of the cases (Figures 3) interaction seems to either increase acceleration at foundation level, or does not affect it at all ($a_{EFM,max}$ / $a_{FFM,max}$ ≈1).

4 RECORDS FROM SHARE DATABASE

In the framework of the European research project "Seismic Hazard Harmonization in Europe" (SHARE) (Yenier et al. 2010) a large database of ground motion records from actual earthquakes has been compiled. We used records from this database to attempt a validation of the main conclusions of above-mentioned parametric analyses, and more specifically on the deviation of effective foundation motion with respect to the free-field because of soil-foundation-structure interaction.

In the present study, we used version v3.1 (March 2010) of the database, which was also used in recent studies (Pitilakis et al. 2012). It consists of 13500 records from 4711 different earthquakes, covering a vast range of earthquake magnitudes (2.8≤Mw≤7.9), epicentral distances (0.46 km≤R≤561 km), soil profiles where the motion was recorded (100 m/s≤V_s≤2400 m/s) and peak ground acceleration values (0.15 cm/s^2≤PGA≤1745 cm/s^2). In case the recording instrument is within a structure, information exists on the number of stories and the floor where the recording device is placed. No specific information is provided on the exact location of the sensors (i.e. centroid/corner of floor plan), or on the type of foundation. Based on the available information, we isolated pairs of recordings at the ground floor of structures and at free-field conditions that matched the following criteria: each pair had to be recorded (a) at almost same soil conditions (same soil type and shear wave velocity *Vs* different up to 5%) and (b) at approximately same distance from source *R* (relative difference of distance from source *ΔR*≤1km).

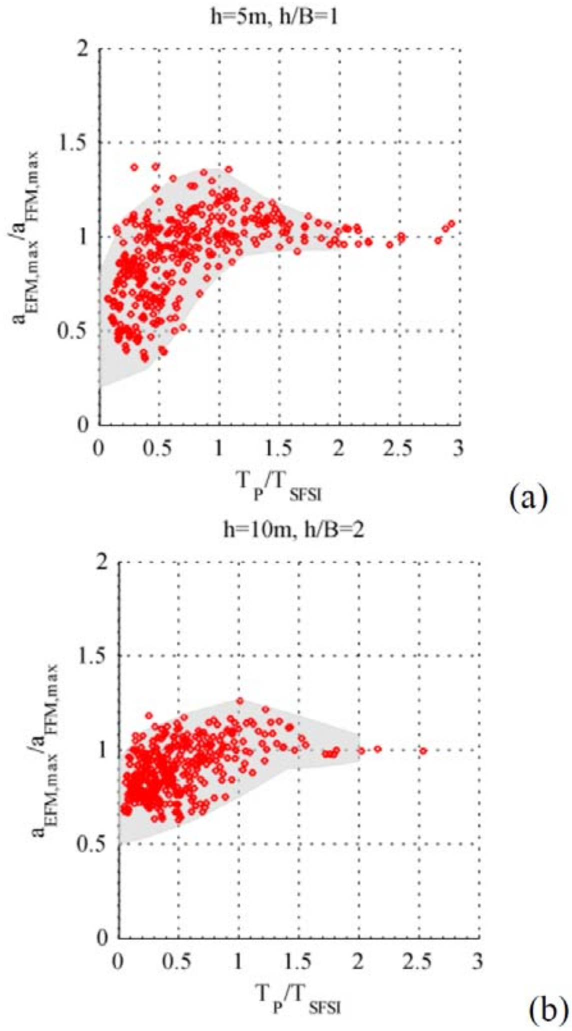

Figure 3. Variation of ratio of maximum acceleration of EFM to FFM ($a_{EFM,max}$ / $a_{FFM,max}$) with respect to the ratio of the predominant earthquake record period T_p to the resonant period of the soil-foundation-structure system, for structures (a) with slenderness *h/B*=1 and for height *h*=5m and (b) with slenderness *h/B*=2 and for height *h*=10m.

Figure 4 shows the peak acceleration values at free-field and at foundation level, from numerical investigation and from the actual recordings. Direct comparison is made only for relatively short structures (*h/B*=1), as our database contains recordings at one-floor buildings. Even though results from numerical analyses cover significant range of peak acceleration values, a mere 17% of the actual recordings fall out of the envelope of the numerical approach.

Nevertheless, significant discrepancies of the order of 50-100% are noted from the average. Such scatter in actual recordings suggests that linear regression for recorded acceleration demand might be out of context, while it is not clear for which cases EFM is amplified or de-amplified from FFM. This deviation from free-field depends on soil conditions, earthquake dynamic characteristics and distance from source. In any case, Figure 4 clearly demonstrates that acceleration at foundation level is certainly not equal to acceleration at free-field, because of both inertial and kinematic interaction.

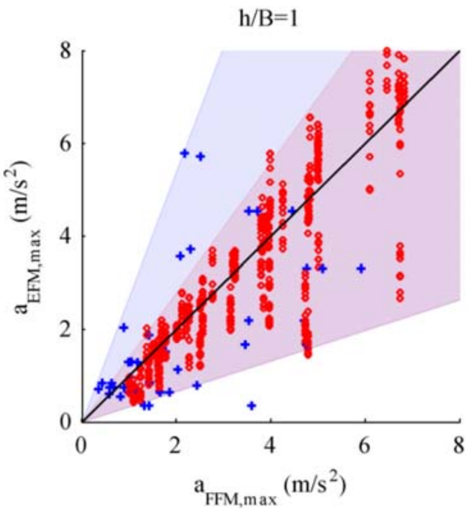

Figure 4. Variation of acceleration demand at free-field $a_{FFM,max}$ and at ground floor (or foundation) $a_{EFM,max}$ between the numerical (red circles) and the recorded (blue crosses) response, for squatty structures (*h/B*=1).

5 CONCLUSIONS

Modification of effective foundation motion from the free-field due to soil-structure interaction results from the combined action of inertial and kinematic interaction. The so-called effective foundation motion includes both aforementioned effects. In literature, inertial interaction tends to be considered detrimental (increasing foundation motion) and kinematic interaction beneficial (decreasing foundation motion) for the structure, with kinematic influence prevailing at foundation level. From the extensive parametric analyses of soil-foundation-structure systems, we concluded that in general effective foundation motion decreases from free-field by 10%-15% for all structures. Deviation from free-field response is, however, significant, especially for squatty structures. In our results, significant discrepancy between foundation and free-field motion is attested for short structures founded on soft soil and excited by either strong or long-pulse earthquake records. Reduction of foundation motion is more significant for squatty structures than for slender ones, due to increased foundation damping.

On the other hand, we observed that foundation motion might as well increase from free-field depending on the dynamic characteristics of the system. This behavior is more pronounced for short squatty structures. This observation is in contrast with recent design guidelines that account for beneficial effect of interaction. More specifically, in our analyses of typical systems there is a non-negligible 30% of squatty and a 15% of the more slender structures, where acceleration demand at foundation increases from freefield. When the predominant period of the pulse coincides with the predominant period of the soil-foundation-structure system, resonance might amplify foundation motion by as much as 50%, depending on the system and earthquake characteristics. Around this resonant period, foundation motion increased in more than 90% of cases.

Finally, comparison between numerical and recorded response at foundation and free-field clearly demonstrates that interaction modifies the recorded response at foundation from free-field. However, it is not clear from strong motion recordings whether interaction will amplify or de-amplify response at foundation level, contrary to current state of practice that, in general, accepts de-amplification of response. Given the continuous improvement of modern earthquake record arrays and databases, more coherent and well-correlated data will provide better insight in the deviation of foundation motion from free-field, towards the improvement of seismic design guidelines.

ACKNOWLEDGEMENT

Part of this work was performed in the framework of the European project "Performance-based approach to earthquake protection of cultural heritage in European and Mediterranean countries (PERPETUATE)", Grant agreement 244229, as well as in the framework of the European project "Seismic engineering research infrastructures for European synergies (SERIES)", Grant agreement 227887. We would like to thank Evi Riga for helping us with the SHARE database, and Konstantina Dastiridou for performing some of the parametric analyses.

REFERENCES

Boore DM, Joyner WB, Oliver AA and Page RA. 1980. Peak acceleration, velocity, and displacement from strong-motion records *Bulletin of Seismological Society of America*, **70(1)**, 305-321.

CE de Normalisation, 1998. Eurocode 8 – Design of Structures for earthquake resistance–Part 1: General rules, seismic actions and rules for buildings.

Federal Emergency Management Agency (FEMA) Report FEMA 440 2005. *Improvement of nonlinear static seismic analysis procedures*, Washington, DC.

Fraino M, Ventura CE, Liam Finn WD and Taiebat M. 2012. Seismic Soil-Structure Interaction Effects in Instrumented Bridges *Proceedings of 15th World Conference on Earthquake Engineering.* Lisbon 24-28 September, paper 5307.

Gazetas, G. 1983. Analysis of machine foundation vibrations: State of the art. *Soil Dynamics and Earthquake Engineering*, **2(1)**, 2–42.

Kim S and Stewart JP. 2003. Kinematic soil-structure interaction from strong motion recordings. *Journal of Geotechnical and Geoenvironmental Engineering*. ASCE **129(4)**: 323 -335, UC Los Angeles.

Lysmer J, Kuhlemeyer AM. 1969. Finite dynamic model for infinite media. *Journal of the Engineering Mechanics Division*, ASCE, **95**:859-877.

Pandey BH, Liam Finn WD and Ventura CE. 2012. Modification of Free-Field Motions by Soil-Foundation-Structure Interaction for Shallow Foundations. *Proceedings of 15th World Conference on Earthquake Engineering*. Lisbon 24-28 September, paper 3575.

PEER 2008. Open system for earthquake engineering simulation (OpenSees)—development platform by the Pacific Earthquake Engineering Research Center (PEER), http://opensees.berkeley.edu/.

Pitilakis, D., Modaressi-Farahmand-Razavi, A., & Clouteau, D. 2013. Equivalent-Linear Dynamic Impedance Functions of Surface Foundations. *Journal of Geotechnical and Geoenvironmental Engineering*, **139(7)**, 1130–1139. doi:10.1061/(ASCE)GT.1943-5606.0000829.

Pitilakis K, Riga E, Anastasiadis A. 2012. Design spectra and amplification factors for Eurocode 8. *Bulletin of Earthquake Engineering*, **10(5)**: 1377-1400, doi: 10.1007/s10518-012-9367-6.

Veletsos AS and Meek JW. 1974. Dynamic behavior of building-foundation systems. *Earthquake Engineering and Structural Dynamics,* **3:**121–138, doi: 10.1002/eqe.4290030203.

Yenier E, Sandikkaya MA, Akkar S 2010. Report on the fundamental features of the extended strong motion databank prepared for the SHARE project (v1.0).

Eurocode 7 and new design challenges using numerical methods with different soil models

Eurocode 7 et de nouveaux défis de conception en utilisant des méthodes numériques avec différents modèles de sol

G. Katsigiannis, H.F. Schweiger, B. Simpson, P. Ferreira and R. Fuentes

ABSTRACT According to Eurocode 7, soil strength factoring can be achieved by applying the material partial factors to the effective stress parameters c′ and φ′ or to the undrained shear strength cu. Thus, in numerical analyses, material factoring is straightforward for constitutive models with c′, φ′ or cu as input parameters. While designers often use simple elastic-perfectly plastic soil models for ULS checks, the use of more advanced constitutive models allows real soil behaviour to be simulated more realistically and can have significant advantages. In this paper, the feasible use of different soil models for ULS design, increasing in sophistication, such as the Mohr-Coulomb (MC), the Hardening Soil (HS), the Hardening Small Strain (HSS) and the Soft Soil (SS) models, is highlighted and better understood in the context of the EC7 requirements using deep supported excavation examples in stiff clay. The challenges of factoring undrained shear strength when using effective stress model parameters are also discussed and the effect of the soil model is investigated.

1 INTRODUCTION

While the Finite Element Method (FEM) has been traditionally used in geotechnical engineering to obtain deformations and check for Serviceability Limit State (SLS), there are still a number of issues that need further research before the Ultimate Limit State (ULS) design can be routinely performed with FEM. Simpson (2012) and Simpson & Junaideen (2013) give a good review of most of the challenges associated with the ULS design with FEM. In this paper, the feasible use of different soil models such as the Mohr-Coulomb (MC), the Hardening Soil (HS), the Hardening Small Strain (HSS) and the Soft Soil (SS) models for ULS design is highlighted and better understood in the context of the EC7 requirements using deep supported excavation examples in stiff clay. The challenges of deriving structural forces using numerical methods and the effect of the soil model used are addressed. The resulting discrepancies are highlighted and better understood using a Crossrail station box case study. The challenges of factoring undrained shear strength when using effective stress model parameters are also discussed while the effect of the soil model is again illustrated by the authors.

2 MATERIAL FACTORING STRATEGIES

EC7 suggests three different Design Approaches (DAs) and each National Standard Body has chosen which approach is preferable. DA1, which is adopted in the UK, has two different combinations (sets of partial factors). In general, we could say that DA1-1 and DA2 are Load Factoring Approaches (LFAs) as the factors are applied to actions or action effects while DA1-2 and DA3 are Material Factoring Approaches (MFAs) as the soil strength parameters have to be factored. There are two different ways to factor soil strength in FEM in staged construction problems which have arisen from the lack of guidance in the code (Katsigiannis et al, 2014). In Strategy 1, the material parameters are factored from the beginning so the analysis is performed with the design values of soil strength. On the other hand, in Strategy 2, calculations are performed with characteristic values and at critical stages the material parameters are reduced to their design values. A good description of the two strategies has been given by Simpson (2012). Katsigiannis et al. (2014) have also discussed the advantages and disadvantages of the two strategies which are summarized in Table 1.

Table 1. Advantages and disadvantages of the two material factoring strategies

Strategy 1	Strategy 2
✓ It is straightforward and easy ✓ It can be applied in many situations, not only in staged construction problems	✓ More critical in terms of design structural forces ✓ It can be used in conjunction with SLS and DA1-1.
X In some cases it might yield design structural forces with inadequate margins of safety	X It requires many extra construction stages X Additional computational effort and time

3 BENCHMARK EXAMPLE

The challenges of deriving design prop forces using FEM and the effect of the soil model used are addressed for deep excavation in stiff, highly overconsolidated clay. The geometry of the problem is given in Figure 1.

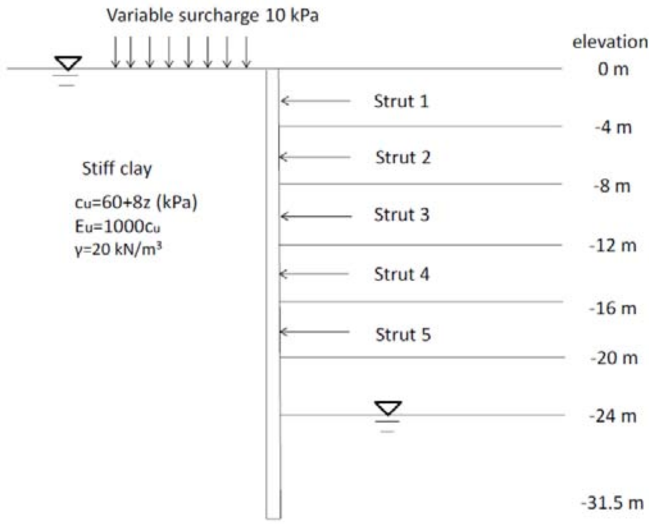

Figure 1. Geometry of deep excavation supported by 5 levels of props

3.1 Analysis Description

The computer software PLAXIS V12.01 was used for the analysis in its two-dimensional version. The analysis was repeated with different soil models assuming undrained conditions: the Mohr-Coulomb (MC), Hardening Soil (HS) and Hardening Small Strain (HSS) models. In all the analyses, typical stiff highly OC clay total stress parameters were used which are listed in Tables 2 and 3. The soil stiffness properties for HS and HSS are taken from Schweiger (2010). The following modelling sequence was analysed (an overdig of 0.5m is considered):

- Stage 0 Initial state conditions
- Stage 1 Wall installation and 10kPa surcharge
- Stage 2, 4, 6, 8, 10 and 12 Excavation of 4m of soil
- Stage 3, 5, 7, 9 and 11 Install strut

3.2 Results

Factoring soil strength from the beginning (i.e. Strategy 1) has a very small effect on the calculated prop loads. In Strategy 2, however, the soil strength is suddenly reduced at each excavation stage. Shifting from characteristic to factored soil strengths has, as result, shown that the lowest prop receives a higher load increment than the props above (see Figure 2). At the final excavation stage the load of the lowest prop increases relative to the characteristic by 17.5%, 25.8% and 32.8% for K_0 values of 1, 1.2 and 1.5 respectively (only the K_0=1.2 case is presented here). The increase of the load of the lowest prop is due to the development of a plastic zone at the bottom of the excavation (see Figure 3). The larger the plastic zone is, the larger is the increase of the prop load when shifting from characteristic to factored strength.

Table 2. Mohr-Coulomb parameters

Total stress parameters	
γ_{sat} (kN/m^3)	20
c_u (kPa)	60+8z
E_u (kPa)	1000c_u
Effective stress parameters	
c' (kPa)	0
φ' (°)	25
ψ (°)	0

Table 3. HS and HSS model parameters

Total stress parameters	
γ_{sat} (kN/m^3)	20
c_u (kPa)	60+8z
E_{50}^{ref} (kPa)	30000
E_{oed}^{ref} (kPa)	30000
E_{ur}^{ref} (kPa)	100000
power m	0.5
R_f	0.9
p_{ref} (kPa)	100
σ_{tens} (kPa)	15
ν'_{ur}	0.2
Effective stress parameters	
c' (kPa)	0
φ' (°)	25
ψ (°)	0
Additional Hardening Small Strain model parameters	
Go	150000
$\gamma_{0.7}$	0.0002

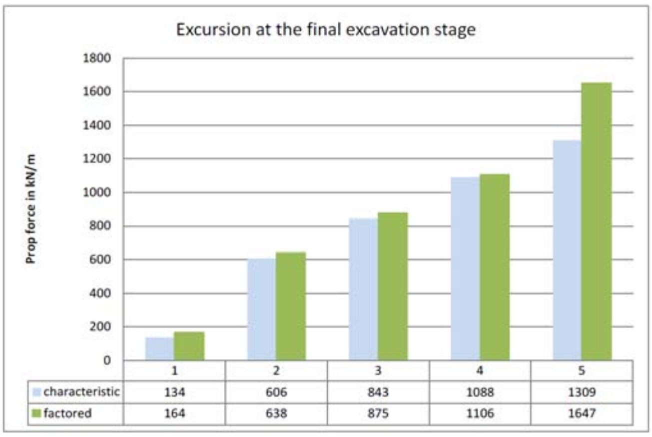

Figure 2. Prop loads before and after factoring soil strength in Strategy 2 at the final excavation stage

Figures 4 to 6 show computed prop loads for three different soil models, increasing in sophistication. In each case, DA1-1 returns the highest prop loads. For the simplest model (elastic-Mohr Coulomb), DA1-2 Strategy 1 returns significantly lower prop loads. Use of more advanced soil models such as the HS and HSS Plaxis models can result in much smaller differences in calculated prop loads from the two material factoring strategies of DA1-2. The difference between the two DA1 combinations becomes smaller too.

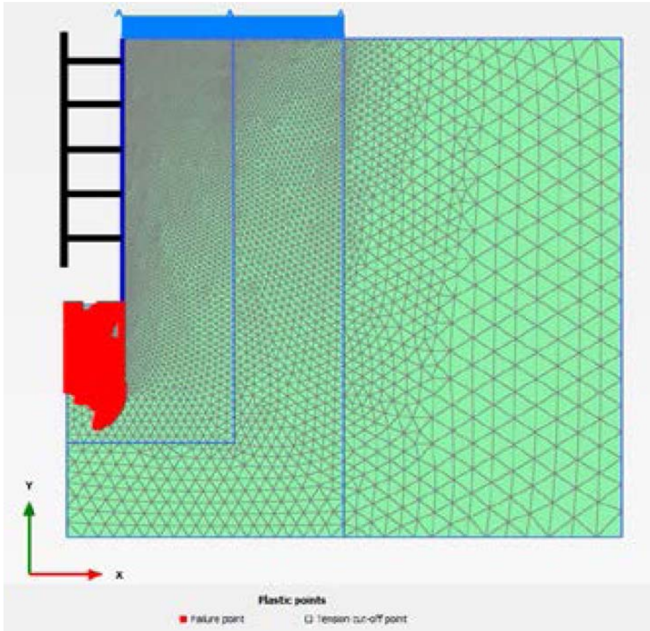

Figure 3. Plastic points developed at the final excavation stage

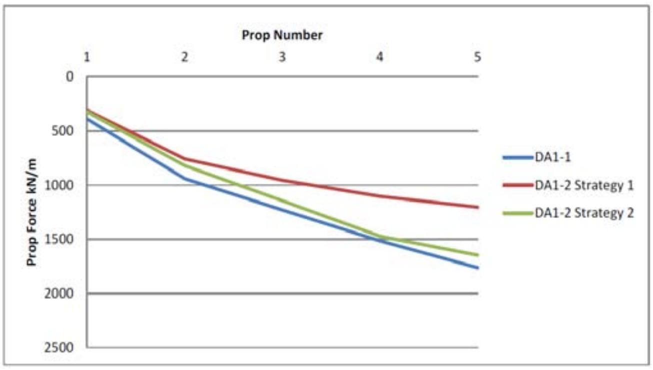

Figure 4. Maximum prop loads from different factoring strategies using MC soil model

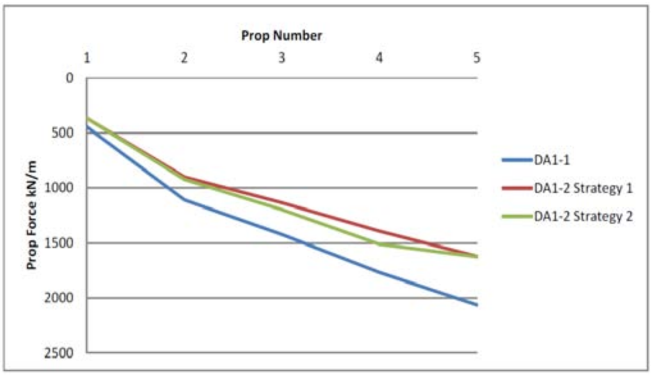

Figure 5. Maximum prop loads from different factoring strategies using HS soil model

4 CROSSRAIL CASE STUDY

The resulting discrepancies are now highlighted using a more realistic and deeper excavation based on the Crossrail Moorgate station box case study. The geometry and construction sequence are related to the proposal made by Zdravkovic et al. (2005). However, a simplification of the geometry was undertaken in order to provide an easier understanding of the different factoring strategies.

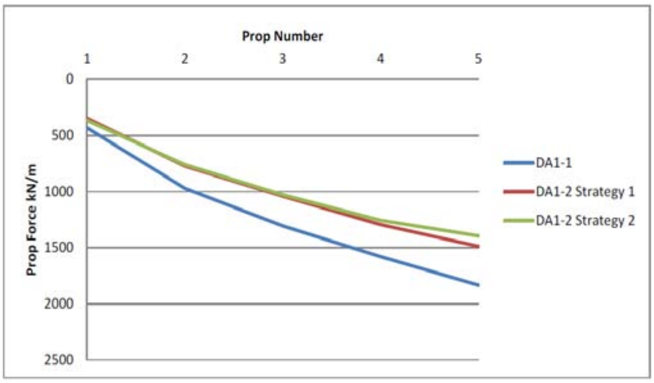

Figure 6. Maximum prop loads from different factoring strategies using HSS soil model

4.1 Analysis Description

The computer software PLAXIS EA was used for the analysis in its 2D version. The Mohr-Coulomb (MC), Hardening Soil (HS) and Hardening Small Strain (HSS) soil models were again chosen. The finite element mesh is shown in Figure 7. The concrete wall is 1.2m thick and is supported by 7 levels of steel tube props. The total stress soil parameters given in Tables 2 and 3 were used for the FEM simulations.

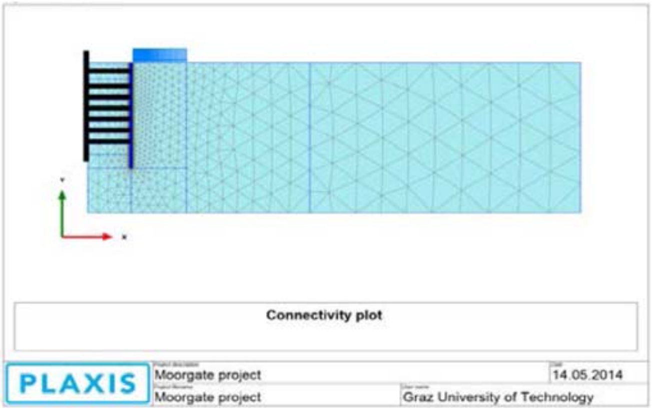

Figure 7. Finite Element mesh

4.2 Results

Factoring soil strength from the beginning (i.e. Strategy 1) has very little effect on calculated prop loads, which is in good agreement with findings in the benchmark example. In general it seems that soil strength is not critical for the materials and geometry considered. In Strategy 2, shifting from unfactored to factored strength has shown that the lowest prop, again, receives a higher load increment. At the final excavation stage the load of the lowest prop increases by 21.64%. DA1-1 governs the prop design in all cases while use of more advanced soil models again results in much smaller differences in calculated prop loads from the two material factoring strategies of DA1-2 (Figures 8 to 10).

5 FACTORING UNDRAINED STRENGTH

How the undrained soil strength should be factored is one of the most common misunderstandings of EC7. In the analyses presented in this paper in Sections 3 and 4, total stress conditions were assumed. The undrained shear strength cu was input, i.e. the analysis was performed in terms of total stresses, so the software user could simply apply the partial factor of 1.4 as the code requires. However, when undrained analysis is performed with effective stress parameters, c_u is not input but it is the result of the soil model used. What is usually overlooked during the design is that the designer should always check that the calculated c_u profile corresponds to the characteristic one, factored by a specified sufficient value. While there is still an ongoing debate, the authors understand that the members of EG4 (the EC7 Evolution Group working on numerical methods) have agreed on a value of 1.4.

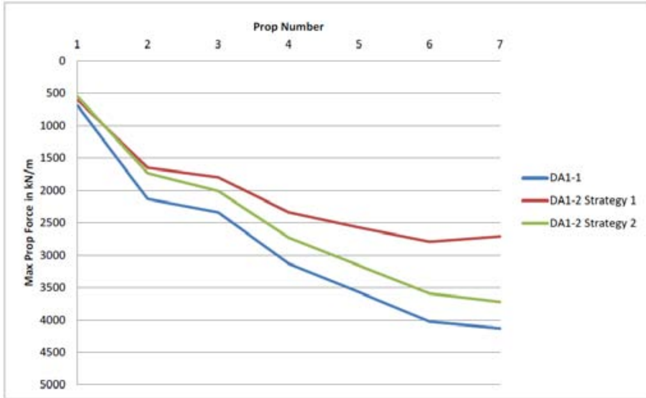

Figure 8. Maximum prop loads from different factoring strategies using MC soil model

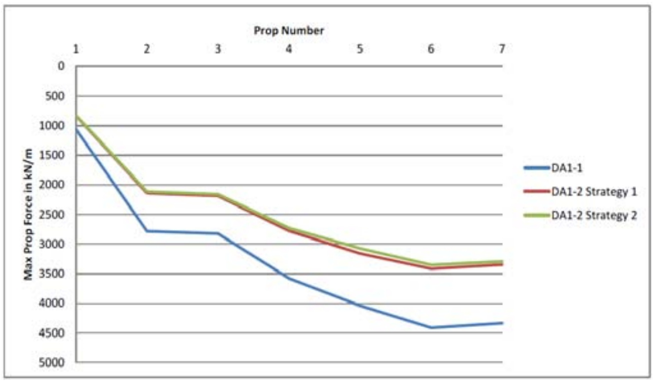

Figure 9. Maximum prop loads from different factoring strategies using HS soil model

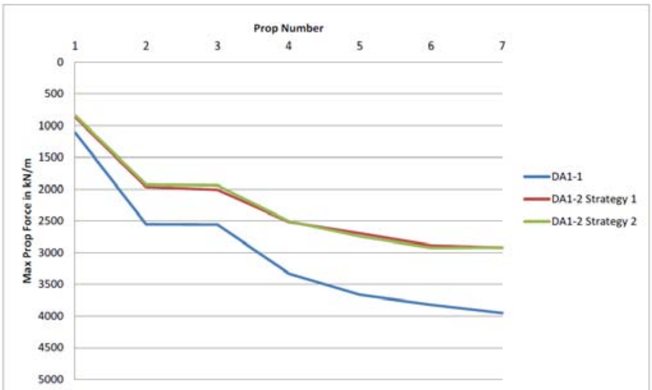

Figure 10. Maximum prop loads from different factoring strategies using HSS soil model

A series of triaxial undrained compression single element tests were performed with MC, SS, HS and HSS soil parameters at different depths (0.5, 2, 5, 10, 15, 30 and 45m below ground level) following isotropic consolidation. The SS parameters are based on the ones used by Schütz (2006). A pre-consolidation pressure of 2000kPa is applied while an underdrained profile is assumed in all cases. It can be seen in Figure 11 that, for this heavily overconsolidated clay, the calculated characteristic undrained shear strength profile from MC, SS and HS triaxial undrained compression tests (in effective stresses) are identical and in close agreement with the assumed c_u profile in total stresses.

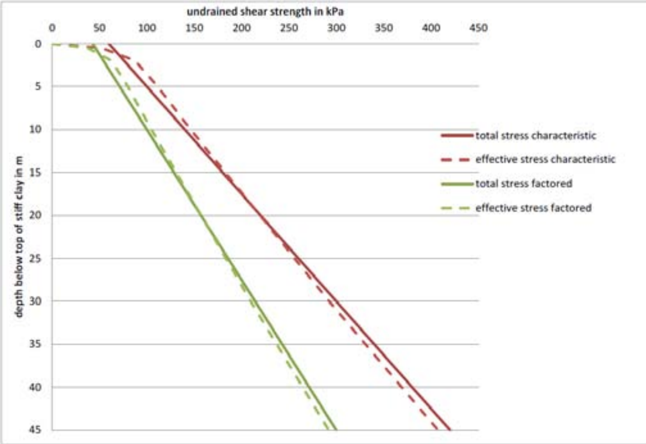

Figure 11. Characteristic and design undrained shear strength profiles using total and effective stress MC, HS and HSS parameters

Also, factoring tanφ' by 1.4 produces a set of undrained strengths equivalent to EC7 requirement where the undrained strength is factored by a partial factor γ_{cu}=1.4. The agreement is not good with HSS model as the stress path is different (see Figure 12).

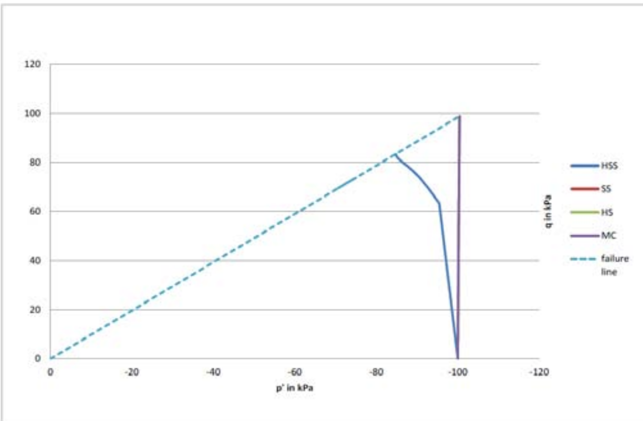

Figure 12. p-q stress paths using different soil models

Figure 13 gives the value of $\gamma_{\tan\varphi'}$ for different values of angle of shearing resistance that results in a calculated c_u profile equal to the characteristic one, factored by 1.4. The graph enables the designer to use appropriate values of $\gamma_{\tan\varphi'}$ when undrained analysis is performed with effective stress parameters. However, the graph is only correct when the triaxial stress path is vertical (in this case for the MC, HS and SS models). It is more difficult to draw general rules for non-vertical stress paths.

6 CONCLUSIONS

While a broader study is needed, some useful conclusions can be drawn from the work done in this article:

- Use of more advanced soil models such as the HS and HSS Plaxis models can result in much smaller differences in calculated prop loads from the different material factoring strategies for the geometries and materials considered in this study and for total stress analysis.

- The choice between the two DA1-2 strategies is not important in practice to DA1 so long as the design is governed by DA1-1.

- When using effective stress parameters for undrained analysis, the designer should always check that the calculated cu profile corresponds to the characteristic one, factored by 1.4 as EC7 requires.

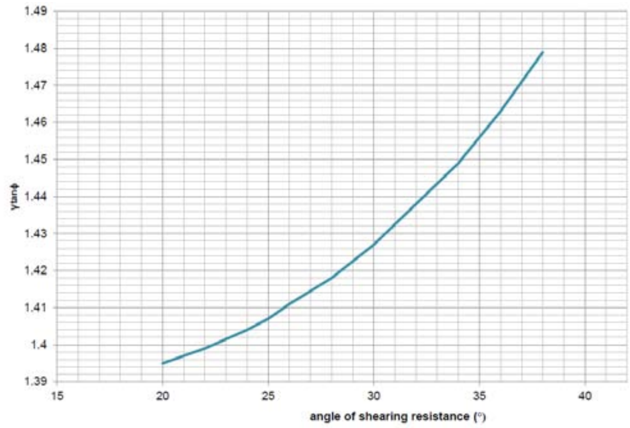

Figure 13. $\gamma_{\tan\varphi'}$ for different values of angle of shearing resistance

REFERENCES

Katsigiannis, G. Ferreira, P. & Fuentes, R. 2014. Ultimate Limit State design of retaining walls with numerical methods. *Proceedings, 8th European Conference on Numerical Methods in Geotechnical Engineering* (Eds: Hicks, M.A., Brinkgreve, R.B.J. & Rohe, A.), Volume 1, 385-389. CRC Press.

Potts, D.M. & Zdravkovic, L. 2012. Accounting for partial material factors in numerical analysis, *Géotechnique* **62**, 1053–1065.

Schütz, R. 2006. Numerical analysis of deep excavations in London Clay. Diploma Thesis Graz University of Technology.

Schweiger, H.F. 2010. Numerical analysis of deep excavations and tunnels in accordance with EC7 design approaches, *Proceedings, Int. Conference Geotechnical Challenges in Megacities* (Eds: Petrukhin, Ulitsky, Kolybin, Lisyuk, Kholmyansky), Moskau, 7.-10.6.2010, Vol. 1, 206-217

Simpson, B. 2012. Eurocode 7 – fundamental issues and some implications for users, Keynote Lecture, *Proceedings, Nordic Geotechnical Meeting 2012***,** *DGF Bulletin 27*.

Simpson, B. & Junaideen, S.M. 2013. Use of Numerical Analysis with Eurocode 7, Keynote Lecture, *Proceedings, 18th Southeast Asian Geotechnical & Inaugural AGSSEA Conference, Singapore*.

Zdravkovic, L. Potts, D.M. & St John, H.D. 2012. Modelling of a 3D excavation in finite element analysis, *Géotechnique* **55**, 497–513.

Triaxial testing of saturated lime-treated high plasticity clay

Essais triaxiaux sur une argile plastique saturée, traitée à la chaux

Z. Kichou, M. Mavroulidou, M. J. Gunn

ABSTRACT The paper investigates the effect of hydrated lime on shear strength properties and behaviour of saturated, lime treated, high plasticity clay (London Clay). A number of Unconsolidated Undrained (UU), Consolidated Drained (CD) and Consolidated Undrained (CU) triaxial tests were performed to identify the effect of lime dosage, compaction water content and curing time on the shear strength parameters of the soil. The results are presented both in terms of the Mohr-Coulomb criterion, commonly used by practicing engineers, as well as through a more modern interpretation of the behaviour of cemented soils (in this case the artificially cemented lime-treated soil), in comparison with the critical state parameters of the uncemented (untreated) soil.

1 INTRODUCTION

Lime treatment is a chemical ground improvement method commonly used in civil engineering applications, in particular for road construction (subgrade and subbase stabilisation), and also embankments and foundations. Despite the widespread use of this technique, most of the results reported in the literature have commonly been obtained based on simple tests, e.g. CBR (due to the applications of the technique in highway engineering) and unconfined compression tests in particular. Conversely there is a relative paucity of results based on more advanced testing such as triaxial testing, probably due to the duration of these tests, which makes it difficult to investigate the number of possible factors that may affect the outcome of the treatment, when such tests are used. These tests are however required to provide the parameters for advanced constitutive models of the mechanical behaviour of the soil.

To address this, the paper investigates the effect of a number of factors on the engineering properties of a high plasticity clay based on triaxial testing. The factors studied included lime amount, curing time and compaction moisture content of the soil. The results are interpreted both in terms of the Mohr-Coulomb criterion, commonly used by practicing engineers, as well as through a more modern interpretation of the behaviour of cemented soils (the artificially cemented lime-treated soil), in comparison with the critical state parameters of the uncemented (untreated) soil.

2 MATERIALS AND PROCEDURES

The high plasticity clay used in this study was London Clay from a deep excavation near Westminster Bridge in London. The soil was air dried for a month and subsequently pulverised. The portion passing through the 425 μm sieve was retained for testing. Particle size distribution showed that the material contained 53% clay and 45% silt (Zhang 2011). The sulphate content of the soil was found to be negligible, hence the application of a calcium based stabiliser would not incur the risk of formation of expansive crystals (e.g. ettringite), with potential detrimental effects. X-Ray Diffraction (XRD) analysis showed the predominant clay mineral to be illite (50% of the clay fraction); montmorillonite, kaolinite and chlorite were also detected at percentages of the clay fraction of 26%, 15% and 9% respectively (Zhang 2011).

Commercially available hydrated lime was used for this study. The required lime percentage for this soil was determined based on the "Initial Consumption of Lime" (ICL) and "Lime Fixation Point" (LFP) methods. According to pH measurements (Figure 1), the ICL was determined as 3.45% (the lime percentage required for a pH of 12.4). The plasticity tests also indicated a LFP of around the same value (Figure 2). Based on these results, an amount of 4% lime per dry soil mass was considered to be sufficient for triggering both cationic exchange and pozzolanic reactions for this soil. This percentage, as well as a second percentage above this value (i.e. 6%), were therefore used in the triaxial tests to assess the effect of the amount of lime.

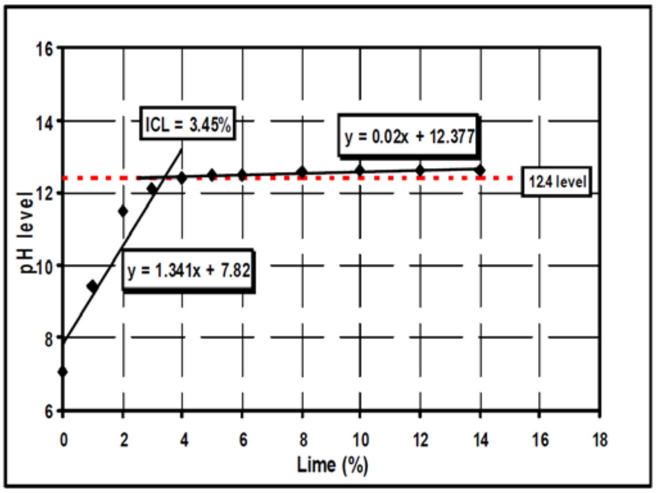

Figure 1. pH variation of lime treated London Clay.

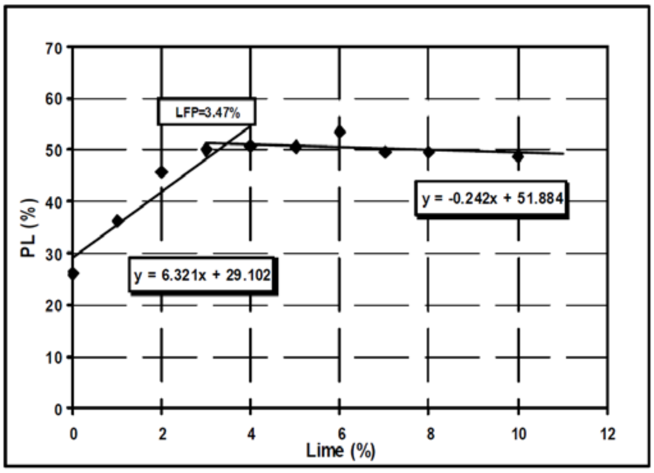

Figure 1. Plasticity tests on lime treated London Clay

A series of statically compacted cylindrical specimens of 38 mm diameter and 76 mm height were then prepared at the following water contents: 25% for untreated London clay (its standard Proctor optimum); 27% for the 4% lime treated specimens (slightly dry of optimum) and 27% and 32% (corresponding to dry and wet of the Proctor optima respectively) for the 6% lime treated specimens. Prior to compaction the treated soil samples mixed with the required amount of water were left to mellow for one day. For consistent comparisons, all specimens were statically compacted to the same dry density (1.43 g/cm^3).

After compaction the lime-treated specimens were then left to cure as required, wrapped in cling film and stored in a humidity controlled cabinet. The curing periods adopted were: 1, 7, 28, 60, 120 and 250 days for Unconsolidated Undrained (UU) triaxial testing (performed on the specimens at as compacted state); 7 and 28 days for Consolidated Drained (CD) triaxial tests (sheared following a q:p'=3 path) and 28 days for Consolidated Undrained (CU) tests. The CD and CU specimens were saturated using a back pressure of 400 kPa to achieve B values of 0.99 and 0.95 or more for untreated and lime treated specimens respectively). Prior to shearing these specimens were isotropically consolidated to effective confining pressures of 100, 200 and 300 kPa for CD and 158, 250 kPa for CU tests.

3 RESULTS AND DISCUSSION

Figure 3(a)-(b) presents UU test results showing predominantly the effect of curing time, and also the effects of lime amount and compaction water content on the peak strength development of the treated soil. It can be seen (Fig 3(a)) that lime treated specimens showed a brittle behaviour which became increasingly pronounced with curing time. From Figure 3(b) it can be noted that for both lime percentages and compaction water contents used, the peak strength of the lime treated soils was twice as much as that of the untreated soil as early as after one day of curing. For the 4% lime treated soil it then remained essentially the same until very later times when it was observed to increase again substantially to a value almost double than that achieved in the previous curing time measurements. The results of specimens treated with 6% lime showed a similar sharp increase in peak strength at long curing periods. However as opposed to the 4% lime treated specimens they also showed continuous peak strength gain with curing time (although at a much slower rate up to 60 days of curing). The trend of a substantial strength gain at later curing times after a period without a considerable strength increase was also shown in Sherwood (1993) for London Clay treated with 10% lime (due to the different lime percentage the strength magnitudes shown in Sherwood were different to the presented ones but the trends were similar). This finding is interesting as it contradicts the common belief that, similarly to concrete, most strength gain upon lime treatment would be achieved within the first 28 days and that henceforth any strength gain would be very small. Overall, other than for the first day of curing, the 6% lime treated specimens developed much higher strengths compared to the 4% lime treated ones, amounting to more than twice the value of the strength of the latter specimens (see in particular the later curing time of 250 days in Fig 3(b)). Finally, concerning the influence of compaction water content it can be seen that the strength values of the specimens compacted at different water contents were initially similar but that at later times the specimens with the 32% compaction water content developed higher strengths than those with 27% water content, showing the beneficial effect of water for the progression of long-term chemical reactions. Overall however the effect of the lime percentage was much more considerable compared to that of the compaction water content (Fig 3(b)).

Figure 4(a)-(b) shows indicative plots of deviator stress versus axial strain and the corresponding volumetric strain versus axial strain plots for CD specimens confined at a 200 kPa effective stress. Note that as the UU results showed no further strength development between 7 and 28 day curing for the 4% lime percentage, no 28 day curing CD or CU tests were performed for specimens treated with 4% lime. The stress-strain plots (Fig 4(a)) showed that lime addition to the minimum requirement i.e. 4% lime cured for 7 days caused an increase of 99% in strength compared to that of the untreated soil. On the other hand all 6% lime treated specimens showed much higher strengths than those achieved by the 4% lime treated one, i.e. on average about 170% higher strengths than the latter (amounting to approximately 430% strength gain, on average, compared to that of the untreated soil). The latter specimens had a higher stiffness (judging from the slope of the initial portion of the curve) and showed a more brittle response compared to the 4% lime treated specimen; the peak strengths of these specimens were reached at axial strains o f 1 .5-2%, after which a very sharp drop in deviator stress was observed. In comparison the 4% lime treated specimen achieved its peak strength at higher axial strains (of 4% or more) and maintained these for axial strains up to 6% after which a more gradual drop in deviator stress (compared to that of the 6% lime treated specimens) was noted. All lime treated specimens developed a rupture on a plane.

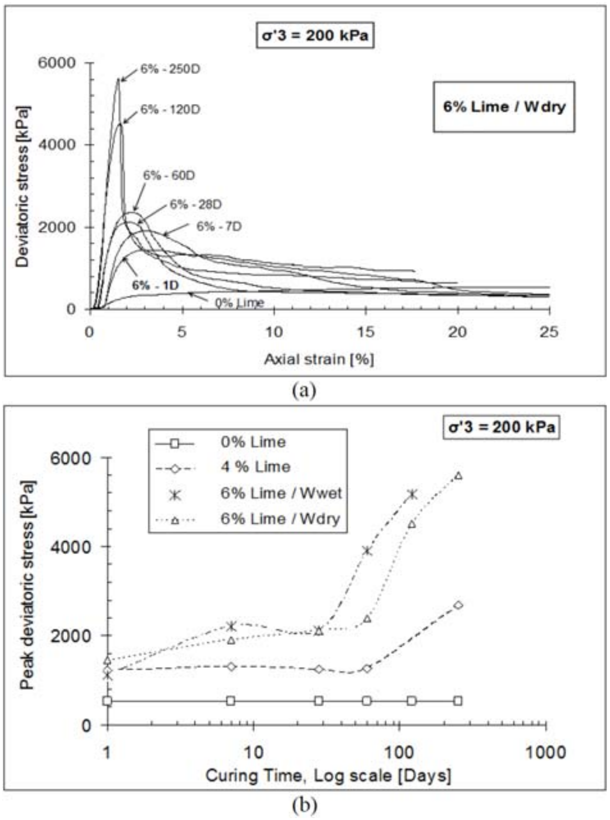

Figure 3. UU testing results: (a) typical stress strain graphs; (b) peak deviatoric stress evolution with curing time

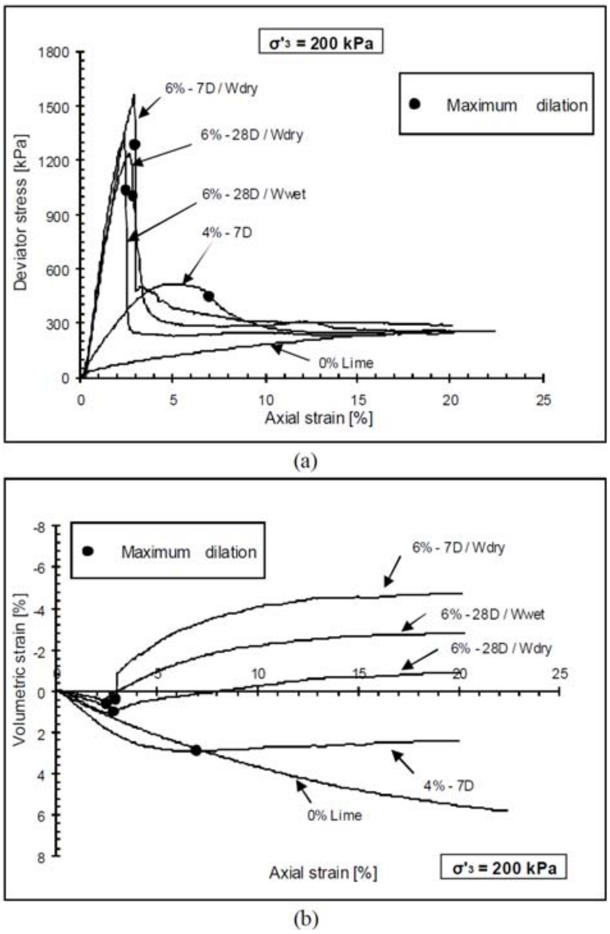

Figure 4. Indicative CD testing results: (a) deviator stress vs. axial strain plots; (b) volumetric strain vs. axial strain plots

The behaviour of the untreated specimen was consistent with that of normally consolidated soils, with the stress increasing continuously towards a maximum value, without any apparent peak and subsequent strain softening. Consistently with these observations, the volumetric strain vs. axial strain plots (Fig. 4(b)) showed a contractive response for the untreated soil as opposed to all lime treated specimens showing an initial contraction followed by dilation, which was particularly pronounced for specimens treated with 6% lime.

It is interesting to note that the maximum rate of dilation of all lime treated specimens was reached after the peak strength, and subsequently decreased as the state of the soil approached an ultimate condition, where the friction angle mobilised on the rupture plane corresponds to the critical state value for untreated specimens (Burland 1990). This corresponds to the typical behaviour of cemented soils (Consoli et al. 2001) and soft rocks (Vaughan 1993). The maximum dilation for the 4% lime treated soil is reached at higher axial strains compared to the 6% lime treated specimens. This is consistent with the stress-strain plots showing that the latter specimens reached and maintained their peak strengths at higher axial strains compared to the 6% lime treated ones. Regardless of curing time and initial water content, the latter specimens showed maximum dilation points occurring at similar axial strains.

An interesting observation based on Figure 4(a) is that the 7 day treated specimen had a higher strength compared to that of the corresponding specimen (i.e. identically prepared and compacted) cured for 28 days. This result was not expected and does not accord with the findings of the UU tests. It was however consistently observed for all 6% lime, 7 day cured, specimens compared to the corresponding 28 day cured ones (see also Figures 6 and 7). Although these findings were consistent throughout the tests, this point requires further investigation and support from complementary testing (e.g. XRD analysis) for the results to be conclusive and explained.

Finally, concerning the differences in the 6% lime treated specimens compacted at wet and dry of optimum water contents respectively, the specimen compacted dry of optimum was slightly stronger and stiffer; however the differences in the peak strength were rather small; it is therefore unlikely that they are of any practical significance.

Figure 5 presents indicative stress paths of CD and CU tests respectively, for 6% lime treated specimens cured for 28 days. It can be seen that the end points of both types of test fell on the Critical State Line (CSL) of the untreated soil. The CD test stress paths corresponded to a compressive failure during the shearing stage, whereas those of the CU tests to a tensile failure (see the points on the tension cut off line) due to the pore water pressure increasing up to a value close to that of the applied cell pressure.

The analyses of all results (including those that were not presented in detailed stress-strain plots due to space limitations) are presented in Figures 6 and 7 (a) and (b) respectively in terms of Mohr circle plots as well as of q:p' plots of peak and post-rupture strengths compared to the Critical State of the untreated soil. Based on these plots the corresponding shear strength parameters of the different specimen types were determined and presented in Table 1.

Based on the above two graphs, the considerable peak strength gains shown earlier in the indicative stress-strain plots can be clearly observed for all lime treated specimens, in particular for those treated with 6% lime. The latter plot much higher than the respective peak values of the 4% lime treated soil. Analysing the results in terms of Mohr-Coulomb criterion parameters, the peak strength increase of the 6% lime treated soil compared to that of the 4% lime treated soil, is manifested as an increase in both the φ'peak as well as the cohesion intercept c', which could be justified by the increased cementation bonding when a higher lime amount was used. Note that for the untreated soil, which showed behaviour typical of a normally consolidated clay, only the parameter φ'_{cs} could be identified. All specimens cured with 6% lime showed similar φ'peak values, with the differences in the peak strengths due to factors other than lime percentage (i.e. curing time and compaction water content) manifested as an increase in the cohesion intercept (as mentioned earlier, the highest peak strengths and consequent cohesion values were observed for the 6% lime, 7 day cured specimen).

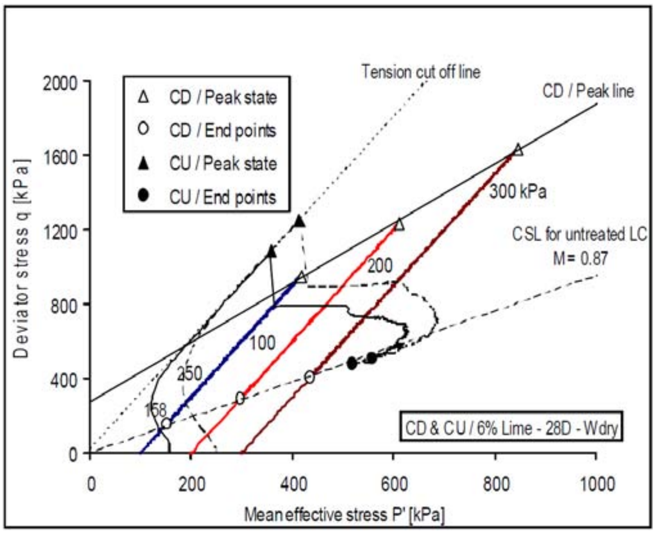

Figure 5. Indicative CD and CU test s tress paths for 6 % lime treated soil

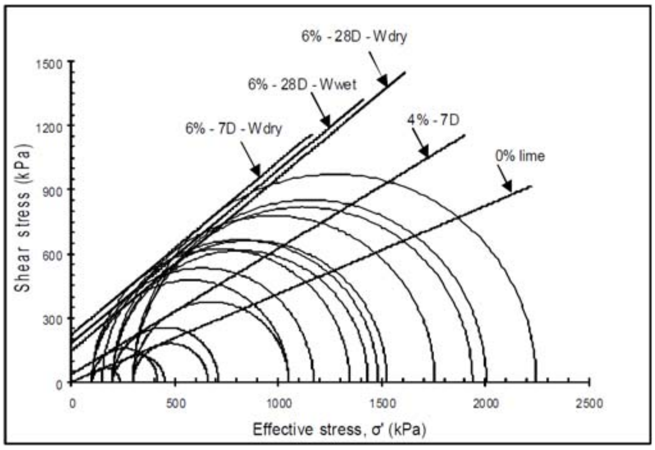

Figure 6. Mohr circle plots of all CD test results

Concerning the post-rupture strength, it can be seen that the best fit straight line of the 4% lime treated soil end of testing strengths (passing through the axis origin) had a gradient very close to that of the Critical State Line (CSL) of the untreated soil (0.88 vs. 0.87 respectively). These gradients can thus be considered as identical, given the usual scatter in the experimental data as well as due to the ambiguity involved in the identification of the post-rupture strength of a brittle soil. On the other hand, the end of testing points of all 6% lime treated specimens (regardless of other differences in the compaction and curing conditions) all defined a straight line of the same gradient as the CSL of the untreated soil, having a non-zero intercept on the q axis (see Table 1).

4 CONCLUSIONS

A number of triaxial tests were carried out to assess the effect of lime on the shear strength parameters and behaviour of statically compacted London Clay and lime-treated London Clay samples respectively. The results showed that the lime-treated soil became increasingly stiffer, stronger but also more brittle with the increase in lime percentage. The volumetric behaviour of lime treated London Clay was consistent with that of bonded materials, showing a contractive-dilatant response with maximum dilation rates after the peak stresses, with the breakage of bonds. Lower lime percentages could thus be recommended to achieve sufficiently high strengths for most common practical applications while avoiding a very brittle behaviour within the range of strains of relevance to engineering design. The initial (compaction) water content was found to have less influence on the resulting strength characteristics and behaviour of the soil compared to the effects of lime percentage. On the other hand it was found that the curing time and conditions could greatly influence the soil strength. The latter point needs further investigation through additional triaxial testing, as well as mineralogical and microstructural analyses.

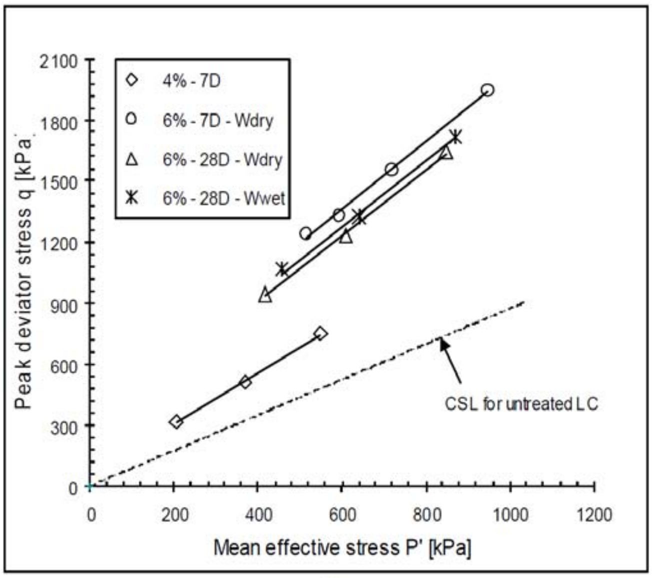

(a)

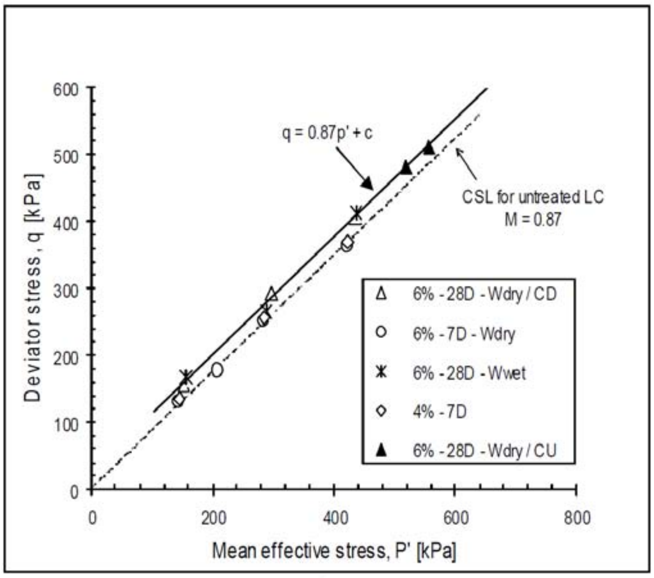

(b)

Figure 7. q:p' plots of the lime treated soil compared to the Critical State Line (CSL) of the untreated London C lay: (a) peak stress envelopes; (b) post-rupture strength envelopes

Table 1. Shear strength parameters of the tested soils.

Lime (%)	Initial w.c. (%)	Curing time (days)	c' (kPa)	φ'_{peak} (°)	φ'_{cs} (°)	M
0	25	N/A	0	N/A	22.33	0.87
4	27	7	35	30.5	22.56	0.88
6	27	7	220	39	22.33	0.87
6	27	28	145	39	22.33	0.87
6	32	28	181	39	22.33	0.87

REFERENCES

Bell, F. G. 1996. Lime stabilisation of clay minerals and soils. *Engineering Geology* **42**, 223–237.

Burland, J.B. 1990. On the compressibility and strength of natural clays. *Géotechnique* **40**, 329-378.

Consoli, N. C., Prietto, P. D. M., Carraro, J. A. H., & Heineck, K. S. 2001. Behavior of compacted soil-fly ash-carbide lime mixtures. *Journal of Geotechnical and Geoenvironmental Engineering* **129**(9), 774-782.

Sherwood, P.T. 1993. *Soil stabilization with cement and lime: State of the Art Review*, HMSO, London.

Vaughan P.R. 1993. Engineering behaviour of soft rocks. Some answers and some questions. *Geotechnical Engineering of Hard Soils – Soft Rocks* (Eds: Anagnostopoulos, A., Schlosser, F., Kalteziotis, N. & Frank R.), 1741-1766. Balkema, Rotterdam.

Zhang, X. 2011. *Hydro-mechanical properties of lime-stabilised London Clay*. PhD Thesis, London South Bank University.

3D simulation of mechanized tunnel excavation

Dimitris Litsas[1], Petros Fortsakis[2], Michael Kavvadas[3]

[1] National Technical University of Athens, Civil Engineer, MSc, PhD Candidate

[2] Deutsche Bahn International, Civil Engineer, MSc, PhD, Tunnel Expert at Qatar Rail

[3] National Technical University of Athens, Civil Engineer, Associate Professor

Abstract

EPBs and slurry machines are commonly used in urban tunnelling projects, since they decrease the displacements induced by tunnel excavation, ensuring high performance in a wide range of ground conditions, low cover depths and high ground water pressures. The calculations related with mechanized tunnelling (settlements, dimensioning of the tunnel lining etc.) are usually carried out by using simplified approaches, such as 2D numerical analyses, empirical methods etc. However, the simulation of the actual construction procedure includes high complexity due to the multiple interfaces, the role of the 3D geometry, the different phases of the grout and the structural system of the segmental lining (radial and longitudinal joints).

This paper presents a realistic full 3D simulation of a shield tunnelling process (EPB or slurry machine) with the finite element code ABAQUS. The objective of this paper is to demonstrate the main modeling techniques employed for the simulation of several key characteristics of the excavation and construction. Indicatively, the main components of the machine (shield, excavation chamber, cutterhead) are simulated using solid elements and the gaps due to overcut and tapered shield are also included in the model via interface elements. The tail void grout is modeled with 3-dimensional finite elements simulating the grout injection pressure and the time-dependent hardening. The segmental lining is modeled with shell elements, considering the coupling behaviour of the joints between the segments, resulting to a more realistic distribution of the internal forces and consequently the dimensioning of the concrete shell.

1. Introduction

The rapid increase of the calculation power and the improvement of the analysis software allows the incorporation of very complex numerical analyses in tunnel design. One of the main objectives of the designer is to determine the optimum balance between the accuracy of the analysis and the required complexity and consequently the time and cost of the design. Many tunnelling problems, especially in the design phase, can be analyzed using simplified approaches as long as the conditions of the project fit with the assumptions of the simplified approach. However, the simulation of certain problems such as face stability, tunnelling in squeezing conditions and mechanized tunnelling demands the development of advanced numerical models.

The main factors that create the complexity of the simulation of the mechanized tunnelling procedure are a) the significant role of the 3D geometry (Gens, 1995), b) the gaps between the shield and the surrounding soil, c) the face pressure, d) the time-dependent behaviour of the grout material and e) the structural system of the segmental lining (radial and longitudinal joints).

The present paper describes the analysis techniques for the simulation of all the aforesaid elements leading to a realistic simulation of the mechanized tunnelling procedure. The first part of the paper focuses on the simulation of the excavation procedure and the second part on the detailed simulation of the segmental lining.

2. Simulation of the excavation procedure

In the present paper the numerical analyses have been carried out using Finite Element code ABAQUS assuming linear geometry. Figure 1 shows a general view of the numerical model. The dimensions of the model have been determined via sensitivity analysis balancing the accuracy of the calculations and the computational cost.

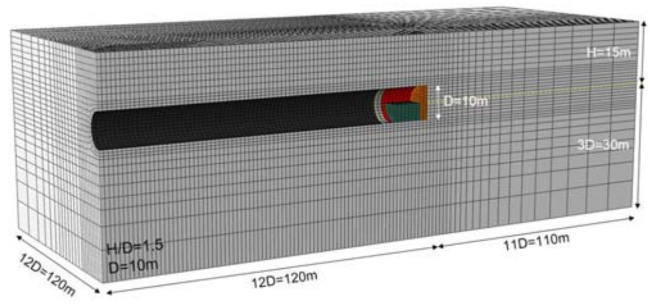

Figure 1. General view of the 3D numerical model.

The tunnel excavation diameter is equal to 10m and the overburden height 15m measured from the tunnel axis. The face pressure varies linearly over the height according to the assumed bulk density of the muck of 13kN/m^3 (Kasper and Meschke, 2006; Sitarenios et al., 2015). The respective reference value in the tunnel axis is equal to 165kPa, i.e. 82.5% of the horizontal geostatic stress (σ_{ho}) and the injection pressure of the grout is assumed to be equal to 200kPa (Table 1).

Table 1. Summary of the main parameters of the numerical analysis.

Geometrical and operational properties			
Depth of tunnel axis (m)	Tunnel diameter (m)	Face pressure in tunnel axis (kPa)	Grout pressure (kPa)
15	10	165	200

Geotechnical properties					
E (MPa)	v (-)	c (kPa)	φ (°)	ψ (°)	k_0 (-)
40	0.3	30	25	4.2	0.5

The surrounding soil has been simulated using 6-sided, 8-noded solid elements. The soil behaviour has been assumed linearly elastic - perfectly plastic following the Mohr-Coulomb failure criterion. The geotechnical parameters for these analyses are presented in Table 1.

The segmental lining in this analysis is modelled as a continuous cylindrical shell neglecting the joints, with width and thickness of the segmental rings equal to 1.5m and 30cm respectively. The EPB machine components are modelled in detail in this analysis (Figure 2). Specifically, the shield has a typical length of 10.5m and thickness of 10cm. The shield diameter is designed with a varying diameter in the longitudinal direction with 3cm overcut at the tunnel face and 6cm tail shield gap at the rear part of the machine (Figure 2-i). The properties of all the EPB and lining components are shown in Table 2.

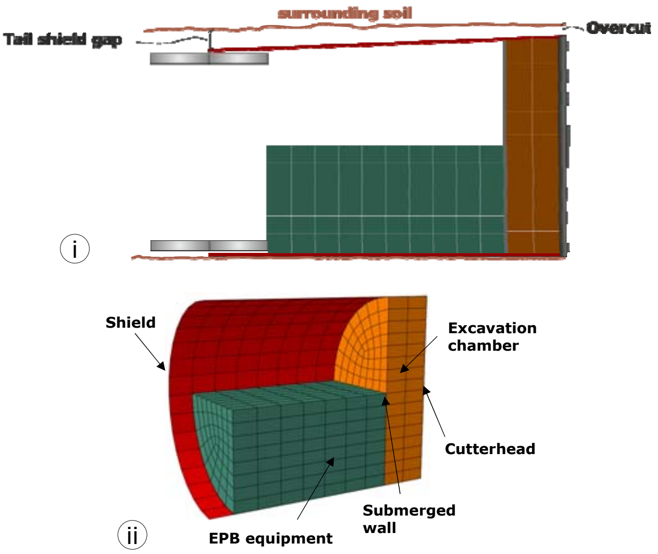

Figure 2. (i) Indicative sketch for the definition of the overcut and tail shield gap (ii) finite elements for the simulation of the EPB.

Table 2. Properties of the machine and the support elements.

Material properties				
Material	Thickness (cm)	Elastic Modulus (GPa)	Poisson ratio (-)	Unit Weight (kN/m^3)
Final lining	30	30	0.3	25.0
Grout (hardened)	11-15	1		20.0
TBM machine components				
Cutterhead	10	200	0.3	78.5
Submerged wall	10	200		78.5
EPB equipment	-	1		20.0
TBM Shield	10	200		78.5

The excavation chamber and the EPB equipment are simulated with 6-sided, 8-noded solid elements assuming elastic response (Figure 2). The main reason for the incorporation of these elements in the model is the simulation of the weight of the TBM which influences the displacements in the bottom of the tunnel especially in case of shallow tunnels. Moreover, the unit weight of the elements in the excavation chamber can be adjusted in case of open or closed mode excavation. It is noted that there is no interaction between the elements of the excavation chamber and the elements at the tunnel face since they have different nodes. The shield, the cutterhead and the submerged wall are simulated using 4-sided, 4-noded elements with elastic behaviour. The gap between the shield and the surrounding soil is created due to the overcut (2cm) of the peripheral cutters of the cutterhead at the tunnel face and the conicity (6cm) of the shield as shown in Figures 2 and 3. The interaction between the shield and the surrounding soil is simulated using an interface.

The normal stiffness of the shield - soil interaction could be ideally described by a "hard" pressure - overclosure relationship (Figure 4-i), i.e. when the two surfaces are in con tact, full transfer of compressive stresses and no transfer of

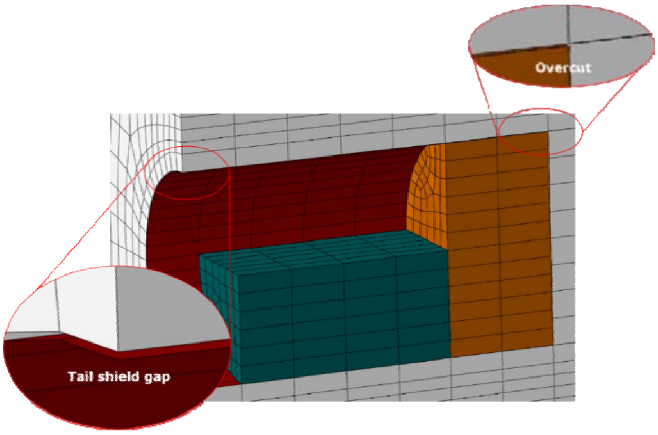

Figure 3. Illustration of the overcut (3cm) and shield conicity (tail shield gap of 6cm) by geometrically defining smaller diameters than the excavation boundary.

tensile stresses is allowed (infinite normal stiffness in compression and zero stiffness in tension). Yet, due to numerical instabilities that are usually imposed by a "hard" contact, a "softened" exponential contact pressure – overclosure relationship was selected (Figure 4-i). In that case the stress transfer initiates when the distance (opening) between the two surfaces in the normal direction is lower than c_0 and it becomes equal to p_0 for zero opening. The normal stiffness of the interface is equal to the slope of the curve. The values of the parameters c_0 and p_0 have been calibrated via parametric numerical analyses for simplified models in the same stress range as the actual model, ensuring the numerical stability of the model and at the same time the accurate simulation of the stress transfer. In the frame of the paper the interaction between the shield and the surrounding soil is assumed to be frictionless without any developed shear stiffness between the two surfaces.

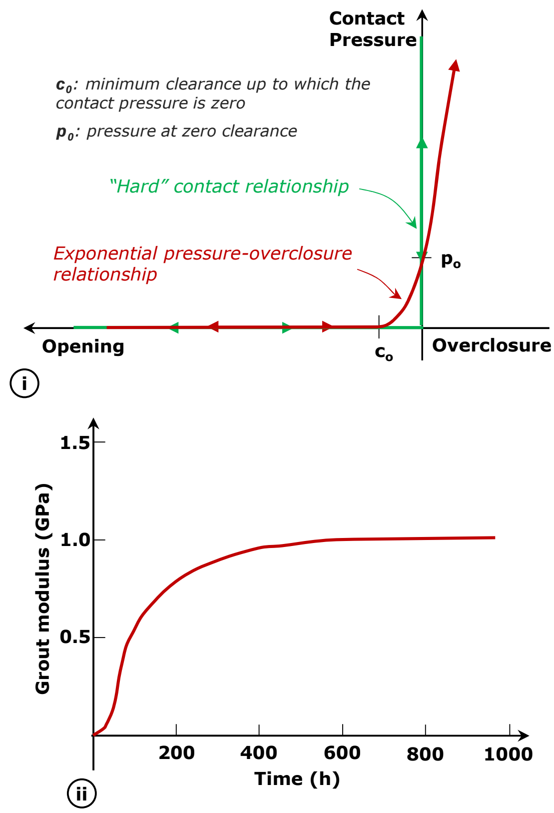

Figure 4. (i) "Hard" contact and "Softened" exponential pressure - overclosure relationship (Abaqus, 2011) (ii) time-dependent elastic modulus of the grout according to Kasper and Meschke (2004).

Mechanized tunnelling involves many different excavation and construction stages (lining installation, TBM advance, grouting, etc.). Thus, analysis steps have a repetitive pattern of substages until the end of the analysis. Figure 5 depicts an indicative representation of a typical step.

- The slice "n" is removed (the dimension of each slice in the longitudinal direction is equal to the width of a segment, i.e. 1.50m).
- Trapezoidal face pressure is applied to the new face location (face of the excavation slice "n+1").
- Due to the advance of the machine, the ring "n-7" that was inside the shield is "left" behind and another ring "n-6" is activated inside the shield (Figure 5-iii) without any interaction with the surrounding shield components.
- In the cavity between the segmental ring "n-7" and the surrounding soil the grout elements are activated (the grout slice "n-7" is depicted in green color in Figure 5-iv. Initially the grout is a fluid under pressure and it is modelled by increasing the value of its isotropic pressure equal to the value of the grout pressure (Lambrughi et al., 2012). The grout material hardens according to Figure 4-ii. Thus, an advance rate of 18m/day has been assumed in order to determine the time dependent grout parameters for every analysis step. It is noted that the stiffness of the grout elements is calculated in the undeformed configuration, since the numerical analyses performed assume linear geometry and therefore the decrease of the grout thickness or the pre-convergence ahead of the tunnel face due to the soil convergence is not taken into account.

Figure 6-i depicts the movements of a specific soil reference node on the tunnel crown as the TBM passes this location and Figure 6-ii the developed pressure on the shield when the soil node attaches it (Litsas et al., 2014). It is evident that due to the relaxation of the advanced core, pre-displacements are developed ahead of the tunnel face and furthermore the removal of a ground "slice" de-confines the surrounding ground which is also translated into an uplift of the TBM. In the first step after the excavation of the specific slice the soil and the shield are not in contact and the pressure in the interface is practically zero. In the second step the interface closes and a rapid increase of the transferred pressure is evident. The continuous decrease of the applied pressure on the shield as the excavation advances is a result of the shield conicity. In the step where the last node of the shield passes from the reference soil node, the interface opens again, due to the applied grout pressure in the next ring. The applied grout pressure pushes upwards the excavation boundary leading to a detachment between the tunnel boundary and the shield. This is a procedure that also allows the numerical calculation of the pressure on the shield skin, which can be used for the estimation of the necessary thrust forces for a TBM advance. This tool may be also valuable in a deep tunnel simulation as well, for the estimation of the probability of the TBM entrapment.

Useful conclusions can also be drawn by Figure 7, which shows the contours of ground displacements. It is evident that the tunnel invert of the model exhibits an uplift due to the ground de-confinement, while the tunnel crown and the surface settles as the machine proceeds. This uplift is also a result of the use of Mohr-Coulomb model for the simulation of the soil behaviour. Mohr-Coulomb is a linearly elastic - perfectly plastic model with constant stiffness parameters for the elastic behaviour and therefore it cannot capture the non-linear elastic behaviour of soils and rocks, leading to an overestimation of the upwards movement due to soil excavation. This is more intense in case of shallow excavations and it must be considered in the calculation of settlements via numerical analyses. Figure 7-iii shows the developed plastic deformations, which are mainly concentrated on the sides of the tunnel, since $k_0 = 0.50 < 1.0$, while the rest of the model remains elastic. The soil at the tunnel face remains in the elastic region due to the high value of the applied face pressure.

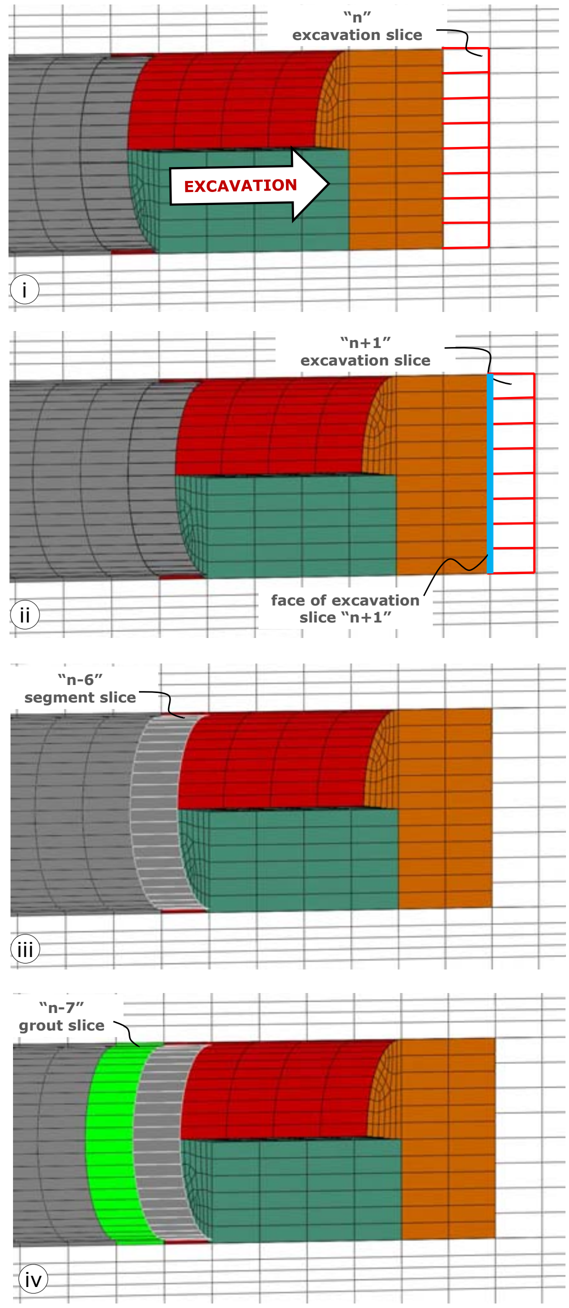

Figure 5. Indicative illustration of the substages in a typical analysis step "n": (i) excavation of slice "n" (ii) face pressure on the "n+1" (iii) slice activation of the ring "n-6" in the shield (iv) activation of the "n-7" slice of the grout.

Similarly, Figure 8-i plots the longitudinal settlement profile of the surface, crown and bottom of the tunnel and Figure 8-ii the evolution of the surface settlements as the excavation advances. The longitudinal settlement profiles reach a steady-state 10R behind the tunnel face. However, only slight differences are observed between the settlement trough of the y/R=5 and y/R=10 behind the tunnel face. The final surface settlement trough results in an inflection point value and volume loss value of 1.2R and 1.21% respectively.

3. Simulation of the segmental lining

Typical shield TBM tunnels are supported using precast concrete segmental linings. A typical segmental lining ring usually consists of five to seven segments and one key-element which is smaller than the others and is installed at the end to complete and stabilize the ring. The main characteristic of a segmental lining is the high degree of jointing. The joints are distinguished to (a) ring joints between the rings

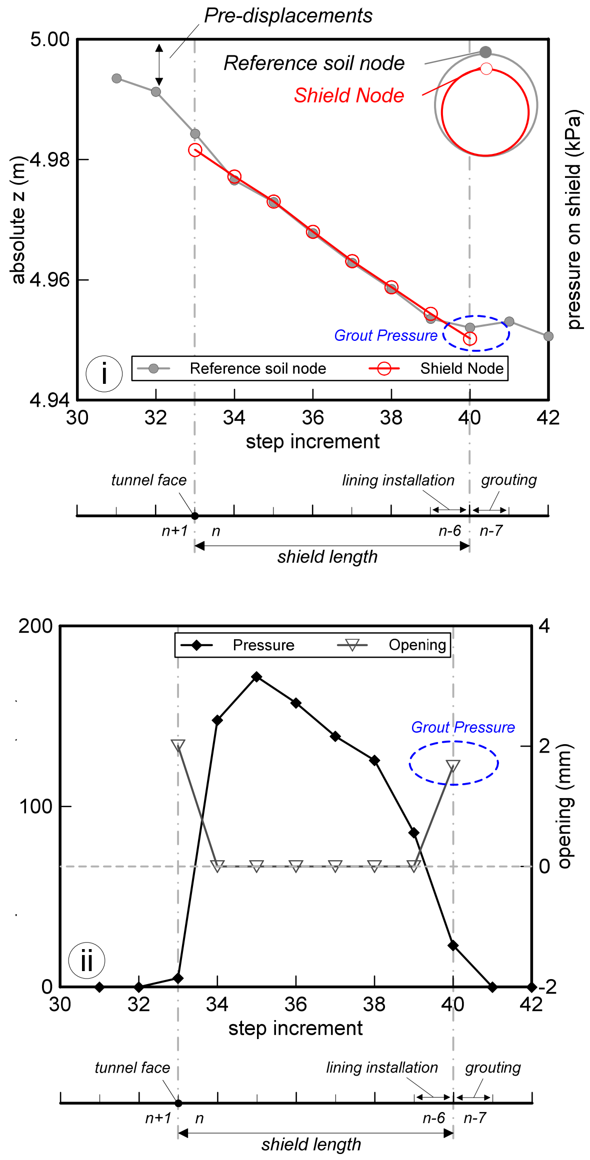

Figure 6. (i) Position of a specific soil reference node on tunnel crown and the nodes of the shield in different steps (ii) applied pressure on the shield and opening of the interface.

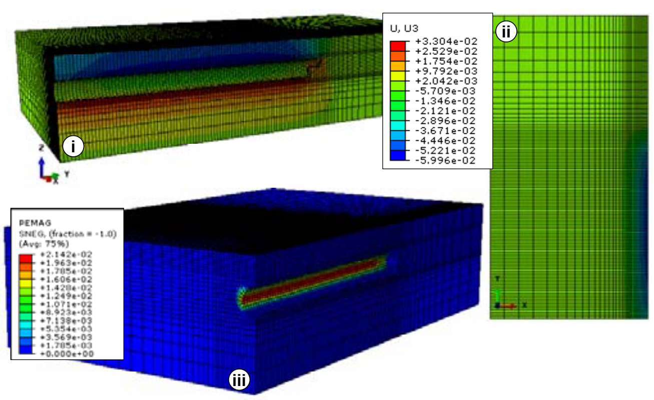

Figure 7. Indicative contour plots from the numerical analyses in ABAQUS: (i) general view of the vertical displacements (ii) plan view of the surface settlements (iii) plastic strain in the surrounding soil of the model.

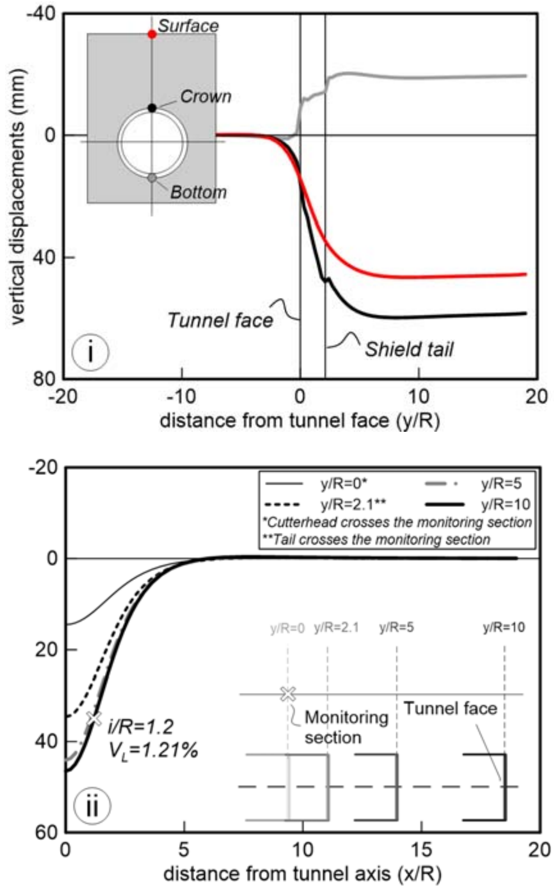

Figure 8. (i) Longitudinal displacements profile at the surface, bottom and crown of the tunnel (ii) evolution of surface settlement trough as the machine proceeds.

and (b) longitudinal joints between the segments of a ring (Figure 9). Longitudinal joints are created by the contact between the segments in order to form a segmental ring and they mostly work in compression (Luttikholt, 2007). On the other hand, ring joints connect the segmental rings with the adjoining ones.

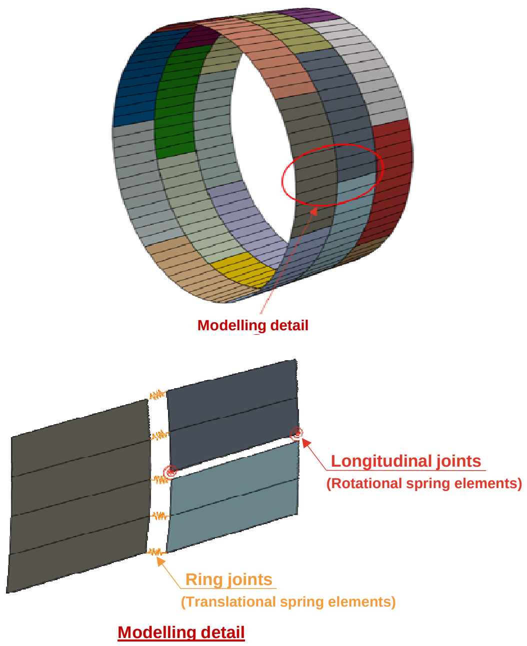

Figure 9. Detailed illustration of the numerical simulation of the segmental lining in ABAQUS; the longitudinal and ring joints have been modelled with JOINTC elements (Litsas et al., 2015).

Due to the complexity of the modelling, segmental linings are usually designed in a simplified way either as a continuous cylindrical shell, without taking into consideration the rotational stiffness of the longitudinal and ring joints between adjacent segments or neglecting the staggered configuration of the longitudinal joints (Figure 9). However, a realistic simulation of the real behaviour of the joints should be taken into account within the structural analyses of segmental lining (Do et al., 2013; Klappers et al., 2006).

In this section a set of 3D numerical analyses has been carried out assuming that the tunnel lining is loaded by the initial geostatic stress field, neglecting the de-confinement due to the pre-convergence. The segmental lining is modelled combining shell elements (S4) and JOINTC elements, which are ideal to model joint interactions, e.g. longitudinal and ring joints. Specifically, JOINTC elements simulate the interaction between two geometrically coincidental nodes, representing a joint with internal stiffness so that the second node of the joint can move and/or rotate with respect to the first node (Abaqus, 2011). The behaviour of such joints is fully defined by six internal stiffness variables (3 rotational and 3 translational). However, as depicted in Figure 9, emphasis is given on the rotational stiffness around the tunnel axis for the longitudinal joints and on the shear stiffness for the ring joints. The rotational stiffness of the longitudinal joint is calculated via 2D analyses assuming a compressive normal force 2000kN (Litsas et al., 2015). The resulted rotational stiffness is compared with analytical solutions (Blom, 2002; Janssen, 1983) in Figure 10-ii giving a sufficiently good correlation.

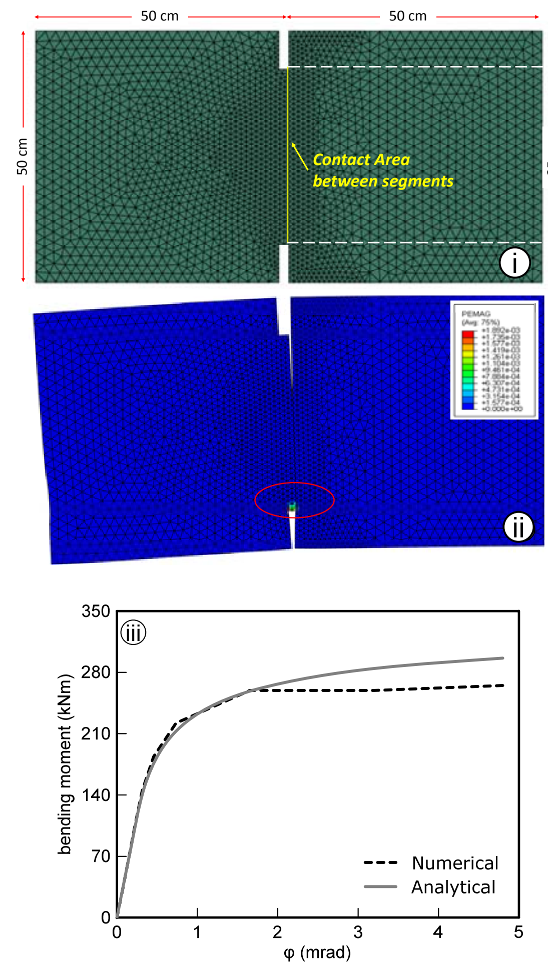

Figure 10. (i) Numerical simulation of the longitudinal joint behaviour in ABAQUS (ii) plastic strain in the concrete at the end of the analysis (iii) comparison between numerical analysis results and analytical solution (Blom, 2002; Janssen, 1983) for the rotational stiffness of the longitudinal joint (Litsas et al., 2015).

Three different assumptions have been made for the lining simulation: a) continuous shell b) simulation of the joints in a staggered pattern, i.e. rotated joints and c) simulation of the joints in a non-staggered pattern, i.e. non rotated joints. Regarding the connection between two successive rings different approaches may be adopted, such as bolts, dowels and bicones influencing the shear stiffness and the interaction between the rings. Furthermore, an experimental research on the shear stiffness between rings was presented by Gijsbers and Hordijk (1997) concluding that the shear stiffness can be assumed constant (linear behaviour) and it is strongly dependent on the applied normal force. Therefore, a sensitivity analysis was performed with two different values for the shear stiffness to investigate the role of this parameter. The parameters of the analyses are presented in Table 3.

Table 3. Parameters for the numerical analysis of the segmental lining.

Parameters	Values	Units
Overburden height (H/D) *(from tunnel axis)*	2	-
Soil unit weight (γ)	20	(kN/m^3)
Elastic modulus of soil (E)	30	(MPa)
Coefficient of lateral earth pressure (k_0)	0.5	-
Tunnel diameter (D)	8	m
Segmental lining thickness (h)	0.5	m
Segmental ring length (b)	1.5	m

Figures 11 and 12 depict the results of the analyses for the assumption of "higher value" of shear stiffness. Figure 11-i shows the bending moment envelope and Figure 11-ii the normal force envelope of the segmental lining. It is evident that, the assumption of the inline configuration compared to the case of rotated joints makes the segmental lining system more flexible and results in significantly smaller developed bending moments. The case of rotated joints results to similar values of maximum and minimum bending moments with the continuous shell, since the rotation of the joints in one ring is partially restrained by the connection with the adjacent rings where the joints are in different positions. This is also shown in the contour plots in Figure 12. Regarding the normal forces all the approaches lead to similar results, since they are not influenced significantly by the decreased rotational stiffness (Figure 11-ii).

The results of the scenario of "lower" shear stiffness of the ring joints are shown in Figure 13. The overall stiffness of the segmental lining decreases by reducing the shear stiffness of the ring joints and consequently the developed bending moments are generally lower than the first scenario. However, the internal forces of the "non-rotated joints" case in both scenarios lead to similar results. Since the overall stiffness of this case follows same pattern in the longitudinal direction due to the inline configuration of the longitudinal joints, the change of the shear stiffness of the ring joints does not influence its response.

4. Conclusions

The present paper describes a set of numerical analyses techniques for the realistic simulation of mechanized tunnelling, taking into account most of the critical components of the procedure. Regarding the excavation procedure the presented approach can provide realistic calculation of the displacements around the tunnel, the settlements, the pressure applied on the shield and the final load on the tunnel lining. The results from simplified approaches can only be assumed realistic in specific cases; for example when the total tunnel convergence after the excavation is lower than the shield overcut. Regarding the simulation of the segmental lining it is evident that the simulation of the actual configuration of the segments can lead to the optimization of the lining design.

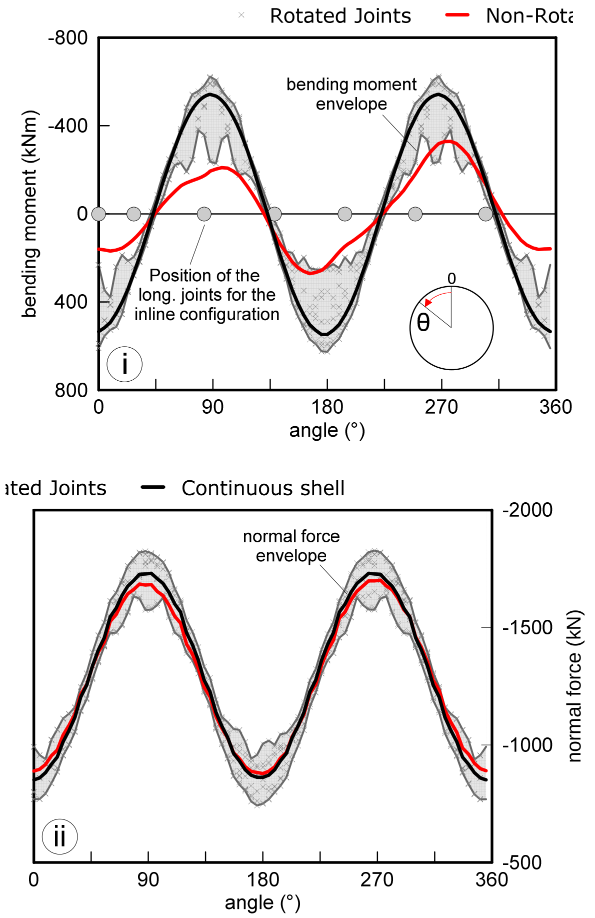

Figure 11. Internal forces in the segmental lining assuming continuous cylindrical shell, rotated and non-rotated joints configuration ("higher value" of shear stiffness in the ring joints).

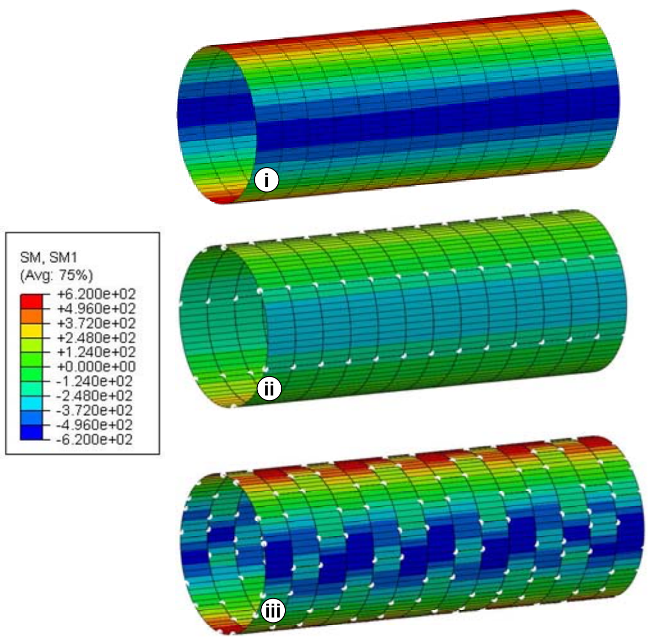

Figure 12. Contour plots of the bending moments for (i) continuous shell (ii) rotated and (iii) non-rotated joints ("higher value" of shear stiffness in the ring joints).

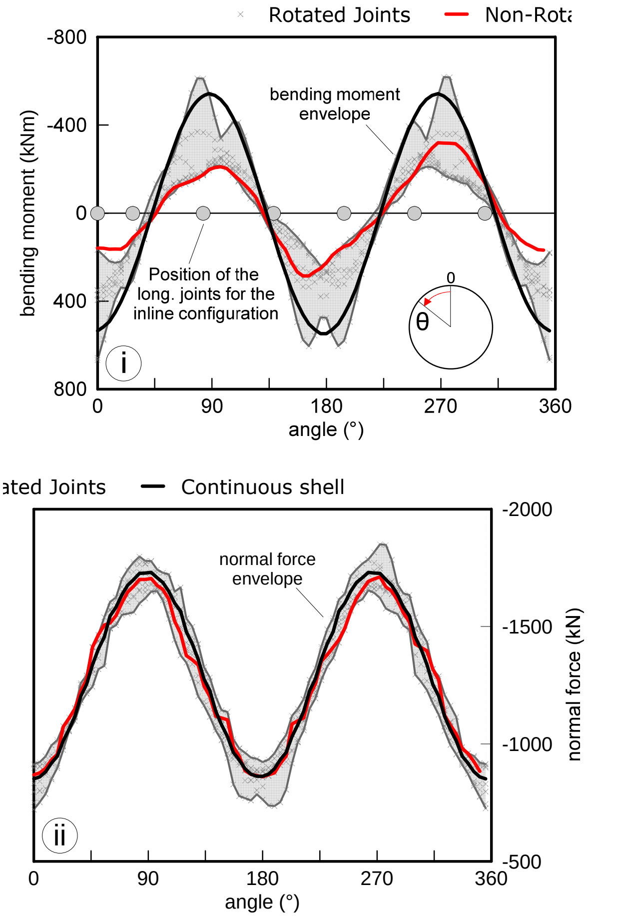

Figure 13. Internal forces for the segmental lining assuming continuous cylindrical shell, rotated and non-rotated joints configuration ("lower value" of shear stiffness in the ring joints).

However, there is space for further improvement of the simulation in order to capture additional elements of the tunnelling procedure that may be significant in some cases. Some characteristic examples are the following:

Implementation of more sophisticated constitutive models for the simulation of soil/rock behaviour. The main focus in this direction should be towards models with non-linear elastic behaviour to decrease the non-realistic development of upwards displacements induced by Mohr-Coulomb.

Coupled analysis for the simulation of the actual hydraulic conditions and the distribution of the pore pressures due to the tunnel advancement.

Assumption of non-linear geometry for the simulation of the actual stiffness of all the elements in the deformed configuration. The influence of the non-linear geometry is significant mainly in deep tunnels and squeezing ground conditions (Vrakas and Anagnostou, 2014).

Remeshing techniques for the simulation of the actual excavation boundaries and the actual stress and strain distribution. The influence of remeshing is also significant mainly in squeezing ground conditions.

Acknowledgements

This research was carried out in the frame of the research programme "NeTTUN: New Technologies for Tunnelling and UNderground works" which is supported by the European Commission under the 7th Framework Programme (FP7). The writers would like to acknowledge Ilias Michalis, Senior Geotechnical and Tunnel Expert at Qatar Rail for his constructive comments.

References

Abaqus, D., 2011. ABAQUS/Standard Analysis User's Manual. USA.

Blom, C., 2002. Design philosophy of concrete linings for tunnels in soft soils, Design Philosophy of Concrete Linings for Tunnels in Soft Soils.

Do, N.A., Dias, D., Oreste, P., Djeran-Maigre, I., 2013. Three-dimensional numerical simulation for mechanized tunnelling in soft ground: the influence of the joint pattern. Acta Geotech. 1-22. doi:10.1007/s11440-013-0279-7

Gens, A., 1995. General report: Prediction, performance and design. Pre-failure Deform. Geomaterials 2, 1233-1256.

Gijsbers, F.B.J., Hordijk, D.A., 1997. Experimenteel onderzoek naar het afschuifgedrag van ringvoegen, CUR/COB K11-W-001.

Janssen, P., 1983. Tragverhalten von Tunnelausbauten Mit Gelenktübbings. Technischen Universitat Carolo-Wilhelmina, Braunschweig.

Kasper, T., Meschke, G., 2006. On the influence of face pressure, grouting pressure and TBM design in soft ground tunnelling. Tunn. Undergr. Sp. Technol. 21, 160-171. doi: 10.1016/j.tust.2005.06.006

Kasper, T., Meschke, G., 2004. A 3D finite element simulation model for TBM tunnelling in soft ground. Int. J. Numer. Anal. Methods Geomech. 28, 1441-1460. doi:10.1002/nag.395

Klappers, C., Grübl, F., Ostermeier, B., 2006. Structural analyses of segmental lining - coupled beam and spring analyses versus 3D-FEM calculations with shell elements. Tunn. Undergr. Sp. Technol. 21, 254-255. doi:10.1016/j.tust.2005.12.116

Lambrughi, A., Medina Rodríguez, L., Castellanza, R., 2012. Development and validation of a 3D numerical model for TBM-EPB mechanised excavations. Comput. Geotech. 40, 97-113. doi:10.1016/j.compgeo.2011.10.004

Litsas, D., Pateriannaki, G., Kavvadas, M., 2015. Investigation of the influence of cracking on the stiffness and capacity of segmental tunnel lining, in: Promoting Tunnelling in See Region, WTC 2015 (Submitted).

Litsas, D., Rachmani, A., Fortsakis, P., Kavvadas, M., 2014. 3D Numerical simulation of shield tunnelling with emphasis on the influence of the tail gap, in: Tunnelling in a Challenging Environment: Proceedings of the 2nd Eastern European Tunnelling Conference. Athens, Greece, pp. 1-9.

Luttikholt, A., 2007. Ultimate Limit State Analysis of a Segmented Tunnel Lining - Results of Full-scale Tests Compared to Finite Element Analysis, Ultimate Limit State Analysis of A Segmented Tunnel Lining - Results of Full-Scale Tests Compared to Finite Element Analysis.

Sitarenios, P., Litsas, D., Papadakos, A., Kavvadas, M., 2015. Effect of Hydraulic Conditions in controlling the Face in EPB Excavated Tunnels, in: SEE Tunnel: Promoting Tunneling in SEE Region. Proceedings of the 41st World Tunnel Congress. Dubrovnik, Croatia.

Vrakas, A., Anagnostou, G., 2014. Relationship between the results of small and large strain elastoplastic analyses of deep tunnels, in: Computer Methods and Recent Advances in Geomechanics. CRC Press, pp. 1975-1980. doi: 10.1201/b17435-351.

(το άρθρο παρουσιάσθηκε από τον δεύτερο των συγγραφέων στο ATC 2015 Arabian Tunnelling Conference & Exhibition 2015, 23-25 November 2015, Dubai, Unaited Arab Emirates, http://www.atcita.com)

ΔΙΑΚΡΙΣΕΙΣ ΕΛΛΗΝΩΝ ΜΗΧΑΝΙΚΩΝ

Σπάνια διάκριση Ελληνίδας φοιτήτριας σε διαγωνισμό των Ηνωμένων Εθνών.

Η φοιτήτρια του Πολυτεχνείου Κρήτης Νάντια Ανθούλη απέσπασε σημαντική διάκριση σε παγκόσμιο διαγωνισμό.

Σύμφωνα με δημοσίευμα του ekriti.gr η Νάντια Ανθούλη είναι τελειόφοιτος της Σχολής Αρχιτεκτόνων Μηχανικών – Πολυτεχνείου Κρήτης και διακρίθηκε στο διαγωνισμό για την καλύτερη αφίσα, που διοργάνωσαν τα Ηνωμένα Έθνη, με αφορμή την 70η επέτειο εξάλειψης των πυρηνικών όπλων και των όπλων μαζικής καταστροφής.

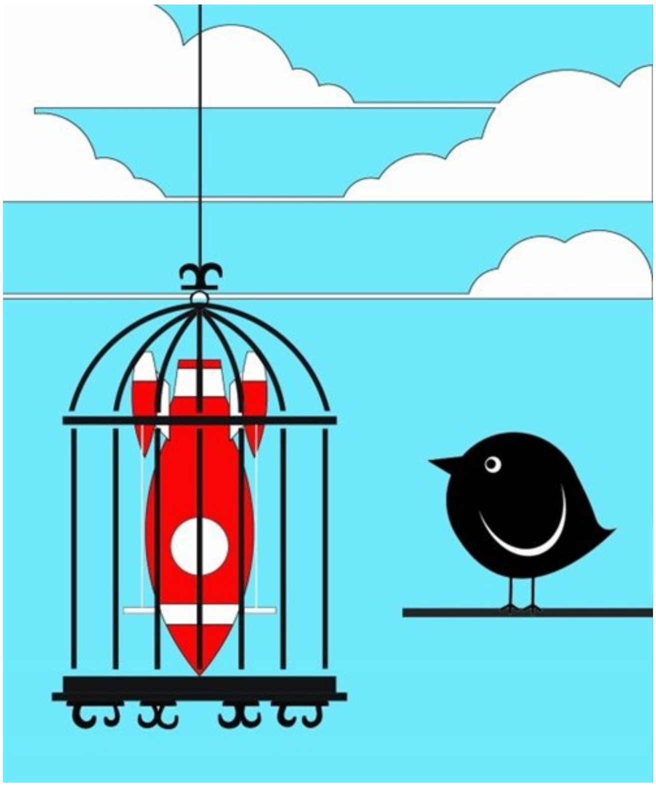

Το θέμα πάνω στο οποίο δούλεψε ήταν κατά των πυρηνικών και το σκίτσο της ήταν απλό και κατανοητό. Στο κλουβί τα πυρηνικά και ελεύθερο το πουλί.

(Κέρδος online / www.kerdos.gr, 11.03.2016)

ΝΕΑ ΑΠΟ ΤΙΣ ΕΛΛΗΝΙΚΕΣ ΚΑΙ ΔΙΕΘΝΕΙΣ ΓΕΩΤΕΧΝΙΚΕΣ ΕΝΩΣΕΙΣ

Volume 18 - December 2015 of the ISRM News Journal is now online

The December 2015 issue of the ISRM News Journal is now available. With Prof. Hudson’s decision to step down after eight years as Editor of the News Journal, an associated modification of the Editorship was required. The new Editors of the ISRM News Journal are Dr Eda Quadros, ISRM President, and Dr José Muralha.

This issue of the News Journal includes the ISRM activities in 2015, a year that saw a new Board being elected and starting its term of office. You will find information about the Board and Council meetings, an article by the previous ISRM President Xia-Ting Feng on the accomplishments of the 2011–2015 Board, the inaugural address of the current ISRM President Eda Quadros, a report of the Technical Oversight Committee on the work done by the Commissions during the last 4 years, reports of events that took place in 2015 and announcements of futures events, reports of the Vice Presidents and many other articles of interest for the rock mechanics fraternity. Two technical articles are presented: the Müller Lecture 2015 given by Prof. John Hudson and the Rocha Medal presentation by Andrea Lisjak Bradley, winner of the Rocha Medal 2015.

The ISRM News Journal is distributed to all members in electronic version. We also print a few copies of the News Journal, which are available at our sponsored symposia. Click here to read it directly on our website or download it.

13th ISRM online lecture by Prof. Peter Kaiser is now online

For the 12th ISRM Online Lecture the ISRM invited Professor **Peter Kaiser** and the title is **“Challenges in rock mass strength determination for the design of underground excavations”**. The lecture was broadcast on 15 March and remains available in a dedicated webpage (https://www.isrm.net/gca/?id=1104).

Dr. Peter Kaiser is a graduate of the Federal Institute of Technology in Zurich, Switzerland, and the University of Alberta in Edmonton, Canada. Since 1987 until his recent retirement, he was Professor and Chair for Rock Engineering and Ground Control at the Bharti School of Engineering of Laurentian University in Sudbury, Canada. In 2000, he was seconded to the Centre for Excellence in Mining Innovation (CEMI) as Founding Director and then as Director of the Rio Tinto Centre for Underground Mine Construction (RTC-UMC). He also holds an Adjunct Professorship at the University of Waterloo in Canada.

Dr. Kaiser is the author of more than 300 technical and scientific geomechanics publications. He has received many awards including, early in his career, the ISRM Schlumberger award in 1993, awards from the Canadian Geotechnical Society and from the Canadian Institute of Mining. He is a Fellow of the Engineering Institute of Canada (EIC) and the Canadian Academy of Engineers and, in 2013, was awarded the Julian C. Smith Medal of for his "Achievements in the Development of Canada" and was named the “Tunneller of the Year” by the Tunnelling Association of Canada. He was recently selected to present the Sir Allan Muir Wood lecture at the WTC 2016 in San Francisco on “Ground Support for the Constructability of Deep Underground Excavations”.

He is a specialist in applied research for underground construction and mining. His interests lie in geomechanics, mine design, rock engineering and the application of innovative technologies to increase mine safety and productivity. He brings extensive experience from both the industrial and academic sectors, having served as consultant to numerous consulting companies, mines, and public agencies. He has supported contractors, mining companies and public sector clients during Coroner’s inquests and litigations on four continents.

Rock Mechanics Principles, an on-line video course by Professor Jian Zhao available from the ISRM website

Rock Mechanics Principles, an on-line course by Professor Jian Zhao, provides an introduction to rock mechanics principles including the mechanics of rock materials, rock joints and rock masses, rock mechanics characterisation and rock mass classifications. The course is prepared for students studying civil and mining engineering, and other science and engineering disciplines concerning rocks.

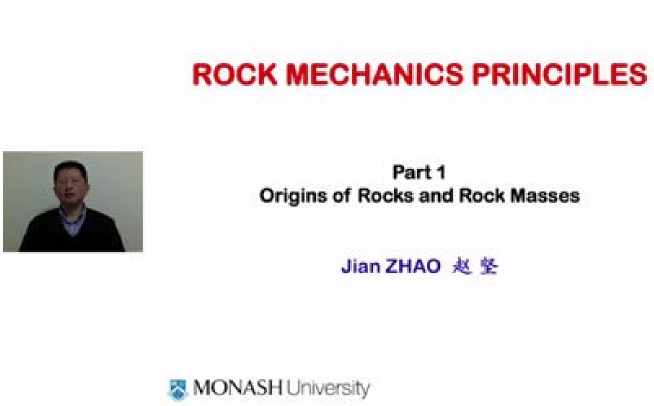

The course is an on-line course, with approximately 30 hours of lectures. It covers 5 parts:

1. Origin of rocks and rock masses (online in March 2016);
2. Properties and mechanics of rock materials (online in March 2016);
3. Properties and mechanics of rock joints (online in June 2016);
4. Rock mass classifications and properties (online in June 2016);
5. Rock mechanics testing and analysis (to be released later).

The lectures are given by Professor Jian Zhao, who has been teaching rock mechanics and rock engineering since 1990, first at Nanyang Technological University of Singapore, then at Ecole Polytechnique Fédérale de Lausanne of Switzerland, and currently at Monash University in Melbourne of Australia. He is a Fellow of the International Society for Rock Mechanics since 2015.

Rock Engineering, a sequential on-line course to Rock Mechanics Principles given by the same lecturer will be made available in near future.

Click here to go to the online course webpage in the ISRM website.

ISRM Suggested Methods videos now on the website

Based on the cooperation between Prof. Seokwon Jeon from Seoul National University (South Korea) and the ISRM Commissions on Testing Methods and on Education, video films on the ISRM Suggested Methods, which are made for educational purposes, started being embedded on the website of the Commission on Testing Methods.

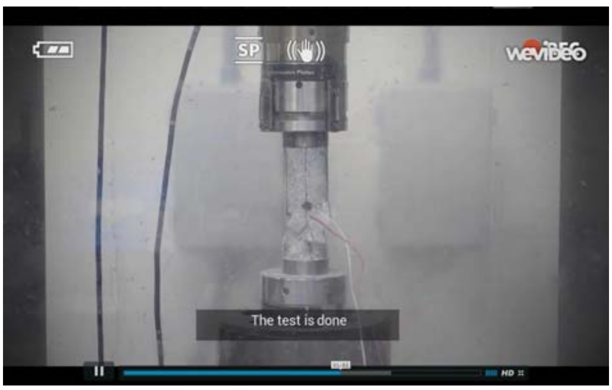

This initiative is an attempt to provide detailed explanations on the ISRM Suggested Methods. The video films are being recorded from the experiments conducted in the Rock Mechanics and Rock Engineering Laboratory of the Seoul National University.

The first video film is on the determination of "Uniaxial Compressive Strength and Deformability of Rock Materials" and is now online. New video films on other Suggested Methods will also appear on the website in near future.

Click here to go to the ISRM Suggested Methods videos webpage.

Public domain rock mechanics research reports

Publicly funded research programmes such as NIOSH in the USA and SIMRAC (MHSC) in South Africa provide free (or at a nominal fee) access to research reports and products on their websites. There must be many more public research domains in different fields of rock mechanics and in different countries. The ISRM would like to create a portal, which will create awareness about and access to public domain rock mechanics research. This portal could assist students and researchers in general. We would like to appeal to all members to provide information and links to public domain research websites. Please send information to the ISRM Secretariat: secretariat@isrm.net.

Digital Library at OnePetro

The ISRM Digital Library makes available to the Rock Mechanics community worldwide the materials published in the ISRM Congresses and sponsored Symposia.

The ISRM Digital Library is part of OnePetro, a large online library managed by the Society of Petroleum Engineers. Papers from more than thirty ISRM Congresses and sponsored Symposia are available (click here for an up to date list) and more are gradually regularly introduced in the Library.

At the beginning of every year, ISRM individual members registered on the ISRM website must follow these instructions to download, at no cost, up to 100 papers from the ISRM conferences.

ΑΝΑΣΚΟΠΗΣΗ ΓΕΓΟΝΟΤΩΝ ΓΕΩΤΕΧΝΙΚΟΥ ΕΝΔΙΑΦΕΡΟΝΤΟΣ ΣΤΗΝ ΕΛΛΑΔΑ

ΕΛΛΗΝΙΚΗ
ΕΠΙΣΤΗΜΟΝΙΚΗ
ΕΤΑΙΡΕΙΑ
ΕΔΑΦΟΜΗΧΑΝΙΚΗΣ
& ΓΕΩΤΕΧΝΙΚΗΣ
ΜΗΧΑΝΙΚΗΣ

10η Αθηναϊκή Διάλεξη Γεωτεχνικής Μηχανικής

Με μεγάλη προσέλευση μελών της ΕΕΕΕΓΜ και συναδέλφων παρουσιάσθηκε στις 23 Φεβρουαρίου 2016 στην Αίθουσα Τελετών του Κτιρίου Διοίκησης του Εθνικού Μετσοβίου Πολύτεχνείου στην Πολυτεχνειούπολη Ζωγράφου η 10η Αθηναϊκή Διάλεξη Γεωτεχνικής Μηχανικής από τον Δρα Σπύρο Καβουνίδη με θέμα "**ΚΑΤΟΛΙΣΘΗΣΕΙΣ ΣΤΗΝ ΕΛΛΑΔΑ. Εδαφομηχανική στην Πράξη**".

Την διάλεξη καθώς και την παρουσίαση του ομιλητή από τον πρόεδρο της ΕΕΕΕΓΜ καθηγητή ΕΜΠ κ. Γ. Γκαζέτα και την αποφώνηση από τον ομότιμο καθηγητή ΕΜΠ κ. Π. Μαρίνο μπορείτε να την παρακολουθήσετε στον παρακάτω σύνδεσμο

https://www.youtube.com/watch?v=KI6yi8WIK6c

ΠΡΟΣΕΧΕΙΣ ΕΚΔΗΛΩΣΕΙΣ ΣΤΗΝ ΕΛΛΑΔΑ ΓΕΩΤΕΧΝΙΚΟΥ ΕΝΔΙΑΦΕΡΟΝΤΟΣ

Ημερίδα με θέμα την Γέφυρα Τσακώνας

Με αφορμή την ολοκλήρωση των εργασιών και την απόδοση στην κυκλοφορία της Γέφυρας Τσακώνας στον Αυτοκινητόδρομο Κορίνθου – Τρίπολης – Καλαμάτας, η Ειδική Υπηρεσία Δημοσίων έργων Κατασκευής και Συντήρησης Συγκοινωνιακών Υποδομών (ΕΥΔΕ ΚΣΣΥ) διοργανώνει ημερίδα, την Τετάρτη 11 Μαΐου 2016, με θέμα: «Η Γέφυρα Τσακώνας».

Η ημερίδα θα διεξαχθή στην Αθήνα, στο Αμφιθέατρο του Υπουργείου Υποδομών, Μεταφορών & Δικτύων, Αναστάσεως 2 και Τσιγάντε, Παπάγου (δίπλα στη στάση του μετρό "Εθνική Άμυνα"). Ακολουθεί το πρόγραμμα της ημερίδας:

09:00-09:15 Προσέλευση

09:15-09:30 Χαιρετισμοί

09:30-09:45 Ιστορικό – Διαχείριση Έργου
Α. Πολάκις, Πολ. Μηχ. Διευθυντής ΕΥΔΕ Κατασκευής και Συντήρησης Συγκοινωνιακών Υποδομών

09:45-10:15 Η κατολίσθηση Τσακώνας και η επιλογή της λύσης γέφυρας

- Η κατολίσθηση
  Σ. Καβουνίδης, Δρ. Πολ. Μηχ., Γ. Ντουνιάς, Δρ. Πολ. Μηχ., Λ. Σωτηρόπουλος, Γεωλόγος, ΕΔΑΦΟΣ ΑΕ
- Η επιλογή της λύσης γέφυρας και η αντιμετώπιση της κατολίσθησης - Αποστραγγιστικά έργα
  Γ. Ντουνιάς, Δρ Πολ. Μηχ., Ι. Φίκιρης, Πολ. Μηχ. MSc., ΕΔΑΦΟΣ ΑΕ
  Μ. Βλαχογιάννης, Πολ. Μηχ., ΣΥΣΤΑΣ ΑΕ, Α. Δραγομάνοβιτς, Πολ. Μηχ.

10:15-11:15 Βασικά στοιχεία σχεδιασμού της γέφυρας

- Σύλληψη και σχεδιασμός, εναλλακτικές λύσεις, κριτήρια επιλογής του τύπου της γέφυρας
  Σ. Σταθόπουλος, Δρ. Πολ. Μηχ., Π. Κοτσανόπουλος, Πολ. Μηχ. MSc., ΔΟΜΗ ΑΕ
- Στοιχεία ανάλυσης, μεθοδολογία ανέγερσης
  Κ. Σταθόπουλος, Δρ. Πολ. Μηχ., Σ. Βλάχος, Πολ. Μηχ. MSc., Π. Θανόπουλος, Δρ. Πολ. Μηχ., ΔΟΜΗ ΑΕ
- Θεμελιώσεις
  Ι. Φίκιρης, Πολ. Μηχ. MSc., ΕΔΑΦΟΣ ΑΕ, Ι. Σπυρόπουλος Δρ. Πολ. Μηχ., ΔΟΜΗ ΑΕ

11:15-11:45 ΔΙΑΛΕΙΜΜΑ

11:45-13.15 Κατασκευή

- Οργάνωση κατασκευής
  Ν. Ντονάς, Πολ. Μηχ., ΤΕΡΝΑ ΑΕ
- Κατασκευή στοιχείων από σκυρόδεμα (θεμέλια, βάθρα, αντηρίδα, προεντεταμένος φορέας)
  Ν. Ντονάς, Πολ. Μηχ., Γ. Τσίρμπας Πολ. Μηχ., ΤΕΡΝΑ ΑΕ, Κ. Σεφέρογλου Πολ. Μηχ., Ι. Βασιλοπούλου Πολ. Μηχ., ΟΔΟΤΕΧΝΙΚΗ ΕΠΕ
- Εργοστασιακή κατασκευή τόξου, καταστρώματος και αναρτήρων
  Ν. Ντονάς, Πολ. Μηχ., Ν. Αλατζόγλου, Μηχ. Μηχ., Η. Σαραντίδης, Μηχ. Μηχ., ΤΕΡΝΑ ΑΕ, Γ. Αθανάσουλας, Αχ. Πατσιούρας, Μηχ. Μηχ., ΕΜΕΚ ΑΕ, Κ. Λιαρομάτης, Ι. Λιαρομάτης Μηχ. Μηχ., Π. Αγγελόπουλος, Μηχ. Μηχ. ΤΕ, ΛΙΑΡΟΜΑΤΗΣ ΑΕ
- Ανέγερση τόξου, αφαψίδωση, εγκατάσταση αναρτήρων και καταστρώματος, ρυθμίσεις
  Ν. Ντονάς, Πολ. Μηχ., Ν. Αλατζόγλου, Μηχ. Μηχ., ΤΕΡΝΑ ΑΕ, Γ. Αθανάσουλας, Αχ. Πατσιούρας, Μηχ. Μηχ., ΕΜΕΚ ΑΕ
- Διαδικασίες συγκολλήσεων, ποιοτικός έλεγχος
  Κ. Ζαχαριάδης, Μηχ. Συγκολλήσεων, Ν. Σκρινή, Μηχ. Συγκολλήσεων, ΤΕΡΝΑ ΑΕ

13.15-13:30 Πρόγραμμα συντήρησης / Ενοργάνωση

- Μ. Λαριντζάκης, Μηχ. Μηχ., Set Point Technologies ΕΠΕ

13.30-14:15 ΕΡΩΤΗΣΕΙΣ – ΣΥΖΗΤΗΣΗ

Δήλωση συμμετοχής (απαραίτητη με τοτ στον αριθμό 210.6417502 ή με ηλ.τα. στην ηλ.δι. nisidr@kssy.gr μέχρι την Παρασκευή 6 Μαΐου) στον δικτυακό τόπο της Γενικής Γραμματείας Δημοσίων Έργων www.ggde.gr.

Μετά την ημερίδα οι παρουσιάσεις θα αναρτηθούν στον δικτυακό τόπο της Γενικής Γραμματείας Δημοσίων Έργων www.ggde.gr.

Διοργάνωση: ΕΥΔΕ Κατασκευής & Συντήρησης Συγκοινωνιακών Υποδομών. Τηλ: 2106417590, Fax: 2106417502, e-mail: nisidir@kssy.gr

ΠΡΟΣΕΧΕΙΣ ΓΕΩΤΕΧΝΙΚΕΣ ΕΚΔΗΛΩΣΕΙΣ

Για τις παλαιότερες καταχωρήσεις περισσότερες πληροφορίες μπορούν να αναζητηθούν στα προηγούμενα τεύχη του «περιοδικού» και στις παρατιθέμενες ιστοσελίδες.

GeoAmericas 2016 3rd Panamerican Conference on Geosynthetics, 11 – 14 April 2016, Miami Beach, USA, www.geoamericas2016.org

International Symposium on Submerged Floating Tunnels and Underwater Structures (SUFTUS-2016), 20-22 April 2016, Chongqing, China, www.cmct.cn/suftus

World Tunnel Congress 2016 "Uniting the Industry", April 22-28, 2016, San Francisco, USA, http://www.wtc2016.us

International Symposium "Design of piles in Europe - How did EC7 change daily practice?", 28-29 April 2016, Leuven, Belgium, www.etc3.be/symposium2016

7th In-Situ Rock Stress Symposium 2016 - An ISRM Specialised Conference, 10-12 May 2016, Tampere, Finland, www.rs2016.org

84th ICOLD Annual Meeting, 15-20 May 2016, Johannesburg, South Africa, www.icold2016.org

Infrastructure Summit 2016, 18 - 19 May 2016, London, United Kingdom, Ilya.Ryndin@emap.com

2nd International Conference on Rock Dynamics and Applications (RocDyn-2), 18 – 20 May 2016, Suzhou, China http://rocdyn.org

6th Annual Underground Infrastructure and Deep Foundations Qatar, 23–24 May 2016, Doha, Qatar, oliver.osea@iqpc.ae

13th International Conference Underground Construction Prague 2016 and 3rd Eastern European Tunnelling Conference (EETC 2016), 23 to 25 May 2016, Prague, Czech Republic, www.ucprague.com

GEOSAFE: 1st International Symposium on Reducing Risks in Site Investigation, Modelling and Construction for Rock Engineering - an ISRM Specialized Conference, 25 – 27 May 2016, Xi'an, China, www.geosafe2016.org/dct/page/1

14th International Conference of the Geological Society of Greece, 25-27 May, Thessaloniki, Greece, www.ege2016.gr

NGM 2016 - The Nordic Geotechnical Meeting, 25 - 28 May 2016, Reykjavik, Iceland, www.ngm2016.com

International Mini Symposium Chubu (IMS-Chubu) New concepts and new developments in soil mechanics and geotechnical engineering, 26 - 28 May 2016, Nagoya, Aichi, Japan, www.jiban.or.jp/index.php?option=com_content&view=article&id=1737:2016052628&catid=16:2008-09-10-05-02-09&Itemid

11th HSTA< International Congress on Mechanics – Mini-Symposium Computational Geomechanics from Micro to Macro, May 27-30, 2016, Athens, Greece, http://11hstam.ntua.gr

19SEAGC – 2AGSSEAC Young Geotechnical Engineers Conference, 30th May 2016, Petaling Jaya, Selangor, Malaysia, seagc2016@gmail.com

19th Southeast Asian Geotechnical Conference & 2nd AGSSEA Conference Deep Excavation and Ground Improvement, 31 May – 3 June 2016, Subang Jaya, Malaysia, seagc2016@gmail.com

ISSMGE TC211 Conference Session within the framework of the 19th Southeast Asian Geotechnical Conference "GROUND IMPROVEMENT works: Recent advances in R&D, design and QC/QA"

ISL 2016 12th International Symposium on Landslides Experience, Theory, Practice, Napoli, June 12th-19th, 2016, www.isl2016.it

2ο Πανελλήνιο Συνέδριο Εξόρυξης και Εναλλακτικών Μεθόδων Διαχείρισης Αποβλήτων, 15-16 Ιουνίου 2016, Αθήνα, www.erasmus.gr/microsites/1091

BCRRA 2017 Tenth International Conference on the Bearing Capacity of Roads, Railways and Airfields, 28 –30 June 2017, Athens, Greece, www.bcrra2017.com

ICONHIC 2016 1st International Conference on Natural Hazards and Infrastructure: Protection, Design, Rehabilitation, 28-30 June 2016, Chania, Greece, http://iconhic2016.com

ICONHIC 2016 Performance-based soil-structure interaction of lifelines and infrastructure, gerolymos@gmail.com, asextos@civil.auth.gr & a.sextos@bristol.ac.uk

4th GeoChina International Conference Sustainable Civil Infrastructures: Innovative Technologies for Severe Weathers and Climate Changes, July 25-27, 2016, Shandong, China, http://geochina2016.geoconf.org

S3: Slopes, Slides and Stabilization, August 1-3, 2016, Denver, USA, events@dfi.org

6th International Conference on Recent Advances in Geotechnical Earthquake Engineering and Soil Dynamics August 1-6, 2016, Greater Noida (NCR), India, www.6icragee.com

EUROC 2016 - ISRM European Regional Symposium Rock Mechanics & Rock Engineering: From Past to the Future, 29-31 August 2016, Ürgüp-Nevşehir, Cappadocia, Turkey http://eurock2016.org

ICEGE 2016 1st International Conference on Energy Geotechnics, 29-31 August 2016, Kiel, Germany, www.iceg-2016.de

3rd ICTG – 3rd International Conference on Transportation Geotechnics 4 - 7 September 2016, Guimaraes, Portugal, www.civil.uminho.pt/3rd-ICTG2016

IAS'5 5th International Conference on Geotechnical and Geophysical Site Characterisation, 5-9 September 2016, Gold Coast, Queensland, Australia, http://www.isc5.com.au

The World Multidisciplinary Earth Sciences Symposium–WMESS 2016, 5-9 September 2016, Prague, Czech Republic www.mess-earth.org

ACCUUS 2016 15th World Conference Underground Urbanisation as a Prerequisite for Sustainable Development, September 12-15, 2016, http://acuus2016.com

SAHC 2016 - 10th international Conference on Structural Analysis of Historical Constructions 13-15 September 2016, Leuven, Belgium, www.sahc2016.be

Flexible hydropower and pump storage generation for a safe renewable electricity system
http://www.wplgroup.com/aci/event/hydropower-development-europe-2016

ACI's Hydropower Development: Europe 2016 Summit, taking place on 14-15 September 2016 in Lyon, France will comprise two days of formal presentations, interactive panel discussions and excellent networking opportunities, providing an ideal setting to convene with your peers to discuss both current operational & future planned hydro power plants, energy markets reform, potential barriers & support policies as well as project economics & finance.

The two days conference will once again bring together senior executives and experts from: hydro power producers, regulatory bodies, engineers and researchers as well as other influential stakeholders to the hydro power industry to examine strategies & technologies to advance hydro power development.

The conference will have a heavy focus on case study examples of hydro power generation projects from leading plant owners as well as engineering contractors focusing on feasibility, planning, financing and technological developments.

Key Topics

- Hydropower of the Future – Adding Storage Capacity & Optimization to Renewable Integration
- How should Market Design for Hydropower Look under Uncertainty Surrounding the Legislative Framework?
- The Flexibility of Hydropower: From Strategy to Implementation
- Asset Management as the key to operations in Hydropower
- Sedimentation of Reservoirs: A Significant Threat in Sustainability
- Economy vs. Ecology
- An Inside in Hydropower Economics
- What Can Hydropower Operators Do to Efficiently Advance in Hydropower Development?
- The Role of Pumped Storage in Energy Storage Arena
- Energy Production and Overcoming Barriers in Small Hydro Development
- Highlighting the Innovative Solutions for a Modern Hydropower Industry

Contact
Stergios Zacharakis
+44 (0) 20 3141 0609
szacharakis@acieu.net

13 Baltic States Geotechnical Conference Historical Experiences and Challenges of Geotechnical Problems in Baltic Sea Region, 15 - 17 September 2016, Vilnius, Lithuania, http://www.13bsgc.lt

ACE 2016 12th International Congress on Advances in Civil Engineering, 21-23 September 2016, Istanbul, Turkey, http://www.ace2016.org

EuroGeo 6 – European Regional Conference on Geosynthetics, 25 – 29 Sep 2016, Istanbul, Turkey, www.eurogeo6.org

8th Nordic Grouting Symposium State of the art – Future Development, 26-27 September 2016, Oslo, Norway, http://nordicgrouting.com

5th International Scientific Conference on Industrial and Hazardous Waste Management, 27 - 30 September 2016, Chania, Crete, Greece, http://hwm-conferences.tuc.gr

2nd International Specialized Conference on Soft Rocks – ISRM 2016 Understanding and interpreting the engineering behavior of Soft Rocks, 6-7 October 2016, Cartagena, Colombia, www.scg.org.co/?p=1634

ARMS 9, 9th Asian Rock Mechanics Symposium, ISRM Regional Symposium, 18-20 October 2016, Bali, Indonesia, http://arms9.com

SFGE 2016 Shaping the Future of Geotechnical Education International Conference on Geo-Engineering Education 20 - 22 October 2016, Minascentro, Belo Horizonte, MG, Brazil, http://cobramseg2016.com.br/index.php/sfge-sobre/?lang=en

10th ICOLD European Club Symposium & Exhibition, 25-30 October 2016, Antalya, Turkey, http://trcold.com

NEMO International Conference Probing the Santorini volcano for 150 years / Διεθνές συνέδριο NEMO 150 χρόνια μελέτης ηφαιστείου της Σαντορίνης, 3-5 November 2016, Santorini, Greece, http://nemo.conferences.gr

GeoAsia 6 - 6th Asian Regional Conference on Geosynthetics 8-11 November 2016, New Delhi, India, http://seags.ait.asia/news-announcements/11704

RARE 2016 Recent Advances in Rock Engineering 16-18 November 2016, Bangalore, India, www.rare2016.in

TBM DiGs Istanbul 2016 2nd International conference on "TBM DiGs in difficult grounds", 16-18 November 2016, Istanbul, Turkey, www.tbmdigsturkey.org

International Symposium on Submerged Floating Tunnels and Underwater Tunnel Structures (SUFTUS-2016), 16—18 December 2016, Chongqing, China, www.cmct.cn/suftus

AfriRock 2017, 1st African Regional Rock Mechanics Symposium, 12 – 17 February 2017, Cape Town, South Africa, www.saimm.co.za/saimm-events/upcoming-events

Water Storage and Hydropower Development for Africa

14-16 March 2017, Marrakech, Morocco

www.hydropower-dams.com/AFRICA-2017.php?c_id=89

Aqua~Media International, in partnership with the International Commission on Large Dams, and with the strong support of the Government of Morocco, is pleased to reconvene the next regional conference for Africa, AFRICA 2017, which will take place in Marrakech. This follows the unfortunate need to postpone AFRICA 2015, at the time of the tragic ebola outbreak, on the advice of various relevant authorities.

In view of the postponement of the 2015 event, we produced a special publication for Africa, also working in collaboration with the African Union and ICOLD. This has been widely disseminated, and proceeds from advertising in the publication were donated to Médecins Sans Frontières, the organization which played the greatest role in bringing the ebola outbreak under control.

The first conference in this series, AFRICA 2013, took place in Addis Ababa, when practical aspects of advancing hydropower and water resources development in Africa were discussed by more than 600 participants from 67 countries. The conference brought together utility CEOs, officers of UNECA, leading experts from the IFIs, Presidents, Vice-Presidents and Secretaries of the water- and energy-related professional associations, eminent engineering consultants, researchers, leading contractors and equipment suppliers.

Outcomes made a practical contribution to the Programme for Infrastructure Development in Africa. A Final Declaration was widely disseminated globally.

Themes

- Potential and planned developments in Africa
- African multipurpose water storage including hydropower, irrigation, water supply, navigation and fisheries
- Quantifying and qualifying the benefits of water infrastructure
- African small dams for irrigation
- Role of storage in river basin management for sustainable development
- The role of risk mitigation in making hydro more competitive
- Concession agreements and construction contracts
- Finance options including resource mobilization and the Africa 50 fund
- Implementation and review of dam safety legislation in Africa
- Monitoring the safety of dams, gates and powerplants
- Public safety around dams
- Dam engineering: design and construction
- Institutions and institutional arrangements
- Case studies from the 'Water Towers': the Congo Basin, the Ethiopian Highlands, the Fouta Djallon and the Lesotho Highlands
- Effects of climate change in Africa: adaptation and mitigation
- Flood control
- The role of hydro in African regional development• Update on the PIDA Energy Priority Action Plan
- Pumped storage; hydro in synergy with other renewable
- Hydro's role in electrical system stability in Africa
- Small hydro in Africa
- Rural electrification in Africa
- Hydro machinery: research and operational issues and, practical examples of innovative low cost technologies
- Environmental and social aspects of African schemes, including water conservation and transfer, and social challenges of transboundary projects
- Reservoir sedimentation mitigation
- Operation, maintenance and rehabilitation challenges; obstacles and solutions

In addition to plenary and parallel sessions exploring the themes above, there will be focused workshops and panel discussions on topics such as project finance, regional co-operation and progress with the Programme for Infrastructure Development in Africa, including Grand Inga and other large regional hydro projects.

For more information please contact:
Mrs Margaret Bourke, Conference Project Manager, Aqua~Media International, PO Box 285, Wallington, Surrey SM6 6AN, UK.
Tel: +44 20 8773 7244 Fax: + 44 20 8773 7255.
Email: mb@hydropower-dams.com

World Tunnel Congress 2017 Surface challenges – Underground solutions, 9 to 16 June 2017, Bergen, Norway, www.wtc2017.no

EUROCK 2017 Human Activity in Rock Masses, 13-15 June 2017, Ostrava, Czech Republic, www.eurock2017.com

GeoMEast2017, 15 - 19 July 2017, Sharm El-Sheik, Egypt, www.geomeast2017.org

July 16 - 19, 2017, Vancouver, Canada

http://pbdiiivancouver.com

It is our pleasure to invite you to participate in the **3rd International Conference on Performance-based Design in Earthquake Geotechnical Engineering (PBD-III)** in Vancouver, BC, Canada, from July 16-19, 2017. The **PBD-III** Conference is organized under the auspices of the International Society of Soil Mechanics and Geotechnical Engineering - Technical Committee TC203 on Geotechnical Earthquake Engineering and Associated Problems (ISSMGE-TC203). The PBD-I and PBD-II events in Japan (2009) and Italy (2012), respectively, were highly successful events for the international geotechnical earthquake engineering community. The PBD events have been excellent companions to the International Conference on Earthquake Geotechnical Engineering (ICEGE) series that TC203 has held in Japan (1995), Portugal (1999), USA (2004), Greece (2007), Chile (2011), and New Zealand (2015).

Come join an international community of geo-professionals working to share and advance performance-based design practices for geotechnical earthquake engineering across a broad range of civil infrastructure problems. The coverage will be diverse, including case histories and practice-oriented papers, recent research findings, innovative technologies, and the emerging arts from across the world. An international mix professional engineers, researchers, specialty contractors, educators, and students will interact across a broad range of keynote and theme lectures, technical sessions, short courses, panel discussions, and field trips.

Everyone involved with **PBD-III** is excited to be hosting this international event and is looking forward to seeing you in Vancouver. The exciting technical and social programs we have planned are only possible though the hard work and dedication of many individuals, including all the conference committee members, local organizing committee members, and TC203 members. Together, we all look forward to a rewarding experience interacting with our international friends and fellow geo-professionals.

Conference Program

PBD-III Vancouver will bring together an international community of geo-professionals working to share and advance performance-based design practices for geotechnical earthquake engineering across a broad range of civil infrastructure problems. An international mix professional engineers, researchers, specialty contractors, educators, and students will interact across a broad range of keynote and theme lectures, technical sessions, short courses, panel discussions, and field trips.

Sunday, July 16 will feature short courses during the day and the opening reception in the evening.

Monday, July 17 through Wednesday, July 19 will include all keynote and theme lectures, concurrent technical sessions, and panel discussions. The concurrent sessions, in combination with the envisioned nine keynote/theme lectures and three panel discussions, are expected to cover the wide range of topics listed under the Conference Themes on the Call for Submissions page. One of the evenings will include a "local color" night for mixing with new and old, local and international, friends and colleagues at an off-site venue, while other evenings will provide opportunities to sample the lively night life of exciting downtown Vancouver. Details on the program and keynote/theme lectures will be provided early in 2016.

Thursday, July 20 will feature a technical tour, enhanced by the natural beauty of Vancouver and its surrounding areas. Details of the technical tour will be provided in the fall of 2016.

Technical Themes

The theme of **PBD-III Vancouver 2017** encompass all aspects of performance based design in earthquake geotechnical engineering. The coverage will be diverse, covering a broad range of civil infrastructure problems and including case histories and practice-oriented papers, recent research findings, innovative technologies, and the emerging arts.

Technical sessions will include oral and poster presentations of individual papers, panel discussions on emerging issues, and mini-symposia on international practices. Individuals interested in proposing a panel discussion or mini-symposium may contact conference co-chair R. W. Boulanger directly.

Researchers and practitioners are invited to submit abstracts describing case histories, emerging design practices, new technologies, or recent research findings in the following topic areas:

- Seismic hazard assessments
- Retaining structures and mechanically stabilized soils
- Port facilities and wharves
- Offshore structures - wind farms, oil and gas facilities
- Bridges
- Lifelines - pipelines, communications, and transportation systems
- Underground structures
- Soil-structure interaction
- Ground improvement techniques
- Landfills
- Education
- Resiliency - emergency response, land use planning, and recovery
- Foundations - deep or shallow
- Slope stability
- Mine stability
- Ground motions and site effects
- Site characterization with in-site and laboratory testing
- Physical modeling - centrifuge, shaking table, or field scale
- Numerical analyses - dynamic or simplified
- Performance based design methodologies - probabilistic frameworks
- Performance based design - codes and guidance
- Sustainability and life cycle cost analyses
- Liquefaction
- Cyclic softening in clays and plastic silts
- Challenging soils - tailings, calcareous soils, gravels
- Embankments, levees, or dams
- Multi-hazard considerations - hurricane, tsunami, flood, sea-level rise

Contact Us

If you have questions about PBD-III Vancouver, please feel free to contact one of the following individuals:

Ross Boulanger
Co-chair, PBD-III Vancouver Organizing Committee
chair@pbdiiivancouver.com

Dharma Wijewickreme
Co-chair, PBD-III Vancouver Organizing Committee
chair@pbdiiivancouver.com

Wayne Gibson
Conference Manager
info@pbdiiivancouver.com

Lisa McJunkin
Conference Administrator
admin@pbdiiivancouver.com

c/o Gibson Group Management Inc.
8828 Pigott Rd
Richmond, BC, V7A 2C4 Canada
(604) 241-1297
(604) 241-1399 (fax)

☙ ❧

19th International Conference on Soil Mechanics and Geotechnical Engineering, 17 - 22 September 2017, Seoul, Korea, www.icsmge2017.org

BCRRA 2017 Tenth International Conference on the Bearing Capacity of Roads, Railways and Airfields, 28th to 30th June 2017, Athens, Greece, www.bcrra2017.com

GeoAfrica 2017
3rd African Regional Conference on Geosynthetics
9 – 13 October 2017, Morocco

11th International Conference on Geosynthetics (11ICG)
16 - 20 Sep 2018, Seoul South Korea
csyoo@skku.edu

10th Asian Rock mechanics Symposium - ARMS10
October 2018, Singapore

Prof. Yingxin Zhou
Address:
1 Liang Seah Street
#02-11 Liang Seah Place
SINGAPORE 189022
Telephone: (+65) 637 65363
Fax: (+65) 627 35754
E-mail: zyingxin@dsta.gov.sg

AFTES International Congress
"The value is Underground"
13-16 November 2017, Paris, France

World Tunnel Congress 2018
20-26 April 2018, Dubai, United Arab Emirates

EUROCK 2018
22-26 May 2018, Saint Petersburg, Russia

Contact Person: Prof. Vladimir Trushko
Address: 21-st line V.O., 2
199106 St. Petersburg
Russia
Telephone: +7 (812) 328 86 71
Fax: +7 (812) 328 86 76
E-mail: trushko@spmi.ru

UNSAT2018 The 7th International Conference on Unsaturated Soils, 3 - 5 August 2018, Hong Kong, China, www.unsat2018.org

11th International Conference on Geosynthetics (11ICG)
16 - 20 Sep 2018, Seoul, South Korea
csyoo@skku.edu

ARMS10
10th Asian Rock Mechanics Symposium
ISRM Regional Symposium
October 2018, Singapore

Contact Person: Prof. Yingxin Zhou
Address: 1 Liang Seah Street
#02-11 Liang Seah Place
SINGAPORE 189022
Telephone: (+65) 637 65363
Fax: (+65) 627 35754
E-mail: zyingxin@dsta.gov.sg

ꟾ ꟾ

14th ISRM International Congress
2019, Foz de Iguaçu, Brazil

Contact Person: Prof. Sergio A. B. da Fontoura
E-mail: fontoura@puc-rio.b

ꟾ ꟾ

The 17th European Conference on
Soil Mechanics and Geotechnical Engineering
1st - 6th September 2019, Reykjavik Iceland
www.ecsmge-2019.com

The theme of the conference embraces all aspects of geotechnical engineering. Geotechnical engineering is the foundation of current as well as future societies, which both rely on complex civil engineering infrastructures, and call for mitigation of potential geodangers posing threat to these. Geotechnical means and solutions are required to ensure infrastructure safety and sustainable development. Those means are rooted in past experiences enhanced by research and technology of today.

At great events such as the European Geotechnical Conference we should: Spread our knowledge and experience to our colleagues; Introduce innovations, research and development of techniques and equipment; Report on successful geotechnical constructions and application of geotechnical design methods, as well as, on mitigation and assessment of geohazards and more.

Such events also provide an opportunity to draw the attention of others outside the field of geotechnical engineering to the importance of what we are doing, particularly to those who, directly or indirectly, rely on our services, knowledge and experience. Investment in quality geotechnical work is required for successful and safe design, construction and operation of any infrastructure. Geotechnical engineering is the key to a safe and sustainable infrastructure and of importance for the society, economy and the environment. This must be emphasized and reported upon.

ΕΝΔΙΑΦΕΡΟΝΤΑ ΓΕΩΤΕΧΝΙΚΑ ΝΕΑ

Living with Shrink-Swell Soils:
A what-to-do pamphlet for home-owners, prepared by ASCE Geo-Institute

The Shallow Foundation Technical Committee of the ASCE Geo-Institute released in February one page pamphlet for homeowners whose house is constructed on expansive soils.

The pamphlet was written for the broad public, because according to the committee Chair, Daniel J. Rich, there is quite a bit of conflicting information on the Internet about how houses built on shrink/swell soil react to changes in the soil moisture content and what can be done to minimize the damage.

When it comes to expansive soils, it is all about the moisture content of the soil, its fluctuation and where water goes. The pamphlet has a cool table of possible problems and action items to reduce the impact on one's structure.

View the pamphlet here
http://www.geoengineer.org/LivingWithShrinkSwellSoils.pdf

(GeoEngineer, Tuesday, 01 March 2016)

Αισθητήρας βαρύτητας κάνει ακτινογραφία στο υπέδαφος

Μια συσκευή σε μέγεθος γραμματοσήμου, ικανή να μετρά απειροελάχιστες μεταβολές στην ένταση του βαρυτικού πεδίου της Γης, θα μπορούσε να χρησιμοποιηθεί για να εντοπίζει μεγάλες δομές στο υπέδαφος, από κοιτάσματα πολύτιμων μετάλλων μέχρι τούνελ για αποδράσεις κρατουμένων.

Η δύναμη της βαρύτητας δεν είναι ακριβώς ίση σε όλο τον κόσμο -η έντασή της σε ένα οποιοδήποτε σημείο της επιφάνειας του πλανήτη εξαρτάται κυρίως από την απόσταση του σημείου αυτού από το κέντρο της Γης, επηρεάζεται όμως και από την πυκνότητα των πετρωμάτων του υπεδάφους.

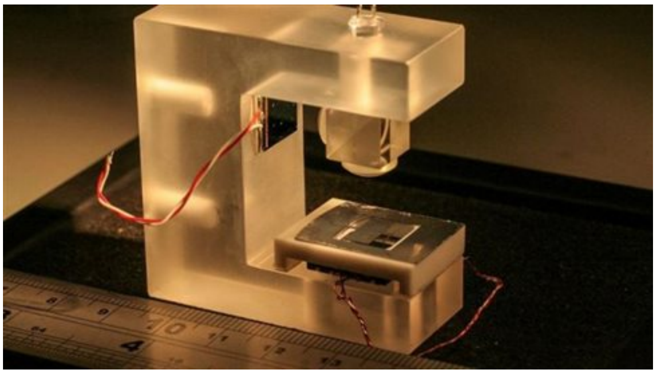

Στην καρδιά της συσκευής κρύβεται ένα βαρύδι από πυρίτιο βάρους 21 mg (Πηγή: Giles Hammond)

Οι διακυμάνσεις αυτές είναι εξαιρετικά μικρές και μπορούν να μετρηθούν μόνο με εξειδικευμένα όργανα που ονομάζονται βαρυτόμετρα. Τα όργανα αυτά μετρούν είτε το χρόνο που χρειάζεται ένα αντικείμενο για να πέσει κατά μια συγκεκριμένη απόσταση (η ταχύτητα πτώσης αυξάνεται όταν η βαρύτητα γίνει ισχυρότερη) είτε το μήκος ενός ελατηρίου από το οποίο έχει αναρτηθεί ένα βαρίδι (το ελατήριο τεντώνεται περισσότερο όταν η δύναμη της βαρύτητας μεγαλώνει).

Τα καλύτερα από τα σημερινά βαρυτόμετρα, επισημαίνει ο δικτυακός τόπος του περιοδικού Science, έχουν μέγεθος μπαταρίας αυτοκινήτου και κοστίζουν πάνω από 100.000 ευρώ.

Το νέο βαρυτόμετρο, αντίθετα, είναι μικρό και ζυγίζει λιγότερο από πούπουλο. Στο κέντρο του φέρει ένα μικροσκοπικό βαρίδι από πυρίτιο, βάρους 25 χιλιοστών του γραμμαρίου, το οποίο συνδέεται σε μια πλάκα πυριτίου μέσω τριών δύσκαμπτων ινών με πάχος 5 μικρόμετρα η καθεμία. Οι τρεις ίνες λειτουργούν ουσιαστικά ως ελατήριο και επιτρέπουν στο κεντρικό βαρίδι να ανεβοκατεβαίνει καθώς το βαρυτικό πεδίο μεταβάλλεται.

Η συσκευή, η οποία αναπτύχθηκε στο Πανεπιστήμιο της Γλασκώβης, είναι τόσο ακριβής ώστε μπορεί να μετρά μεταβολές κατά ένα μέρος ανά δισεκατομμύριο -μεταβολή που θα αντιστοιχούσε σε αύξηση του υψομέτρου κατά μόλις 3 χιλιοστά.

Χάρη το μικρό μέγεθος και κόστος, το μίνι βαρυτόμετρο θα μπορούσε να χρησιμοποιηθεί σε drone για εναέριες μελέτες του υπεδάφους, αναφέρουν οι δημιουργοί της στο περιοδικό Nature.

Οι πρακτικές εφαρμογές της νέας τεχνολογίας είναι δυνητικά πολλές και σημαντικές: οι γεωλόγοι θα μπορούσαν να αναζητούν κοιτάσματα μετάλλων ή ακόμα να παρακολουθούν τη ροή του μάγματος κάτω από ηφαίστεια. Θα μπορούσαν ακόμα να εντοπίζουν κρυμμένα σπήλαια, θαμμένες αρχαιότητες, ακόμα και να υπολογίζουν τα εναπομείναντα αποθέματα σε κοιτάσματα πετρελαίου.

Και αν η αστυνομία ενδιαφερθεί να εντάξει το βαρυτόμετρο στο οπλοστάσιό της, οι κρατούμενοι που σχεδιάζουν να αποδράσουν από τούνελ θα αντιμετωπίζουν μεγαλύτερο ρίσκο.

(Βαγγέλης Πρατικάκης / Newsroom ΔΟΛ, 31 Μαρ. 2016, http://news.in.gr/science-technology/article/?aid=1500068460)

ΕΝΔΙΑΦΕΡΟΝΤΑ - ΠΕΡΙΒΑΛΛΟΝ

This river kills everything that falls into it

Legend or fact? A young explorer traveled deep into a remote jungle to find out.

With maximum temperatures of over 200 degrees Fahrenheit, the Boiling River is not quite at boiling point, but it's hot enough to poach your egg—and kill anything that falls into it.

It sounds like a Jules Verne tale: a boiling river that seems to flow from the center of the earth and kills anything that falls into it. Andrés Ruzo, a National Geographic Young Explorer, first heard about it from his Peruvian grandfather. When Ruzo became a geophysicist, he decided to investigate whether this story could be true—and whether science could explain it. In "*The Boiling River: Adventure and Discovery in the Amazon*", he travels deep into the Peruvian jungle to unravel the mystery.

I first heard the story of the Boiling River as a boy in Lima from my grandfather as part of a legend of a lost city of gold in the Amazon. Much later, when I was working on my PhD in geophysics, I started looking at this detail from a scientific viewpoint. The focus of my dissertation was to create the first detailed heat flow map of Peru in order to identify areas of potential geothermal energy.

The Boiling River is in the central Peruvian Amazon, in the middle of low jungle. From Lima it's about an hour flight to the city of Pucallpa, the largest city in the central Peruvian Amazon. From Pucallpa, it was a two-hour drive mostly on red dirt roads to the Pachitea river, a tributary of the Amazon over 300 meters wide. From there, we took a *peke-peke*, or motorized canoe, upriver for about 30 minutes to the mouth of the Boiling River. It's called a *peke-peke* because the motor goes *pekepekepekepekepeke.*

As we approached the confluence of the two rivers, the shaman's apprentice, who was at the prow, said "Stick your hand in"! So we put our hands into the cold waters of the Pachitea. As the boat glided into this olive-green plume that was the mouth of the Boiling River, immediately the temperature went up. But there was no steam and the temperature was only like hot bath water.

What's curious about the river is that it actually starts off as a cold stream, heats up, then cools back down slightly at night. It goes from roughly 27 degrees Celsius to about 94 degrees Celsius at its hottest. There are also *very* hot springs, which inject water into the river to produce this amazing feature.

The total river system is about 9 kilometers (5.5 miles), but it is the 6.24 kilometers (3.8 miles) on the lower part of the river that are hot. Most of that flow, particularly during the dry season, is hot enough to kill you. Small mammals, reptiles, or amphibians regularly fall in and are boiled alive. One of the things I love about being there is that it forces you to be extremely intentional with every step, because there can be really serious consequences if you do fall in.

According to local traditions, the Boiling River is a place of tremendous spiritual power. Here, a shaman plays a song to the Spirit of the Vapor, which he believes "carries the prayers of the rocks, jungle, and all creation to their Creator."

When I first got to the river, my biggest concern was whether it was natural or not. To create a large geothermal system like this, you need three things: a tremendous source of heat, a large volume of water, and a plumbing system that will take this hot water from depth all the way up to the surface.

One of the hypotheses was that this was a volcanic feature, a magmatic system that the scientists had missed. It could also have been a non-volcanic feature, i.e. hot water flowing out of the earth at an anomalously high rate. The deeper we go into the earth the hotter it gets. That's called the geothermal gradient. At these temperatures the water would have to be coming up from pretty deep down and at *very* fast rates.

One hypothesis about the origins of the Boiling River is that a company drilling for gas accidentally ruptured a geothermal system, as happened in 2007 in Lusi, Indonesia. The resulting mud flow (above) covered an area twice the size of Central Park and displaced 40,000 people.

The final theory, which was really the scary one for me, was that this place was not natural at all but the result of an oil field accident. The river is only 2-3 kilometers from the oldest active oil field in the Peruvian Amazon. If there was an oil and gas flow that only produces hot water but no hydrocarbons or gas, they might just have abandoned it. Another possibility is that an oil and gas flow accidentally drills into a geothermal system. The biggest and most frightening example of this was the Lusi mud volcano on Java. Over 40,000 people have been displaced and the thing's still erupting.

But, in fact, the Boiling River is a natural feature: a non-volcanic, geothermal feature flowing at anomalously high rates.

(Simon Worrall/NATIONAL GEOHRAPHIC, Sun Mar 13, 2016 http://news.nationalgeographic.com/2016/03/160313-boiling-river-amazon-geothermal-science-conservation-ngbooktalk)

Ημισυνθετικό υλικό
«Διάφανο ξύλο» για φωτεινούς τοίχους

Το διάφανο ξύλο υπόσχεται ένα πιο φωτεινό μέλλον

Για να κάνουν το σπίτι πιο φωτεινό, οι διακοσμητές χρησιμοποιούν ανοιχτά χρώματα, καθρέπτες και τρικ στο φωτισμό. Όλα όμως θα ήταν απλούστερα αν οι τοίχοι ήταν διάφανοι.

Αυτό ίσως θα μπορούσε να γίνει στο εγγύς μέλλον χάρη στο «διάφανο ξύλο» που δημιουργήθηκε σε εργαστήριο της Σουηδίας με χημική κατεργασία του φυσικού ξύλου.

Πρόσφατες εξελίξεις που επέτρεψαν την παραγωγή διαφανούς χαρτιού κινητοποίησαν το ενδιαφέρον των ερευνητών για την ανάπτυξη παρόμοιων αλλά πιο ανθεκτικών υλικών.

Ο Λαρς Μπέργκλουντ και οι συνεργάτες του στο Βασιλικό Ινστιτούτο Τεχνολογίας της Στοκχόλμη πειραματίστηκαν με το ξύλο του δέντρου μπάλα, ένα σπογγώδες, ελαφρύ και μαλακό ξύλο που χρησιμοποιείται μεταξύ άλλων σε σανίδες του σερφ και αρχιτεκτονικές μακέτες.

Σε πρώτη φάση, το ξύλο υποβλήθηκε σε χημική επεξεργασία για την αφαίρεση της λιγνίτης, ενός δομικού πολυμερούς που χαρίζει σταθερότητα στο ξύλο αλλά απορροφά το 80 με 95 τοις εκατό του φωτός που πέφτει πάνω του.

Το υλικό που προέκυψε δεν ήταν διάφανο αλλά άσπρο επηδή διαθλούσε το φως αντί να περάσει κατευθείαν από μέσα του. Για να γίνει πιο διάφανο, το υλικό υποβλήθηκε σε μια δεύτερη χημική κατεργασία κατά την οποία ενσωματώθηκε στην επιφάνειά του το ακρυλικό υλικό που γνωρίζουμε ως Plexiglass.

Το τελικό προϊόν δεν είναι απόλυτα διάφανο σαν το γυαλί, προσφέρει όμως διπλάσια αντοχή από το Plexiglass και σύμφωνα με τους ερευνητές είναι κατάλληλο για χρήση ως οικοδομικό υλικό.

Επιπλέον, το διάφανο ξύλο θα μπορούσε να αντικαταστήσει το γυαλί στα φωτοβολταϊκά πάνελ, δεδομένου ότι παγιδεύει ένα μέρος του φωτός που δέχεται και θα μπορούσε έτσι να αυξήσει την απόδοση.

Επόμενος στόχος της ομάδας είναι να πειραματιστεί και με άλλα είδη ξύλου και να αυξήσει περαιτέρω τη διαφάνεια του υλικού.

Αν το νέο προϊόν αποδειχθεί οικονομικά βιώσιμο και πρακτικό, οι τοίχοι του μέλλοντος θα μπορούσαν να παίζουν και ρόλο φεγγίτη.

Η μελέτη δημοσιεύεται στην επιθεώρηση Biomacromolecules (http://pubs.acs.org/doi/abs/10.1021/acs.biomac.6b00145)

(Βαγγέλης Πρατικάκης / Newsroom ΔΟΛ, 31 Μαρ. 2016, http://news.in.gr/science-technology/article/?aid=1500068399)

Optically Transparent Wood from a Nanoporous Cellulosic Template: Combining Functional and Structural Performance

Yuanyuan Li[‡], Qiliang Fu[‡], Shun Yu[‡], Min Yan[§], and Lars Berglund[*‡]

[‡]Wallenberg Wood Science Center, Department of Fiber and Polymer Technology, and [§]School of Information and Communication Technology, KTH Royal Institute of Technology, SE-10044 Stockholm, Sweden

Abstract

Optically transparent wood (TW) with transmittance as high as 85% and haze of 71% was obtained using a delignified nanoporous wood template. The template was prepared by removing the light-absorbing lignin component, creating nanoporosity in the wood cell wall. Transparent wood was prepared by successful impregnation of lumen and the nanoscale cellulose fiber network in the cell wall with refractive-index-matched prepolymerized methyl methacrylate (MMA). During the process, the hierarchical wood structure was preserved. Optical properties of TW are tunable by changing the cellulose volume fraction. The synergy between wood and PMMA was observed for mechanical properties. Lightweight and strong transparent wood is a potential candidate for lightweight low-cost, light-transmitting buildings and transparent solar cell windows.

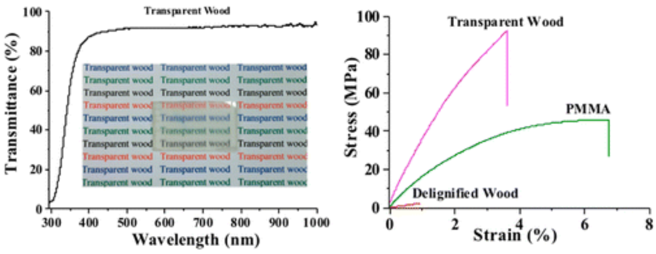

ΕΝΔΙΑΦΕΡΟΝΤΑ – ΛΟΙΠΑ

Zaha Hadid, Groundbreaking Architect, Dies at 65

Dame Zaha Hadid, the Iraqi-born British architect whose soaring structures left a mark on skylines and imaginations around the world and in the process reshaped architecture for the modern age, died in Miami on Thursday. She was 65

She was not just a rock star and a designer of spectacles. She also liberated architectural geometry, giving it a whole new expressive identity. Geometry became, in her hands, a vehicle for unprecedented and eye-popping new spaces but also for emotional ambiguity. Her buildings elevated uncertainty to an art, conveyed in the odd ways one entered and moved through those buildings and in the questions her structures raised about how they were supported.

Her work, with its formal fluidity — also implying mobility, speed, freedom — spoke to a worldview widely shared by a younger generation. "I am non-European, I don't do conventional work and I am a woman," she once told an interviewer. "On the one hand all of these things together make it easier — but on the other hand it is very difficult."

Strikingly, Ms. Hadid never allowed herself or her work to be pigeonholed by her background or her gender. Architecture was architecture: it had its own reasoning and trajectory. And she was one of a kind, a path breaker. In 2004, she became the first woman to win the Pritzker Prize, architecture's Nobel; the first, on her own, to be awarded the RIBA Gold Medal, Britain's top architectural award, in 2015.

Inevitably, she stirred nearly as much controversy as she won admiration, provoking protests from human rights advocates when her $250 million cultural center in Baku, Azerbaijan, forced the eviction of families from the site. A commission to design a stadium in Qatar — a sensuous plan that more than a few observers likened to female anatomy — became, in truth unfairly, a lightning rod for critics who decry the treatment of foreign laborers by the government there. She sued for defamation one critic who falsely reported that 1,000 workers had died building her stadium — before construction had even begun. She won a settlement and an apology.

Zaha Hadid was born in Baghdad on Oct. 31, 1950. She attended a Catholic school where students spoke French, and Muslims and Jews were welcome. After that, she studied mathematics at the American University in Beirut (she would later say her years in Lebanon were the happiest of her life).

Then, in 1972, she arrived at the Architectural Association in London, a center for experimental design. Her teachers included Elia Zenghelis and Rem Koolhaas. They "ignited my ambition," she would recall, and "taught me to trust even my strangest intuitions."

Ms. Hadid's concept was a jagged, gravity-defying composition of beams and floating shards cantilevered into the rock face. It encapsulated the 1980s movement called Deconstructivism. During these years Ms. Hadid turned out an astonishing, super-refined variety of futuristic drawings and paintings. She used her art to test spatial ideas that she couldn't yet make concrete without the aid of computer algorithms. She soon developed an insiders' reputation as a leading theoretical designer of groundbreaking forms with unrealized projects like the Cardiff Bay opera house in Wales.

In 1994, she realized her first commission, a fire station on the corporate campus of Vitra, a furniture company, in Weil am Rhein, Germany. It inspired a design of typically outsized imagination: a winged composition, all sharp angles and protrusions. Architects were impressed. The firefighters, not so much. They moved out, and the station became an event space.

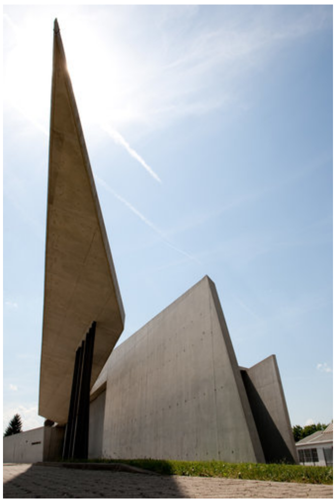

A fire station Ms. Hadid designed in Weil am Rhein Germany

Not one to compromise or concede much to those who called her works impractical, indulgent and imprudent, from early on she made the most, creatively speaking, of what commissions she got. When her Rosenthal Center for Contemporary Art in Cincinnati, a relatively modest project, opened in 2003, Herbert Muschamp, then architecture critic for The New York Times, declared it "the most important American building to be completed since the end of the Cold War."

Projects followed, like the Phaeno Science Center in Wolfsburg, Germany; the Bridge Pavilion in Zaragoza, Spain; and an opera house in Guangzhou, China, whose rock crystal-shaped design she likened to "pebbles in a stream smoothed by erosion."

The Guangzhou Opera House in Guangzhou, China.

Her sources were nature, history, whatever she thought useful. Ms. Hadid's design for the Maxxi, a modern art museum in Rome, alluded distantly to Baroque precedents, and became one of the rare modern buildings in the city to vie for attention with its numerous historical sites. Like the fire station it wasn't entirely practical, but it was a voluptuous and muscular building, multi-tiered, with ramps that flowed like streams and floors tilted like hills, many walls swerving and swooning.

The towering lobby inside Maxxi Art Museum, Rome, 2009

It took years before Ms. Hadid won major commissions in Britain, where she became a citizen and established a thriving office. Her Aquatics Center in London, built for the 2012 Olympics, was a cathedral for water sports, with an undulating roof and two 50-meter pools. It has become a city landmark and neighborhood attraction, bustling with kids and recreational swimmers.

Ms. Hadid's Serpentine Sackler Gallery in London.

Ms. Hadid embodied, in its profligacy and promise, the era of so-called starchitects, who roamed the planet in pursuit of their own creative genius, offering miracles, occasionally delivering. "She was bigger than life, a force of nature," as Amale Andraos, the dean of Columbia University's architecture school, put it on Thursday. "She was a pioneer."

She was. For women, for what cities can aspire to build and for the art of architecture.

(Michael Kimmelman / The New York Times, March 31, 2016)

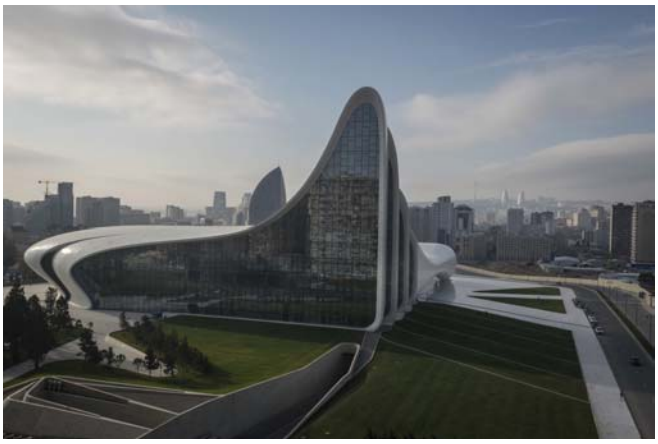

Heydar Aliyev Center, Azerbaijan, 2013

Al Wakrah Stadium, Qatar, in progress

ΗΛΕΚΤΡΟΝΙΚΑ ΠΕΡΙΟΔΙΚΑ

No. 33 - March 2016
www.isrm.net/adm/newsletter/ver_html.php?id_newsletter=123&ver=1

Κυκλοφόρησε το τεύχος αρ. 33. Μαρτίου 2016 του NEWSLETTER της ISRM με τα ακόλουθα περιεχόμενα:

- 2016 ISRM International Symposium - EUROCK 2016, 29-31 August, in Cappadocia, Turkey
- ARMS9, Bali, Indonesia, 18-20 October 2016
- 13th ISRM online lecture by Prof. Peter Kaiser
- Stravos Bandis 1951-2016
- Volume 18 - December 2015 of the ISRM News Journal is now online
- New ISRM National Group of Malaysia
- Rock Mechanics Principles, an on-line video course by Professor Jian Zhao
- ISRM Suggested Methods videos now on the website
- ISRM Online Rock Mechanics Glossary: Norwegian and French now available
- Public domain rock mechanics research reports
- Digital Library at OnePetro
- ISRM Board meeting and ISRM Workshop in Zagreb, Croatia, 3-4 March 2016
- 2017 ISRM International Symposium - AfriRock 2017 2-7 October, in Cape Town, South Africa
- Rock Stress 2016, 10–12 May, Tampere, Finland, an ISRM Specialised Conference
- RockDyn-2, 18-20 May 2016, Suzhou, China, an ISRM Specialised Conference
- Geosafe 2016, 25–27 May, Xi'an, China, an ISRM Specialised Conference
- US Rock Mechanics/Geomechanics Symposium program comes together
- 2nd ISCSR, 28-30 September, Cartagena de Indias, Colombia, an ISRM Specialised Conference
- VIII SBMR, 19-22 October 2016, Belo Horizonte, Brazil, an ISRM Specialised Conference
- RARE-2016, 16-18 November, Bengaluru, India, an ISRM Specialised Conference
- ISRM Sponsored Meetings

❧ ❧

www.geoengineer.org

Κυκλοφόρησε το Τεύχος #132 του **Newsletter του Geoengineer.org** (Μαρτίου 2016) με πολλές χρήσιμες πληροφορίες για όλα τα θέματα της γεωμηχανικής. Υπεν-θυμίζεται ότι το Newsletter εκδίδεται από τον συνάδελφο και μέλος της ΕΕΕΕΓΜ Δημήτρη Ζέκκο (secretariat@geoengineer.org).

❧ ❧

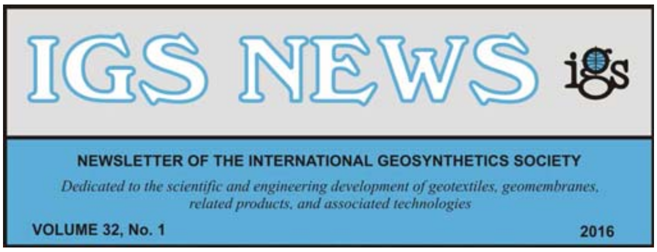

http://files.ctctcdn.com/15018a1b201/7f2364d2-7223-4203-bc7b-7e9bdee1c77f.pdf

Κυκλοφόρησε το Τεύχος 1 του Τόμου 32, των IGS NEWS με τα παρακάτω περιεχόμενα:

General Information for IGS Members

- Election for IGS Council: Term 2016 to 2020
- Obituary Late Professor Fukuoka, Masami, Founding Member of IGS
- Memories of Professor Masami Fukuoka

Technical Committees IGS-TC

- IGS TC-B Activities Report
- IGS TC-H Activities Report 2016-02

Announcements of Regional Conferences of IGS

- GeoAmericas 2016 3rd Pan-American Congress on Geosynthetics
- EuroGeo6 6th European Regional Conference on Geosynthetics
- GeoAsia6 6th Asian Regional Conference on Geosynthetics

Announcements of Conferences under the Auspices of IGS

- 3rd International Conference on Transportation Geotechnics (3rd ICTG 2016)
- Geotechnical Frontiers 2017

News from the IGS Chapters and the Membership

- News from the Australasian IGS Chapter (ACIGS)
- GEOS PERÚ 2015 – 3rd National Conference on Geosynthetics
- 24th Geotechnical Conference of Torino (CGT 2016)
- International Seminar on Natural Disaster Mitigation with Geosynthetics and other Advanced Methods
- 15th Asian Regional Conference on Soil Mechanics and Geotechnical Engineering (15ARC)
- New German Recommendation for Geosynthetics in Earthworks for Road Constructions
- Proceedings of FS-KGEO 2015

- Serviceability of geogrid reinforced base course layers – Lars Vollmert received the PhD for his contribution

List of IGS Chapters

Official Journals of the IGS

- Geosynthetics International
- Geotextiles & Geomembranes

Corporate Membership

- Case studies – use the chance!
- Midshore I Landfill Exposed Geomembrane Cover, Easton, MD, USA
- Corporate Members of the IGS

IGS News Publisher, Editor and Chapter Correspondents

IGS Council

IGS Officers

IGS Membership Application

Calendar of Events

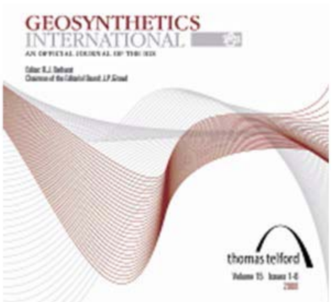

Content of Volume: 22, Issue: 6 (December 2015)

Best *Geosynthetics International* Paper for 2014, R. J. Bathurst

Method to increase seam efficiency for woven geotextile materials, W. Guo, J. Chu, B. Zhou

Numerical studies on the performance of hybrid-geosynthetic-reinforced soil slopes subjected to rainfall, D. Bhattacherjee, B. V. S. Viswanadham

Full-scale load test and finite-element analysis of soft ground improved by geotextile-encased granular columns, I. Hosseinpour, M. S. S. Almeida, M. Riccio

Evaluation of a calculation method for embankments reinforced with geocells over soft soils using finite-element analysis, J. O. Avesani Neto, B. S. Bueno, M. M. Futai

The application of water-absorbing geocomposites to support plant growth on slopes, K. Lejcuś, J. Dąbrowska, D. Garlikowski, M. Śpitalniak

Infiltration into unsaturated reinforced slopes with nonwoven geotextile drains sandwiched in sand layers, J. N. Thuo, K. H. Yang, C. C. Huang

Note of Appreciation to Paper Reviewers

Content of Volume: 23, Issue: 1 (February 2016)

Ultimate bearing capacity of saturated reinforced horizontal ground, C.-C. Huang

Slope stabilisation using EPS block geofoam with internal drainage system, O. Akay

An analytical solution for contaminant extraction in a radial flow field using PVD-enhanced system, H.-Y. Wang, X.-W. Tang, Q. Tang, Y. Wang, P.-L. Gan

Behaviour of anchored geosynthetic-reinforced slopes subjected to seepage in a geotechnical centrifuge, A. Raja-bian, B. V. S. Viswanadham

Monitoring and numerical modelling of an instrumented mechanically stabilised earth wall, N. Cristelo, C. Félix, M. L. Lopes, M. Dias

Interface shear properties of geosynthetics and construction and demolition waste from large-scale direct shear tests, C. S. Vieira, P. M. Pereira

Please find the download of the articles at: http://www.icevirtuallibrary.com/content/issue/gein/22/6
For the IGS members to have FREE access to the papers they MUST log in through the IGS website.

Content of Volume 44, issue 1 (February 2016)

Numerical and physical modeling of geofoam barriers as protection against effects of surface blast on underground tunnels, Anirban De, Alberto N. Morgante, Thomas F. Zimmie

Model tests on geotextile-encased granular columns under 1-g and undrained conditions, Yung-Shan Hong, Cho-Sen Wu, Yi-Sheng Yu

Road surface permanent deformations with a shallowly buried steel-reinforced high-density polyethylene pipe un-der cyclic loading, Zhigang Cao, Jie Han, Changjie Xu, Deep K. Khatri, Ryan Corey, Yuanqiang Cai

Mitigating the bridge end bump problem: A case study of a new approach slab system with geosynthetic reinforced soil foundation, Qiming Chen, Murad Abu-Farsakh

Transient hydraulic behavior of two GMBs–GCLs composite liners, H. Bannour, N. Touze-Foltz, P. Pierson

Application of EPS geofoam in attenuating ground vibrations during vibratory pile driving, D.S. Liyanapathirana, S.D. Ekanayake

Experimental and numerical studies of the performance of the new reinforcement system under pull-out conditions, M. Mosallanezhad, S.H. Sadat Taghavi, N. Hataf, M.C. Alfaro

Experimental study on performance of geosynthetic-reinforced soil model walls on rigid foundations subjected to static footing loading, Chengzhi Xiao, Jie Han, Zhen Zhang

Performance evaluation of geogrid reinforced soil walls with marginal backfills through centrifuge model tests, S. Balakrishnan, B.V.S. Viswanadham

Evaluation of permanent deformation of geogrid reinforced asphalt concrete using dynamic creep test, Sina Mirza-pour Mounes, Mohamed Rehan Karim, Ali Khodaii, Mohamad Hadi Almasi

Electrical resistance method for assessing spatial variation of water content in geosynthetics clay liners at laborato-ry scale, Hossam M. Abuel-Naga, Abdelmalek Bouazza

Vertical-drain consolidation using stone columns: An analyt-ical solution with an impeded drainage boundary under mul-ti-ramp loading, G.H. Lei, C.W. Fu, C.W.W. Ng

Content of Volume 44, issue 2 (April 2016)

Three-dimensional reinforced slopes: Evaluation of required reinforcement strength and embedment length using limit analysis, Yufeng Gao, Shangchuan Yang, Fei Zhang, Ben Leshchinsky

Modelling of deformable structures in the general frame-work of the discrete element method, Anna Effeindzourou, Bruno Chareyre, Klaus Thoeni, Anna Giacomini, François Kneib

Tensile force of geogrids embedded in pile-supported rein-forced embankment: A full-scale experimental study, R.P. Chen, Y.W. Wang, X.W. Ye, X.C. Bian, X.P. Dong

Microgrid inclusions to increase the strength and stiffness of sand, Ben Leshchinsky, T. Matthew Evans, Jordan Vesper

Statistical-experimental study of geosynthetics performance on reflection cracking phenomenon, Fereidoon Moghadas Nejad, Saeid Asadi, Shahab Fallah, Morteza Vadood

Centrifuge evaluation of the time-dependent behavior of geotextile-reinforced soil walls, Carina Maia Lins Costa, Jorge Gabriel Zornberg, Benedito de Souza Bueno, Yuri Da-niel Jatobá Costa

Study of a small scale tyre-reinforced embankment, Lihua Li, Henglin Xiao, Pedro Ferreira, Xilin Cui

Numerical and field test verifications for the deformation behavior of geotextile tubes considering 1D and areal strain, Hyeong-Joo Kim, Myoung-Soo Won, Jay C. Jamin, Jeong-Hoon Joo

Please find the download of the articles at:
http://www.sciencedirect.com/science/journal/02661144
For IGS members to have FREE access to the G&G journal articles they MUST log in through the IGS website.

ΟΣ ΣΟ

ITA@NEWS

ASSOCIATION INTERNATIONALE DES TUNNELS ET DE L'ESPACE SOUTERRAIN AITES | ITA INTERNATIONAL TUNNELLING AND UNDERGROUND SPACE ASSOCIATION

The ITA@NEWS #59 – March 2016
www.ita-aites.org

Message from SØREN DEGN ESKESEN, ITA President

WTC 2016 is in one month

ITA WGs and Committees Publications

At WTC a Workshop on BIM will be organized

At WTC ITAtech session will deal with Internet of Things (IoT)

ITACUS 'THINK DEEP' SESSION

ITA Tunnelling Awards 2016 registration is open.

A successful first training session by video-conference
Saudi Arabia hosts a training session on landslides and tun-nels

13th International Conference Underground Construction & EETC, 23-25th May 2016, Prague

1st National Congress on Tunnelling and Underground Space & Roads, Bridges and Tunnels Fair, 26-28 May 2016, Ankara, Turkey

TBM Applications II, Bergen, Norway from 6th to 7th June 2016.

8th Nordic Grouting Symposium, 26-27 September 2016, Oslo, Norway

ΕΚΤΕΛΕΣΤΙΚΗ ΕΠΙΤΡΟΠΗ ΕΕΕΕΓΜ (2015 – 2018)

Πρόεδρος	:	Γεώργιος ΓΚΑΖΕΤΑΣ, Δρ. Πολιτικός Μηχανικός, Καθηγητής Ε.Μ.Π. president@hssmge.gr, gazetas@ath.forthnet.gr
Α' Αντιπρόεδρος	:	Παναγιώτης ΒΕΤΤΑΣ, Πολιτικός Μηχανικός, ΟΜΙΛΟΣ ΤΕΧΝΙΚΩΝ ΜΕΛΕΤΩΝ Α.Ε. otmate@otenet.gr
Β' Αντιπρόεδρος	:	Μιχάλης ΠΑΧΑΚΗΣ, Πολιτικός Μηχανικός mpax46@otenet.gr
Γενικός Γραμματέας	:	Μιχάλης ΜΠΑΡΔΑΝΗΣ, Πολιτικός Μηχανικός, ΕΔΑΦΟΣ ΣΥΜΒΟΥΛΟΙ ΜΗΧΑΝΙΚΟΙ Α.Ε. mbardanis@edafos.gr, lab@edafos.gr
Ταμίας	:	Γιώργος ΝΤΟΥΛΗΣ, Πολιτικός Μηχανικός, ΕΔΑΦΟΜΗΧΑΝΙΚΗ Α.Ε.- ΓΕΩΤΕΧΝΙΚΕΣ ΜΕΛΕΤΕΣ Α.Ε. gdoulis@edafomichaniki.gr
Έφορος	:	Γιώργος ΜΠΕΛΟΚΑΣ, Δρ. Πολιτικός Μηχανικός, Επίκουρος Καθηγητής ΤΕΙ Αθήνας gbelokas@teiath.gr, gbelokas@gmail.com
Μέλη	:	Ανδρέας ΑΝΑΓΝΩΣΤΟΠΟΥΛΟΣ, Δρ. Πολιτικός Μηχανικός, Ομότιμος Καθηγητής ΕΜΠ aanagn@central.ntua.grn
		Βάλια ΞΕΝΑΚΗ, Δρ. Πολιτικός Μηχανικός, ΕΔΑΦΟΜΗΧΑΝΙΚΗ Α.Ε. vxenaki@edafomichaniki.gr
		Μαρίνα ΠΑΝΤΑΖΙΔΟΥ, Δρ. Πολιτικός Μηχανικός, Αναπληρώτρια Καθηγήτρια Ε.Μ.Π. mpanta@central.ntua.gr
Αναπληρωματικό Μέλος	:	Κωνσταντίνος ΙΩΑΝΝΙΔΗΣ, Πολιτικός Μηχανικός, ΕΔΑΦΟΜΗΧΑΝΙΚΗ Α.Ε. kioannidis@edafomichaniki.gr
Εκδότης	:	Χρήστος ΤΣΑΤΣΑΝΙΦΟΣ, Δρ. Πολιτικός Μηχανικός, ΠΑΝΓΑΙΑ ΣΥΜΒΟΥΛΟΙ ΜΗΧΑΝΙΚΟΙ Ε.Π.Ε. editor@hssmge.gr, ctsatsanifos@pangaea.gr

ΕΕΕΕΓΜ

Τομέας Γεωτεχνικής
ΣΧΟΛΗ ΠΟΛΙΤΙΚΩΝ ΜΗΧΑΝΙΚΩΝ
ΕΘΝΙΚΟΥ ΜΕΤΣΟΒΙΟΥ ΠΟΛΥΤΕΧΝΕΙΟΥ
Πολυτεχνειούπολη Ζωγράφου
15780 ΖΩΓΡΑΦΟΥ

Τηλ. 210.7723434
Τοτ. 210.7723428
Ηλ-Δι. secretariat@hssmge.gr ,
geotech@central.ntua.gr
Ιστοσελίδα www.hssmge.org (υπό κατασκευή)

«ΤΑ ΝΕΑ ΤΗΣ ΕΕΕΕΓΜ» Εκδότης: Χρήστος Τσατσανίφος, τηλ. 210.6929484, τοτ. 210.6928137, ηλ-δι. ctsatsanifos@pangaea.gr, editor@hssmge.gr, info@pangaea.gr

«ΤΑ ΝΕΑ ΤΗΣ ΕΕΕΕΓΜ» «αναρτώνται» και στην ιστοσελίδα www.hssmge.gr